STUDY OF LARGE CIRCULAR LOOP ANTENNAS BY FULL-MAXWELL TREATMENT OF THE CURRENT DISTRIBUTION

BY

BHARAT KUMAR SAHA

A THESIS

SUBMITTED TO THE DEPARTMENT OF ELECTRICAL AND ELECTRONIC ENGINEERING

IN PARTIAL FULLFILLMENT OF THE REQUIREMENTS FOR

THE DEGREE

OF

MASTER OF SCIENCE IN ENGINEERING (ELECTRICAL & ELECTRONIC)

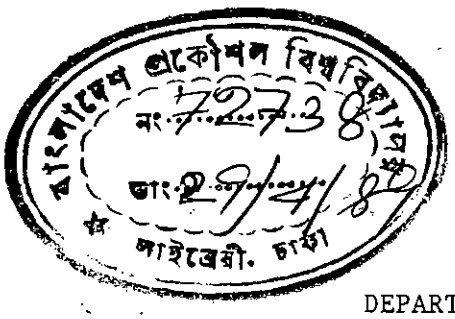

DEPARTMENT OF ELECTRICAL AND ELECTRONIC ENGINEERING

BANGLADESH UNIVERSITY OF ENGINEERING AND TECHNOLOGY (BUET),

DHAKA, BANGLADESH.

March 1989

CERTIFICATE

This is to certify that this work has been done by me and has not been submitted elsewhere for the award of any degree or diploma.

Signature of the candidate.

Bharat Kumar Saha

31.3.1989

Bharat Kumar Saha

The thesis titled, "Study of Large Circular Loop Antennas by Full-Maxwell Treatment of the Current Distribution," submitted by Bharat Kumar Saha of M. Sc. Engineering (EEE) Roll No. 871304F of the session 1985-86, has been accepted as satisfactory for partial fulfilment of the requirements for the degree of Master of Science in Engineering (Electrical and Electronic).

BOARD OF EXAMINERS

1. M. A. Matin 31.3.1989 — Chairman (Supervisor)
   Dr. Md. Abdul Matin
   Professor
   Department of Electrical and Electronic Engineering, Bangladesh University of Engineering and Technology (BUET),Dhaka.

2. M. A. Matin 31.3.1989 — Member
   Head of the Department,
   Department of Electrical and Electronic Engineering, BUET, Dhaka.

3. Saiful Islam 31.3.89 — Member
   Dr. Saiful Islam
   Professor
   Department of Electrical and Electronic Engineering, BUET, Dhaka.

4. Rezwan Khan 31.3.89 — Member
   Dr. Md. Rezwan Khan
   Assistant Professor
   Department of Electrical and Electronic Engineering, BUET, Dhaka.

5. Shamsuddin Ahmed 31.3.89 — Member (External)
   Prof. Shamsuddin Ahmed
   Head, Department of Electrical and Electronic Engineering, Islamic Centre for Technical and Vocational Training and Research (ICTVTR) Dhaka,Board Bazar, Gazipur.

ACKNOWLEDGEMENT

The author expresses his deep sense of gratitude and indebtness to Dr. Md. Abdul Matin, Professor and Head, Department of Electrical and Electronic Engineering, Bangladesh University of Engineering and Technology (BUET), Dhaka for advice, guidance and constant supervision throughout the course of this research work.

The author is highly indebted to Dr. Md. Mujibur Rahman, Professor and former Head, Department of Electrical and Electronic Engineering,BUET for constant support and encouragement with this work.

The author is grateful to Professor Shamsuddin Ahmed, Head of the Department of Electrical and Electronic Engineering, ICTVTR, Dhaka; to Prof. Saiful Islam and to Dr. Md. Rezwan Khan of the Department of Electrical and Electronic Engineering, BUET, Dhaka for their valuable suggestions.

The author wishes to express his sincere gratitude to Professor, J. R.Chowdhury, Director, Computer Centre, BUET for kind permission to work at the Computer Centre where almost all the computations were performed.

The author is thankful to Dr. Syed Mahbubur Rahman, Head of the Department of Computer Science and Engineering, BUET, Dhaka for kind permission to use the Microcomputers of his department.

Finally, the author would like to thank all who were involved directly or indirectly in successful completion of this work.

ABSTRACT

The distribution of current of a thin circular loop antenna has been derived by rigorous treatment of the fields in the loop region. Computations have been carried out for circular loops radiating in air. The current distribution is obtained in an infinite series converging rapidly after a few terms. Using this distribution of current the other characteristics of the antenna such as radiation pattern, radiation resistance, directivity and gain have been investigated. It reveals that circular loops having circumferences shorter than a half-wavelength can be treated as small loops supporting approximately a uniform current distribution. Loops of longer circumferences are affected by the non-uniformity of the current distribution arising from harmonics. The electric field of a large circular loop has been found to be cross-plorized in all planes other than the plane in which the loop lies. The cross polarizing effects are such that broadside and endfiring properties can be observed by varying the operating frequency. From calculation of the radiated power of the antenna it has been found that the lowest resonance of a thin circular loop take place when $L/\lambda = 1.5$ where L is the length of the loop and λ is the free space wavelength. Some other resonances occur at L/λ =3.4, 6.75, 10.0 which can be identified as the maxima of the second order Bessel's function $J_2 (L/\lambda)$. Antiresonances take place at L/λ =2.45,5.6, 8.7 corresponding to zeros of the zero-order Bessel's function $J_0 (L/\lambda)$. Numerical results or radiation resistance and gain are illustrated for upto L/λ =10. From studies of the directional gain of the antenna it is observed that for loop sizes $L/\lambda < 1.3$ the main beam of the antenna is in the endfire direction. For larger loops beyond this limit the main beam is along the axis of the loop for some ranges of frequency. For other ranges of frequency the radiation pattern is splitted into several lobes in various directions.

CONTENTS

List of Principal Symbols

ε_o = free space electric permittivity, 8.854×10^{-12} farad/m.

μ_o = free space magnetic permeability, $4\pi \times 10^{-7}$ henry/m.

ω = angular operating frequency, radian/sec.

f = frequency, Hz

λ = wave-length, m.

ρ = wire-radius of the conducting loop, m.

a = radius of the loop, m.

L = $2\pi a$, length of the loop, m

v = speed of the electromagnetic wave, m/sec.

$\bar{i}$ = current density, Amp/m^2

$\bar{E}$ = electric field intensity, volt/m.

$\bar{D}$ = electric flux density, $coulomb/m^2$.

$\bar{H}$ = magnetic field intensity, Amp/m

$\bar{B}$ = magnetic flux density, weber/m

$\bar{A}$ = vector magnetic potential, volt-sec/m

K_o = $\omega\sqrt{\mu_o \varepsilon_o} = 2\pi/\lambda =$ free space propagation constant, radian/m.

η = 120π = free space intrinsic impedance, ohms

$\bar{N}$ = radiation vector, Amp-m

$\bar{P}$ = Pointing vector, $Watt/m^2$

P_R = radial component of the Poyinting vector, $Watt/m^2$

K = radiation intensity, Watt per steredian

W = total radiated power, Watt

R_r = radiation resistance, Ohm

G_n = gain

D = directivity

CHAPTER - 1

GENERAL INTRODUCTION

1.1 Introduction

Antenna helps to convey electromagnetic energy from one place to another under the condition where running of wires, transmission line or waveguide becomes impossible or uneconomic such as aircraft or space communication, communication with ships, mobile vehicular communication or in radio and television broadcasting.

While small circular loops are very small compared to a wavelength, large circular loop antennas have circumferences comparable to or greater than the free space wavelength at the frequency of operation. Radiation from large loops is expected to be much greater than small loops and may sometimes be of practical interest for VHF and UHF communications.

1.2 Historical Review

The first general analysis of the circular loop as a transmitting antenna appears to be that of Hallen [1] who derived the current distribution in Fourier series. However, owing to the occurrence of a singularity or a very large value when the number of terms in the summation is sufficiently great, Hallen concluded that the series was divergent. Storer [2] avoided the contribution from the large term by replacing the Fourier series by the corresponding integral and evaluating this in the sense of the Cauchy's principal value. He provided extensive tables and graphs of the impedance, admittance and distribution of current for loops upto a wavelength in circumference with a number of different wire sizes. Wu [3] re-examined the problem of evaluating the Fourier series. He considered Storer's expedient to be of doubtful validity and devised an alternative and improved method with approximations.

Kraichman's [4] analysis is based on a Postulated uniform distribution of current around the loop which is valid only for electrically small loops if these are bare or covered with a very thin layer of dielectric. The work of chen and King [5] makes use of Storer's analysis but retains only the first two terms in the Fourier series. Although this is a considerably better approximation than that of Kraichman [4], it is also limited to electrically rather small loop. King et al. [6, 7] derived the distribution of current and admittance in bare circular loop- antennas using the theory of W_u [3]. Galejs [8] presented a method of analysis using two term trial functions for the current distribution. Whiteside and King [9] studied the loop antenna as a probe. They considered the receiving loop antenna as a magnetic probe. The ideal probe for this purpose would be an infinitesimal magnetic dipole for which the small loop is usually considered as an approximation.

Richtscheid [10] calculated the radiation resistance of loop antennas assuming a sinusoidal current distribution. Tsukiji and Tou [11] studied the characteristics of a polygonal loop antennas. They observed that the bandwidth of a loop depends largely on the shape of the loop. Some loop configurations exhibit more broadband property than the others. This property is explained by examining the current distributions on the loops obtained by the moment-method [28].

Michaski and Pearson [12] studied equivalent circuit synthesis for a loop antenna based on the singularity expansion method. The synthesized circuit have been analyzed under various excitation and loading conditions, Awadalla and Sharshar [13] presented an equivalent transmission line representation of the reactance of a loop antenna assuming the loop as a shorted transmission line.

The equivalent circuit and principles of operation of a miniloop antenna has been established by Barrick [14]. He used both classical and moment method for determining the circuit parameters.

Studies on loop antennas under various constraints have been reported by many authors. An insulated loop antenna in a conducting spherical shell has been studied by Row [15]. Self and mutual admittances of two identical circular loop antennas in a conducting medium and in air have been evaluated by Iizuka et al. [16]. Two identical coplanar rectangular loops have been analyzed by TsuKiji[17]. In this work, the current distribution is based on integral equation techniques.

Devore et al. [18] presented an analytical modelling of electrically small magnetically loaded multiturn loop antenna. A design procedure of receiving antenna for miniature receivers has been described by Pettengill et al. [19]. The problem concerning the mutual coupling of two parallel thin-wire loop antennas in air has been analysed by Abul-Kassem et al. [20]. They have chosen two coupled integral equations for the current on the loops. Shoamanesh and Shafai [21] studied the characteristics of Yagi arrays of two concentric loops with loaded elements. The electromagnetic field of an electrically small loop antenna with a cylindrical core has been investigated by Burton et al. [22]. A room-TV receiving antenna with a voltage standing-wave ratio (VSWR) less than two in the full-band VHF has been described by Ju et al. [23]. Metwally et al. [24] studied the problem of mutual coupling between loops on or above the surface of a layered lossy earth by applying the image theory.

1.3 Objective of the Study

The objective of this research is to study the characteristics of a large circular loop antenna. The current distribution of a loop antenna has been obtained by solving Maxwell's equations. The other characteristics for loops of different sizes have been obtained using this current distribution.

1.4 Thesis Layout

In the present work in studying the radiation characteristics of a circular loop antenna the analysis has been carried out in a straight-forward manner from Maxwell's equations. In chapter-2, solution of Maxwell's equations in a region enclosed by a circular loop antenna has been obtained. Chapter-3 deals with the derivation of the current distribution of a circular loop antenna. In Chapter-4 radiation pattern of a circular loop antenna has been studied for different loop sizes. Chapter-5 deals with the radiated power and radiation resistance of a circular loop antenna for different loop sizes. Chapter-6 deals with the evaluation of directivity and gain of the antenna. A general discussion and suggestions for future works is presented in Chapter-7.

CHAPTER - 2

SOLUTION OF MAXWELL'S EQUATIONS IN A REGION ENCLOSED BY A CIRCULAR LOOP ANTENNA

2.1 Introduction

The circular loop antenna under consideration is a single circular turn of a highly conducting wire carrying high frequency current. Fields are produced both inside and outside the loop region. The fields inside the loop region applying the necessary boundary conditions shall be investigated.

2.2 Field Equations in Circular Co-ordinates

The performance of antennas is primarily described by Maxwell's field equations. In a source-free region Maxwell's equations for time periodic fields are written as

$$\nabla \times \bar{E} = -j\omega\mu_o \bar{H} \tag{2.1}$$

$$\nabla \times \bar{H} = j\omega\varepsilon_o \bar{E} \tag{2.2}$$

where $\bar{E}$ and $\bar{H}$ are the electric and magnetic field intensities in volt/m and Amp/m respectively. The surrounding medium is considered to be air characterized approximately by the free-space electric permittivity ε_o and the magnetic permeability μ_o

Corresponding to the circular cylindrical co-ordinates shown in Fig. 2.1, eqns (2.1) and (2.2) can be expressed as [30],

$$\frac{1}{r}\begin{vmatrix} \bar{a}_r & r\bar{a}_\phi & \bar{a}_z \\ \frac{\partial}{\partial r} & \frac{\partial}{\partial \phi} & \frac{\partial}{\partial z} \\ E_r & rE_\phi & E_z \end{vmatrix} = -j\omega\mu_o\left(\bar{a}_r H_r + \bar{a}_\phi H_\phi + \bar{a}_z H_z\right) \tag{2.3}$$

$$\frac{1}{r}\begin{vmatrix} \bar{a}_r & r\bar{a}_\phi & \bar{a}_z \\ \frac{\partial}{\partial r} & \frac{\partial}{\partial \phi} & \frac{\partial}{\partial z} \\ H_r & rH_\phi & H_z \end{vmatrix} = j\omega\varepsilon_o\left(\bar{a}_r E_r + \bar{a}_\phi E_\phi + \bar{a}_z E_z\right) \tag{2.4}$$

Where $\bar{a}_r$, $\bar{a}_\phi$ and $\bar{a}_z$ are unit vectors in the radial, circumferential and axial directions respectively.

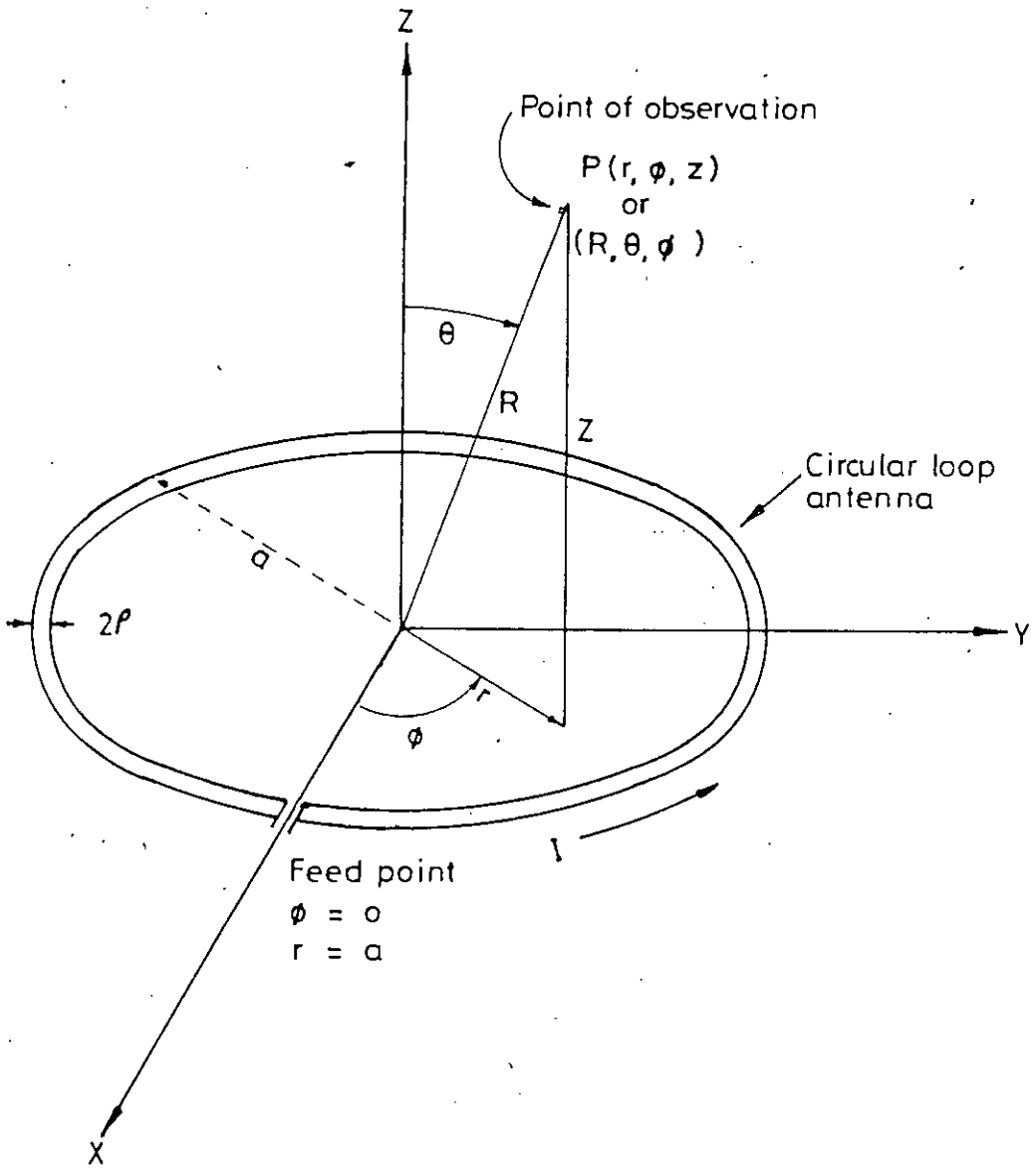

Fig. 2.1 A circular loop antenna and its co-ordinate system.

Equating the vector components on both sides of eqns. (2.3) and (2.4) we get

$$\frac{1}{r}\left\{\frac{\partial E_z}{\partial \phi} - \frac{\partial}{\partial z}(rE_\phi)\right\} = -j\omega\mu_o H_r \tag{2.5}$$

$$\frac{\partial E_r}{\partial z} - \frac{\partial E_z}{\partial r} = -j\omega\mu_o H_\phi \tag{2.6}$$

$$\frac{1}{r}\left\{\frac{\partial}{\partial r}(rE_\phi) - \frac{\partial E_r}{\partial \phi}\right\} = -j\omega\mu_o H_z \tag{2.7}$$

$$\frac{1}{r}\left\{\frac{\partial H_z}{\partial \phi} - \frac{\partial}{\partial z}(rH_\phi)\right\} = j\omega\epsilon_o E_r \tag{2.8}$$

$$\frac{\partial H_r}{\partial z} - \frac{\partial H_z}{\partial r} = j\omega\epsilon_o E_\phi \tag{2.9}$$

$$\frac{1}{r}\left\{\frac{\partial}{\partial r}(rH_\phi) - \frac{\partial H_r}{\partial \phi}\right\} = j\omega\epsilon_o E_z \tag{2.10}$$

2.3 The Boundary Conditions

As the current is ϕ -directed, then in the plane of the loop the field conditions can be assumed to be $H_r = 0$, $H_\phi = 0$, $E_z = 0$. Then from(2.5) and (2.6) $\frac{\partial}{\partial z}$ of all field quantities will be zero. Now, looking into field at the feed-point where the feeding gap is very small the electric field is entirely ϕ-directed so that

$$E_r = 0 \quad \text{at} \quad r = a \;,\; \phi = 0 \tag{2.11}$$

2.4 The Field Solution in the Region Enclosed by a Circular Loop Antenna

Applying the field conditions stated in section 2.3 in the eqns (2.5)-(2.10) we obtain the following equations for fields inside the circular loop:

$$\frac{1}{r}\left\{\frac{\partial}{\partial r}(rE_\phi) - \frac{\partial E_r}{\partial \phi}\right\} = -j\omega\mu_o H_z \tag{2.12}$$

$$\frac{1}{r}\frac{\partial H_z}{\partial \phi} = j\omega\epsilon_o E_r \tag{2.13}$$

$$\frac{\partial H_z}{\partial r} = -j\omega\epsilon_o E_\phi \tag{2.14}$$

From eqns (2.13) and (2.14)

$$E_r = \frac{1}{j\omega\varepsilon_o} \cdot \frac{1}{r} \frac{\partial H_z}{\partial \phi} \tag{2.15}$$

$$E_\phi = - \frac{1}{j\omega\varepsilon_o} \frac{\partial H_z}{\partial r} \tag{2.16}$$

Substituting (2.15) and (2.16) into eqn. (2.12) we find that H_z satisfies the following equation:

$$r^2 \frac{\partial^2 H_z}{\partial r^2} + r \frac{\partial H_z}{\partial r} + K_o^2 r^2 H_z + \frac{\partial^2 H_z}{\partial \phi^2} = 0 \tag{2.17}$$

where, K_o is the free-space propagation constant

$$K_o = \omega\sqrt{\mu_o \varepsilon_o} \tag{2.18}$$

The solution of eqn (2.17) can be carried out by applying the separation of variable technique. Let,

$$H_z (r, \phi) = R(r) \cdot F_\phi (\phi) \tag{2.19}$$

Substituting (2.19) into (2.17) and dividing althrough by RF we get

$$r^2 \frac{R''}{R} + r \frac{R'}{R} + K_o^2 r^2 + \frac{F_\phi''}{F_\phi} = 0 \tag{2.20}$$

Now let,

$$\frac{F_\phi''}{F_\phi} = - \nu^2 \tag{2.21}$$

Where ν is an integer. Then (2.20) takes the form

$$\frac{d^2R}{dr^2} + \frac{1}{r} \frac{dR}{dr} + \left(K_o^2 - \frac{\nu^2}{r^2} \right) R = 0 \tag{2.22}$$

The general solution of the above equation is [32],

$$R(r) = A\ J_\nu (K_o r) + B\ N_\nu (K_o r) \tag{2.23}$$

where $J_\nu (K_o r)$ and $N_\nu (K_o r)$ are respectively Bessel's function and Neuman's function of order ν. A and B are arbitrary constants. The solution of eqn. (2.21) is given by

$$F_\phi = C \cos \nu\phi + D \sin \nu\phi \tag{2.24}$$

where C and D are arbitrary constants.

Thus the general solution of eqn. (2.17) becomes

$$H_z(r,\phi) = R(r)\, F_\phi(\phi)$$
$$= [A J_\nu(k_o r) + B N_\nu(k_o r)][C \cos\nu\phi + D \sin\nu\phi] \quad (2.25)$$

Since at $r = 0$, H_z must be finite, then it is such that $B = 0$

Denoting $AC = C_\nu$ and $AD = D_\nu$, we have the harmonic solution of H_z given by

$$H_z(r,\phi) = \sum_{\nu=0}^{\infty} J_\nu(k_o r)(C_\nu \cos\nu\phi + D_\nu \sin\nu\phi) \quad (2.26)$$

Substituting H_z from eqn (2.26) into eqn. (2.15), we get

$$E_r = \frac{1}{j\omega\epsilon_o} \sum_{\nu=0}^{\infty} \frac{\nu}{r} J_\nu(k_o r)(D_\nu \cos\nu\phi - C_\nu \sin\nu\phi) \quad (2.27)$$

Similarly substituting H_z from eqn (2.26) into eqn. (2.16), we get,

$$E_\phi = -\frac{1}{j\omega\epsilon_o} \sum_{\nu=0}^{\infty} [\frac{\nu}{r} J_\nu(k_o r) - k_o J_{\nu+1}(k_o r)][C_\nu \cos\nu\phi + D_\nu \sin\nu\phi] \quad (2.28)$$

Applying the boundary condition at the feed-point,

i.e., at $r = a$, $\phi = 0$, $E_r = 0$ in eqn (2.27) we get

$$D_\nu = 0 \quad (2.29)$$

Thus the field components in the region enclosed by the circular loop antenna are obtained as :

$$E_r = -\frac{1}{j\omega\epsilon_o} \sum_{\nu=0}^{\infty} C_\nu \frac{\nu}{r} J_\nu(k_o r) \sin\nu\phi \quad (2.30)$$

$$E_\phi = -\frac{1}{j\omega\epsilon_o} \sum_{\nu=0}^{\infty} C_\nu [\frac{\nu}{r} J_\nu(k_o r) - k_o J_{\nu+1}(k_o r)] \cos\nu\phi \quad (2.31)$$

$$H_z = \sum_{\nu=0}^{\infty} C_\nu J_\nu(k_o r) \cos\nu\phi \quad (2.32)$$

2.5 Discussion

The solution of Maxwell's equations in the plane of a circular loop antenna is obtained by applying the condition that the magnetic lines of forces are perpendicular to the plane and the electric field in the loop region is polarized with the radial and circumferential components. The feedpoint of the loop is assumed to be a small gap such that no radial electric field component is developed in the gap. The solution appears in a series of harmonics involving higher order Bessel's functions multiplied by sine and cosine harmonics.

CHAPTER - 3

CURRENT DISTRIBUTION OF A CIRCULAR LOOP ANTENNA

3.1 Introduction

In Chapter-2 we obtained the solution of source-free Maxwell's equations in the region enclosed by a circular loop antenna. The solution can now be used to obtain the current distribution of a loop antenna.

3.2 Derivation of the Current Distribution

The current distribution in a circular loop antenna can be evaluated from the concept of surface current

$$\bar{J} = \bar{n} \times \bar{H} \tag{3.1}$$

Where $\bar{J}$ is the surface current density in amp/m and $\bar{n}$ is a unit vector normal to the conducting loop. $\bar{n} = -\bar{a}_r$ for a radially inward normal and $\bar{n} = \bar{a}_r$ for a radially outward normal. Considering $\bar{n} = -\bar{a}_r$

$$\begin{aligned} \bar{J} &= -\bar{a}_r \times \bar{a}_z H_z \\ &= \bar{a}_\phi H_z \end{aligned} \tag{3.2}$$

Hence the current flow is ϕ -directed as it is expected.

Similarly for $\bar{n} = \bar{a}_r$ we have to consider the magnetic field just outside the loop where it should be oppositely directed.

Hence,

$$\begin{aligned} \bar{J} &= \bar{a}_r \times -\bar{a}_z H_z \\ &= \bar{a}_\phi H_z \end{aligned} \tag{3.3}$$

This is similar to eqn (3.2). Now, if, the loop is very thin, then the magnetic field just arround the wire can be considered uniform. Hence the current is given by

$$\begin{aligned} I &= 2\pi\rho J \Big|_{r=a} \\ &= 2\pi\rho H_z \Big|_{r=a} \end{aligned} \tag{3.4}$$

where ρ is the wire radius.

Substituting the value of H_z from eqn (2.32), the current distribution becomes

$$I(\phi) = \sum_{\nu=0}^{\infty} I_\nu \; J_\nu(K_0 a) \cos \nu\phi \tag{3.5}$$

where

$$I_\nu = 2\pi\rho C_\nu \tag{3.6}$$

The series in eqn (3.5) indicates that the net current in the loop is the superposition of infinite number of current components. It also indicates that each component of a ϕ -dependent current series of the form $\sum_{\nu=1}^{\infty} I_\nu \cos\nu\phi$ has been reduced by a factor $J_\nu(K_0 a)$ which accounts for the effect of the loop-size on the current. Hence let us investigate the ϕ -dependence of the current by studying the series

$$f(\phi) = \sum_{\nu=0}^{\infty} I_\nu \cos\nu\phi \tag{3.7}$$

Taking out the Zero order term, this can be written as

$$f(\phi) = I_0 + \sum_{\nu=1}^{\infty} I_\nu \cos\nu\phi \tag{3.8}$$

This becomes the Fourier series representation of a periodic even function. A family of periodic even functions can be called upon to represent the above series. But, if it is assumed that the harmonic effects will be severe due to energy trapping in a closed circular region, then a square wave sketched in Fig. 3.1 poses to the problem very well. Also, it complies with the concept that the major charge concentration will take place around the feed point.

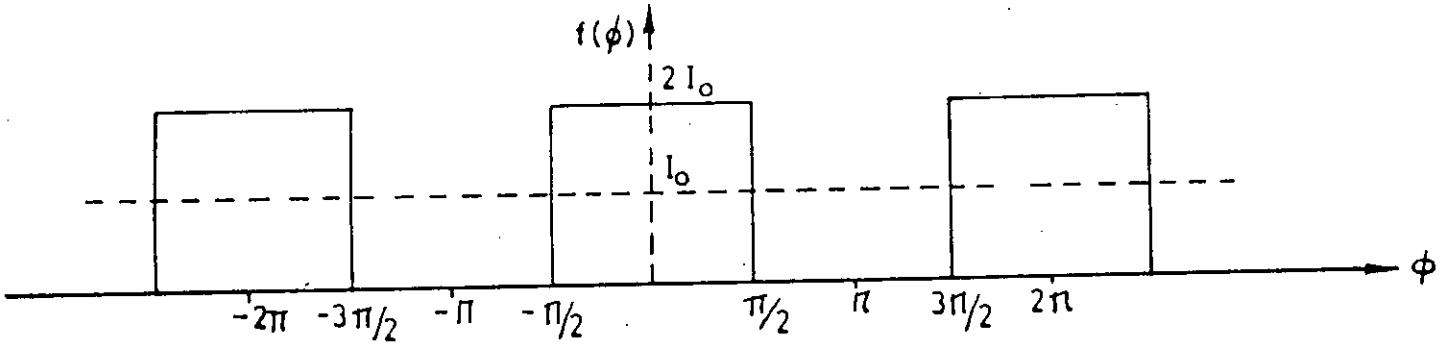

Fig. 3.1 Square wave representation of the fuction $f(\phi)$

The function $f(\phi)$ referred to Fig. 3.1 is such that

$$f(\phi) = 2I_o \quad , \quad 0 < \phi < \pi/2$$
$$= 0 \quad , \quad \pi/2 \, \phi < \pi \tag{3.9}$$

Hence the coefficient I_ν is given by [25],

$$I_\nu = \frac{2}{\pi} \int_0^{\pi/2} 2I_o \cos\nu\phi \, d\phi$$
$$= \frac{4I_o}{\pi} \frac{\sin \nu\pi/2}{\nu} \tag{3.10}$$

Again I_o in eqn (3.8) is the half of the Zero order Coefficient

$$I_o = \frac{1}{2} \cdot \frac{2}{\pi} \int_o^{\pi/2} f(\phi) \, d\phi = \lim_{\nu \to o} \frac{I_\nu}{2}$$

Now taking out the zero order term from (3.5) and substituting I_ν by eqn. (3.10) we get,

$$I(\phi) = I_o J_o(K_o a) + \frac{4I_o}{\pi} \sum_{\nu=1}^{\infty} \frac{\sin \nu\pi/2}{\nu} J_\nu(K_o a) \cos\nu\phi \tag{3.11}$$

This series can be tested for d.c. or extremely low frequency excitation. In such cases $K_o a \to o$, so that $J_o(K_o a) \to 1$, and for ν = 1, 2, 3 .. etc. $J_\nu(K_o a) \to 0$.

Hence for d.c. or low frequency excitation we get the uniform current distribution,

$$I(\phi) = I_o \tag{3.12}$$

Thus the current component I_o defined in the above discussions is actually the direct current or the low frequency effective current of the circular loop.

For high frequency excitation where the current is affected by the loop-size, the first term in eqn. (3.11) constitutes a uniform component of the current.

But the higher order terms in eqn (3.11) will have ϕ-variations and will constitute a non-uniform part of the current distribution. The appearances of cosine harmonics in the current distribution were also predicted by King et al. [7] and Galejs [8]. But their functional representations of the current distribution are not so regular as obtained above. The reason is that in their approaches they imposed additional boundary conditions at the feed point in order to evaluate the Fourier Co-efficient I_ν . In these attempts the Fourier series does not converge. However, in our analysis the series is regular and converges to a finite value rapidly after a few terms due to the occurences of higher order Bessel's functions accounting for the effects of the loop size on the current.

3.3 Numerical Results

Numerical calculations of the current distribution of loop antennas of different sizes were carried out by using sub-programs of higher order Bessel's functions with $\nu = q$ for which the current series converges completely. The results are illustrated in Figs.3.2 and 3.3 for various loop sizes L/λ , where $L = 2\pi a$ is the loop length and λ is the free space wavelength. For $L/\lambda = 1.0$ the current is maximum at the feed point and minimum at the diametrically opposite point. For still larger loops there are several maxima and minima and the current may flow in the opposite direction. The common feature is that each current wave swings about a uniform value of current on the loop. The current wave stands on the loop in a compressed manner indicating a slower speed of electromagnetic wave along the wire of the loop.

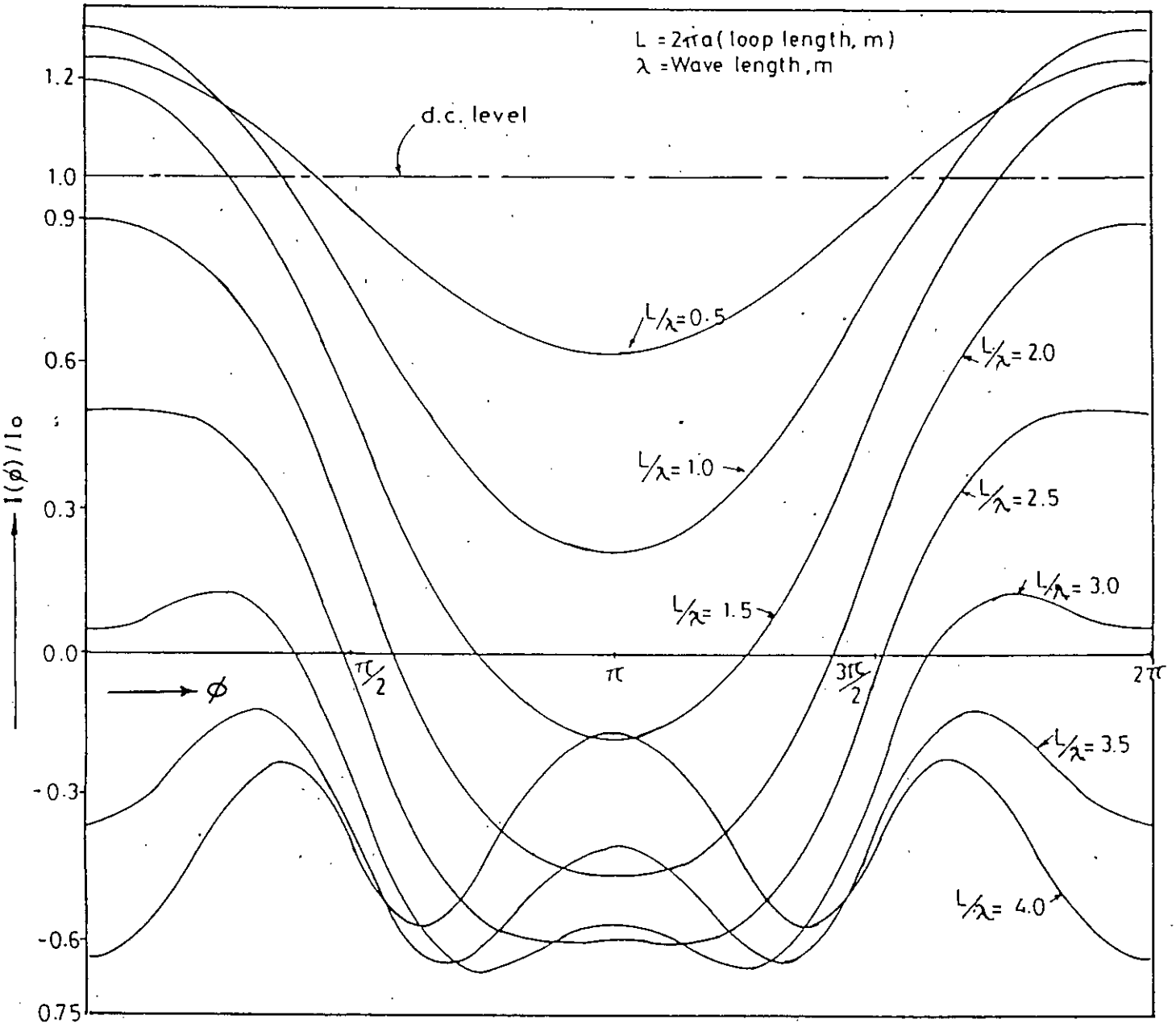

Fig. 3.2 Current distribution of a circular loop antenna for different loop-sizes.

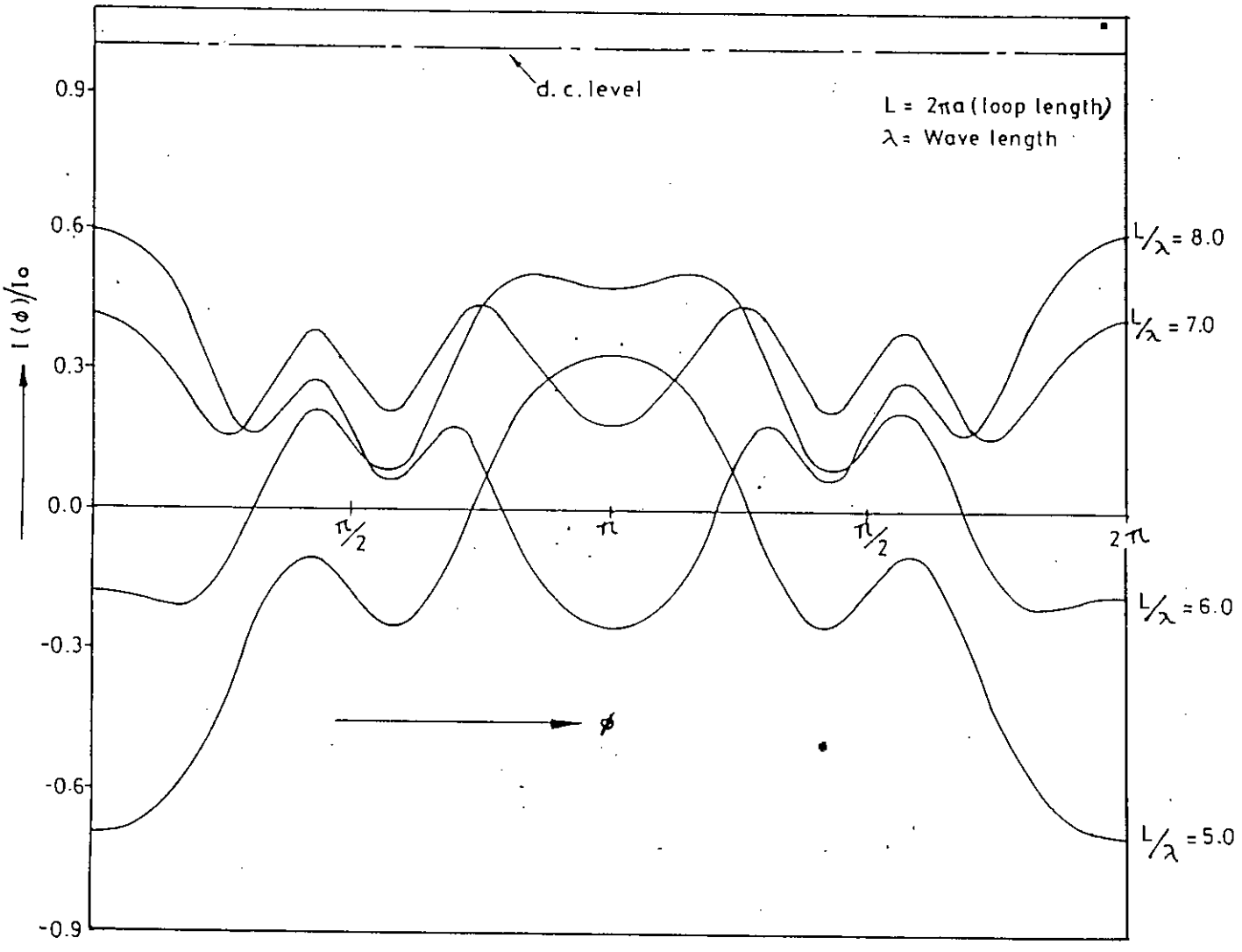

Fig. 3.3 Current distribution of a circular loop antenna for different loop-sizes.

3.4 Discussion

In the above the current distribution of a circular loop antenna has been derived using the field solution in the region enclosed by the loop. The current has been found to consist of a uniform component and a series of harmonic components. The harmonic components of the current appear as the products of higher order Bessel's functions and harmonic cosine functions. Numerical plots of the current wave are illustrated in Figs. 3.2 and 3.3 for different loop sizes.

CHAPTER - 4

RADIATION PATTERN OF A LARGE CIRCULAR LOOP ANTENNA

4.1 Introduction

The radiation pattern of an antenna is its basic property [29] - [31], since it represents the spatial distribution of the radiated energy. Antennas do not radiate uniformly in all directions in space. Consequently it is of interest to plot the relative strength of the radiation intensity as a function of the angle θ and ϕ for a constant value of R in spherical co-ordinates. The resultant surface describes the radiation pattern of the antenna. In this chapter radiation intensity has been derived with the help of the far field. Numerical plots of radiation pattern are also illustrated.

4.2 Far Field Evaluation

The far field or radiation field of an antenna can be calculated using the method suggested by Schelkunoff [26]. For ready reference the method is described in appendix-A. The vector magnetic potential A at the far field is given by eqn. (A-4)of the appendix,

$$\bar{A} = \mu_0 \frac{e^{-jk_0R}}{4\pi R} \bar{N} \tag{4.1}$$

where $\bar{N}$ is given by eqn.(A-3)of appendix as

$$\bar{N} = \int_{v'} \bar{i}_s e^{jk_0R'\cos\psi} dv' \tag{4.2}$$

For a line current this becomes

$$\bar{N} = \int_{l'} I(l') e^{jk_0R'\cos\psi} d\bar{l}' \tag{4.3}$$

In the present case, the source co-ordinates are such that the loop lies in the plane where $\theta' = \pi/2$. The direction cosine is given by

$$\cos\psi = \sin\theta \cos(\phi - \phi') \qquad (4.4)$$

Also

$$R' = a, \quad dl' = a\,d\phi', \quad I(l') = I(\phi')$$

Now if the vector $\bar{N}$ is calculated at a point (r, ϕ, Z) by integrating the contributions from differential current elements at $(a, \phi', 0)$, then it can be checked, $\bar{N}$ will have both circumferential and radial components given by

$$\bar{N} = \bar{a}_\phi N_\phi + \bar{a}_r N_r \qquad (4.5)$$

where

$$N_\phi = a\int_0^{2\pi} I(\phi')\, e^{jk_0 a \sin\theta \cos(\phi-\phi')} \cdot \cos(\phi-\phi')\, d\phi' \qquad (4.6)$$

$$N_r = a\int_0^{2\pi} I(\phi')\, e^{jk_0 a \sin\theta \cos(\phi-\phi')} \cdot \sin(\phi-\phi')\, d\phi' \qquad (4.7)$$

For a circularly symmetric current $N_r = 0$. But in the present case since the current has got ϕ -variations, then $N_r \neq 0$. In evaluating (4.6) and (4.7) we shall make use of the following identities [27].

$$\int_0^{2\pi} e^{jp\cos\alpha} \cdot \cos n\alpha\, d\alpha = 2\pi J_n(p) j^n \qquad (4.8)$$

$$\int_0^{2\pi} e^{jp\cos\alpha} \cdot \sin n\alpha\, d\alpha = 0 \qquad (4.9)$$

Using the above identities we can evaluate the following integrals:

$$\int_0^{2\pi} e^{jp\cos(\beta-\alpha)} \cdot \cos(\beta-\alpha)\cos n\alpha \, d\alpha = \pi\left\{j^{n+1}J_{n+1}(p) + j^{n-1}J_{n-1}(p)\right\} \times \underset{\cos n\beta}{} \quad (4.10)$$

$$\int_0^{2\pi} e^{jp\cos(\beta-\alpha)} \cdot \sin(\beta-\alpha)\cos n\alpha \, d\alpha = \pi\left\{j^{n-1}J_{n-1}(p) - j^{n+1}J_{n+1}(p)\right\} \times \underset{\sin n\beta}{} \quad (4.11)$$

Hence for n = 0 we get by using $J_{-1}(p) = -J_1(P)$,

$$\int_0^{2\pi} e^{jp\cos(\beta-\alpha)} \cdot \cos(\beta-\alpha)\, d\alpha = j\,2\pi J_1(p) \quad (4.12)$$

$$\int_0^{2\pi} e^{jp\cos(\beta-\alpha)} \cdot \sin(\beta-\alpha)\, d\alpha = 0 \quad (4.13)$$

Now, substituting $I(\phi')$ from eqn. (3.11) into (4.6) and (4.7) and then applying the identities (4.10) - (4.13) N_ϕ and N_r are determined as

$$N_\phi = jI_o 2\pi a J_0(k_0 a) J_1(k_0 a \sin\theta) - 4aI_o \sum_{\nu\ odd} \frac{1}{\nu} J_\nu(k_0 a)\left\{J_{\nu+1}(k_0 a\sin\theta) - J_{\nu-1}(k_0 a\sin\theta)\right\}\cos\nu\phi \quad (4.14)$$

$$N_p = 4aI_o \sum_{\nu\ odd} \frac{1}{\nu} J_\nu(k_0 a)\left\{J_{\nu+1}(k_0 a\sin\theta) + J_{\nu-1}(k_0 a\sin\theta)\right\}\sin\nu\phi \quad (4.15)$$

Eqn (4.15) indicates that N_r is non-vanishing except for $\nu = o$.

Now, the cylindrical vector $\bar{a}_r N_r$ can be resolved into spherical components as

$$\bar{a}_r N_r = \bar{a}_\theta N_\theta + \bar{a}_R N_R \tag{4.16}$$

where

$$N_\theta = N_r \cos\theta \tag{4.17}$$

$$N_R = N_r \sin\theta \tag{4.18}$$

As shown in appendix-A, N_R does not exist in the far field radiation vector. Rather N_θ exists. Thus the appearance of N_θ and N_ϕ in the radiation vector will produce cross-polarized field. However, N_θ vanishes only at $\theta = 90^o$ indicating that only the ϕ - polarization of the electric field exists in the far field radiation along the plane of the circular loop.

4.3 Radiation Intensity

Radiation intensity is defined as the power radiated in a given direction per unit solid angle. It determines the spatial distribution of the radiated energy. From eqn. (A-12) of the appendix the radiation intensity of the circular loop is given by

$$K(\theta, \phi) = \frac{\eta}{8\lambda^2}\left(|N_\phi|^2 + |N_\theta|^2\right)$$

$$= 15\pi I_o^2 (K_o a)^2 |S(\theta,\phi)|^2 \tag{4.19}$$

where

$$|S(\theta,\phi)|^{\nu} = S_{\phi}^{\nu} + S_{\theta}^{\nu} \tag{4.20}$$

$$S_{\phi} = \sqrt{a_0^{\nu} + \left(\sum_{\nu\ odd} a_{\nu}\right)^{\nu}} \tag{4.21}$$

$$S_{\theta} = \sum_{\nu\ odd} b_{\nu} \tag{4.22}$$

$$a_0 = J_0(K_0 a)\, J_1(K_0 a \sin\theta) \tag{4.23}$$

$$a_{\nu} = \frac{2}{\nu\pi} J_{\nu}(K_0 a) \left\{ J_{\nu-1}(K_0 a \sin\theta) - J_{\nu+1}(K_0 a \sin\theta) \right\} \cos\nu\phi \tag{4.24}$$

$$b_{\nu} = \frac{2}{\nu\pi} \cos\theta\, J_{\nu}(K_0 a) \left\{ J_{\nu-1}(K_0 a \sin\theta) + J_{\nu+1}(K_0 a \sin\theta) \right\} \sin\nu\phi \tag{4.25}$$

$S(\theta, \phi)$ has been computed for $\nu = 9$ for which the infinite series converges to finite value. Numerical plots of the θ and ϕ dependence of the radiation intensity $K(\theta, \phi)$ are shown in Figs. 4.1-4.15. The dotted patterns in Figs. 4.1, 4.4 and 4.10 are for loop size, $L/\lambda = .5$ assuming a uniform current distribution. These are shown for comparison with the solid patterns calculated by using the non-uniform current distribution. The radiation pattern in the yx-plane i.e. in the plane of the loop is elliptical (Fig. 4.1) for upto $L/\lambda = 2.0$ However, for larger loop-sizes pattern distortion takes place. For $L/\lambda = 7.0$(Fig. 4.3)radiation in the yx-plane is very little compared with the loops having $L/\lambda =$ 6.0 and 8.0.

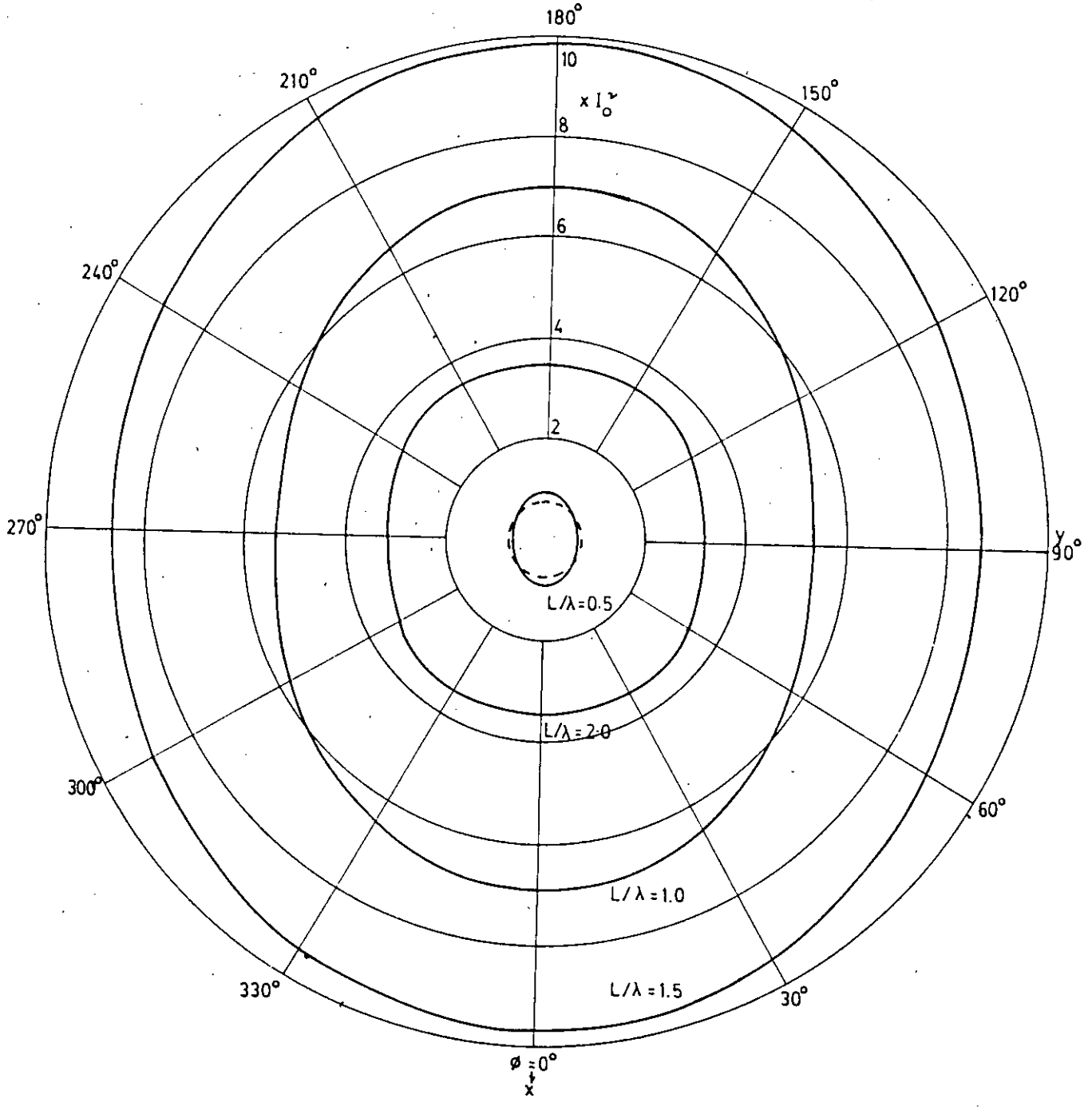

Fig. 4.1 Radiation pattern of a large circular loop antenna in yx-plane for $L/\lambda = 0.5, 1.0, 1.5$ and 2.0

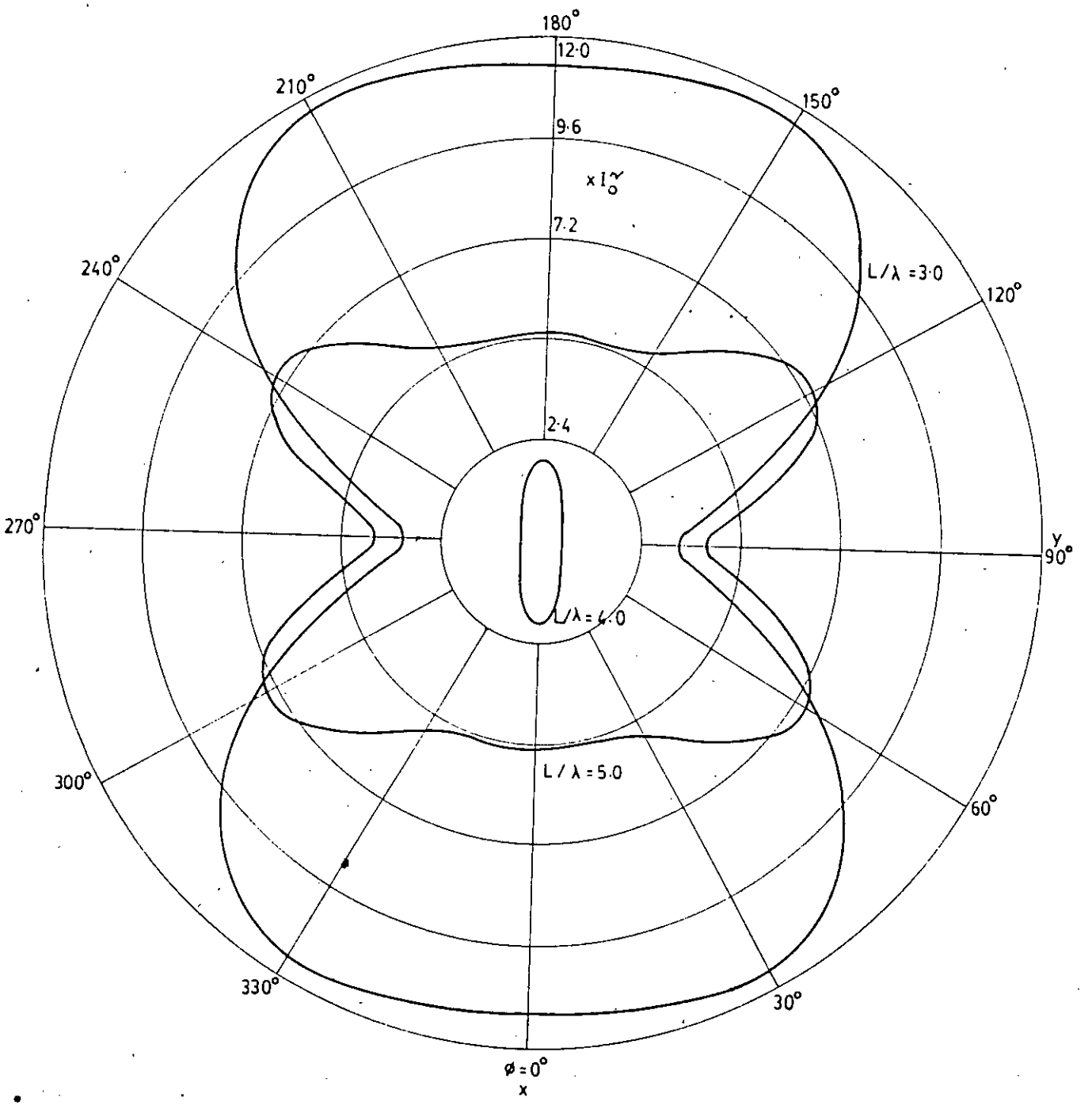

Fig. 4·2 Radiation pattern of a large circular loop antenna in yx-plane for L/λ=3·0,4·0 and 5·0

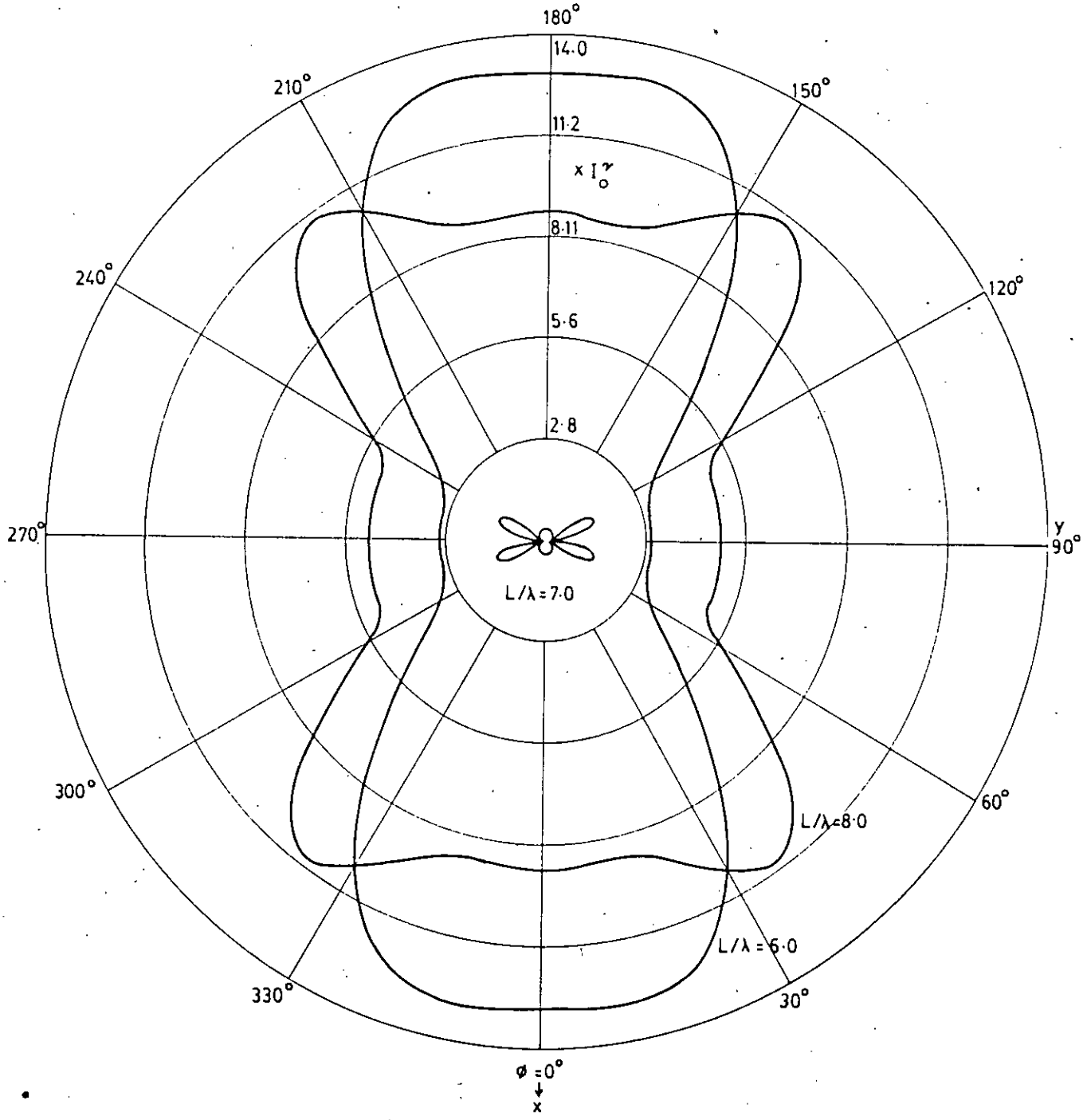

Fig. 4·3 Radiation pattern of a large circular loop antenna in yx-plane for $L/\lambda = 6{\cdot}0, 7{\cdot}0$ and $8{\cdot}0$

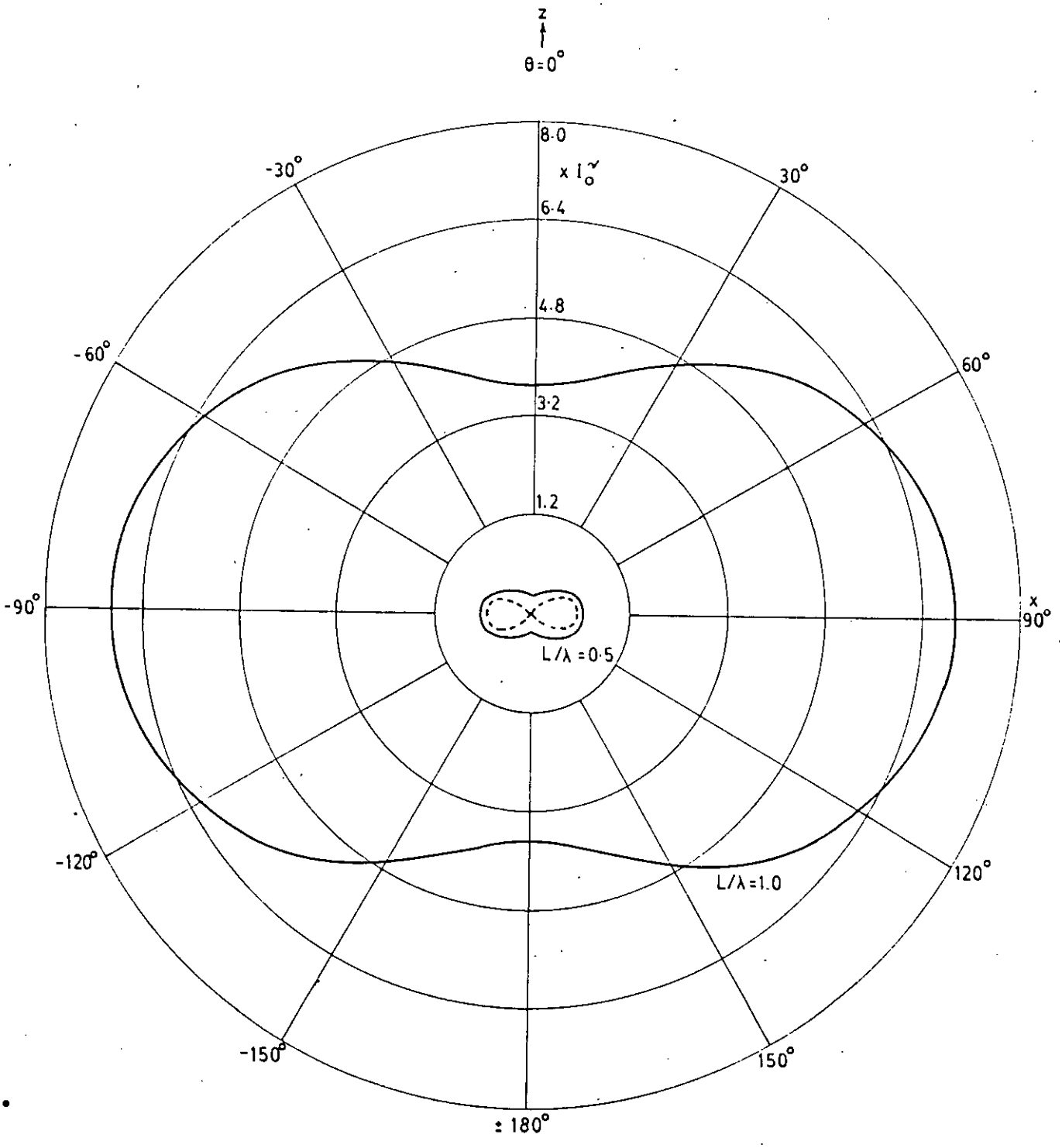

Fig. 4.4 Radiation pattern of a large circular loop antenna in xz-plane for L/λ=0.5, and 1.0

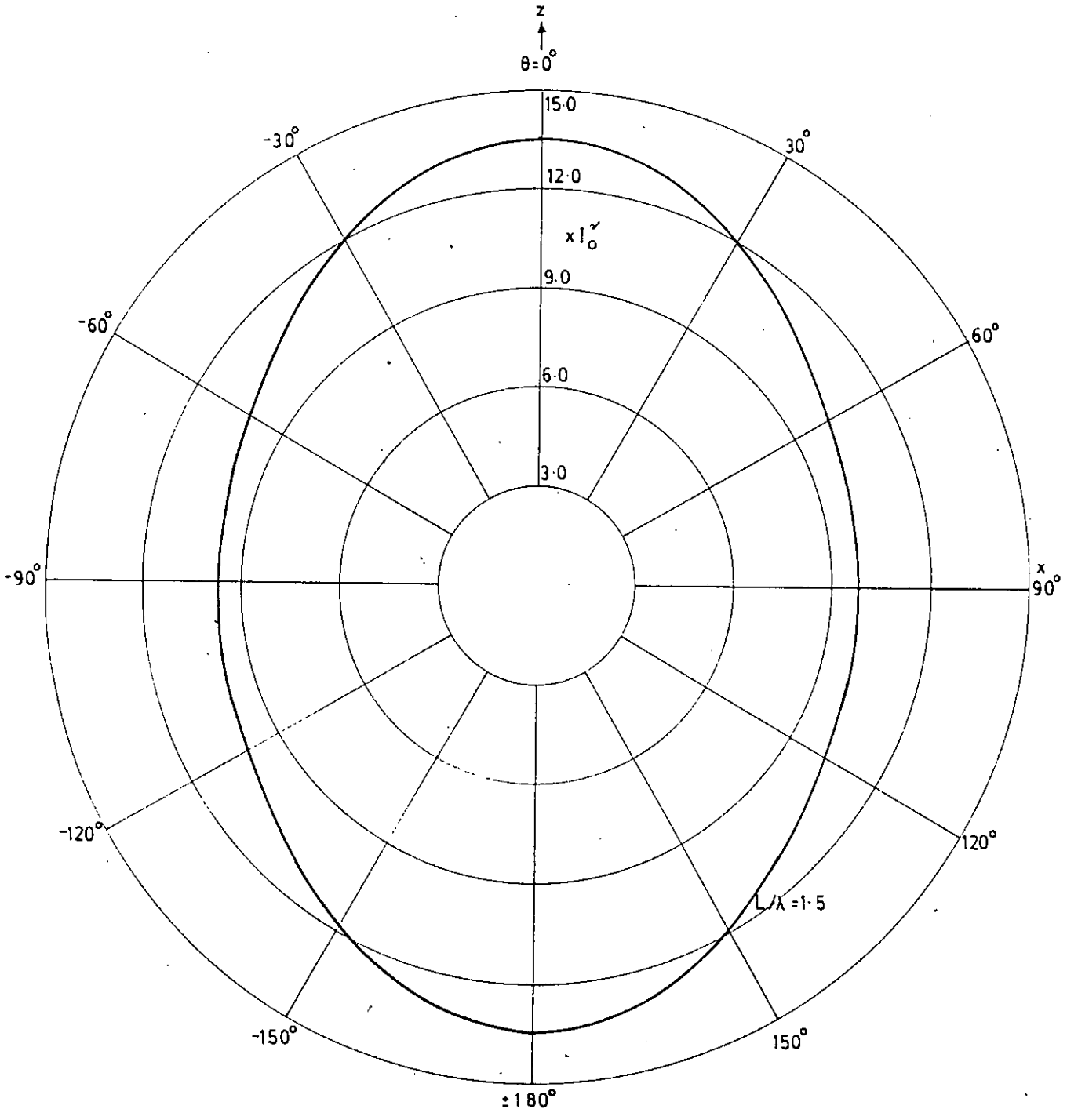

Fig. 4·5 Radiation pattern of a large circular loop antenna in xz-plane for $L/\lambda = 1{\cdot}5$

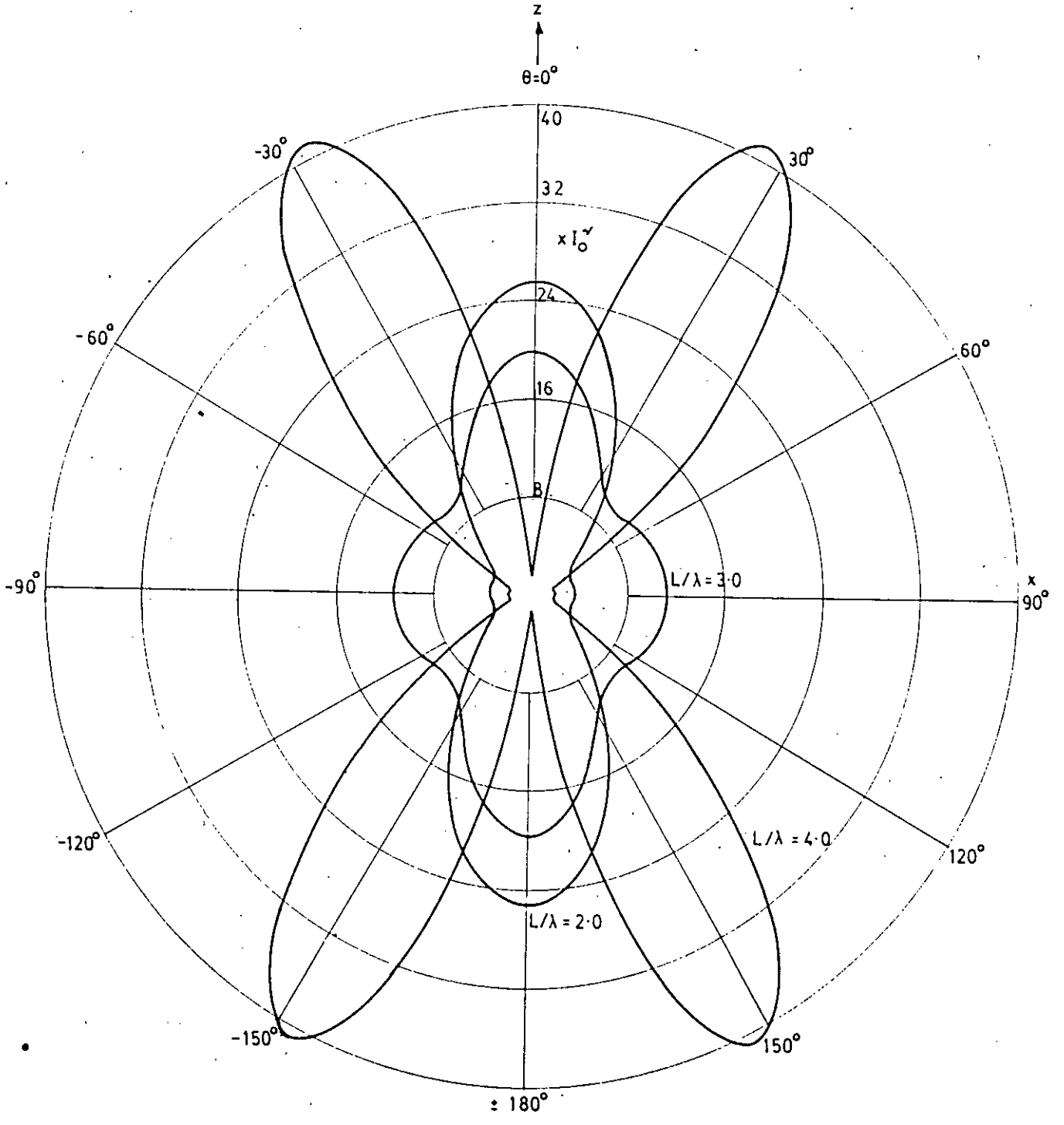

Fig 4·6 Radiation pattern of a large circular loop antenna in zx-plane for L/λ = 2·0, 3·0 and 4·0

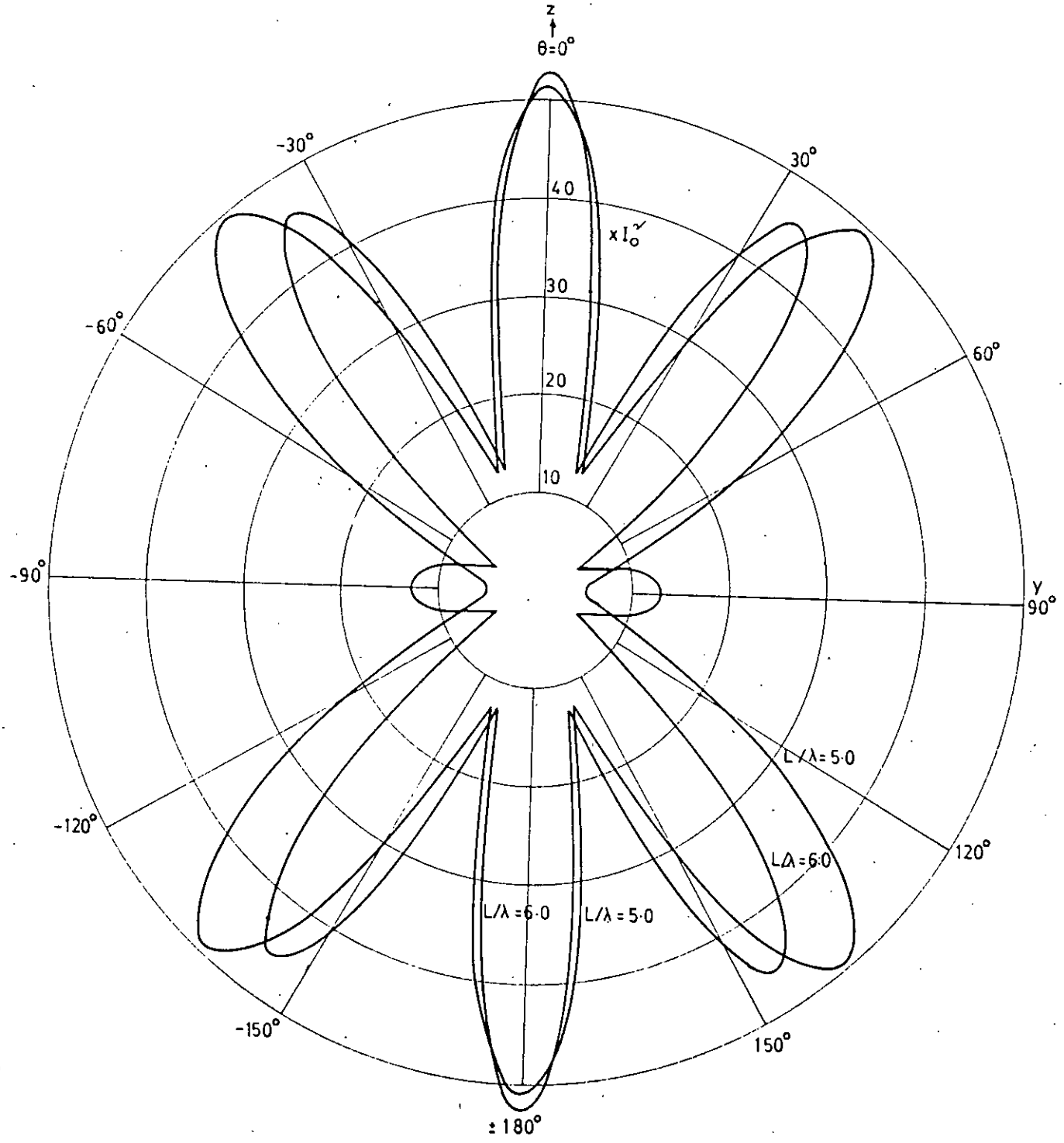

Fig. 4·7 Radiation pattern of a large circular loop antenna in xz-plane for $L/\lambda = 5.0$ and 6.0

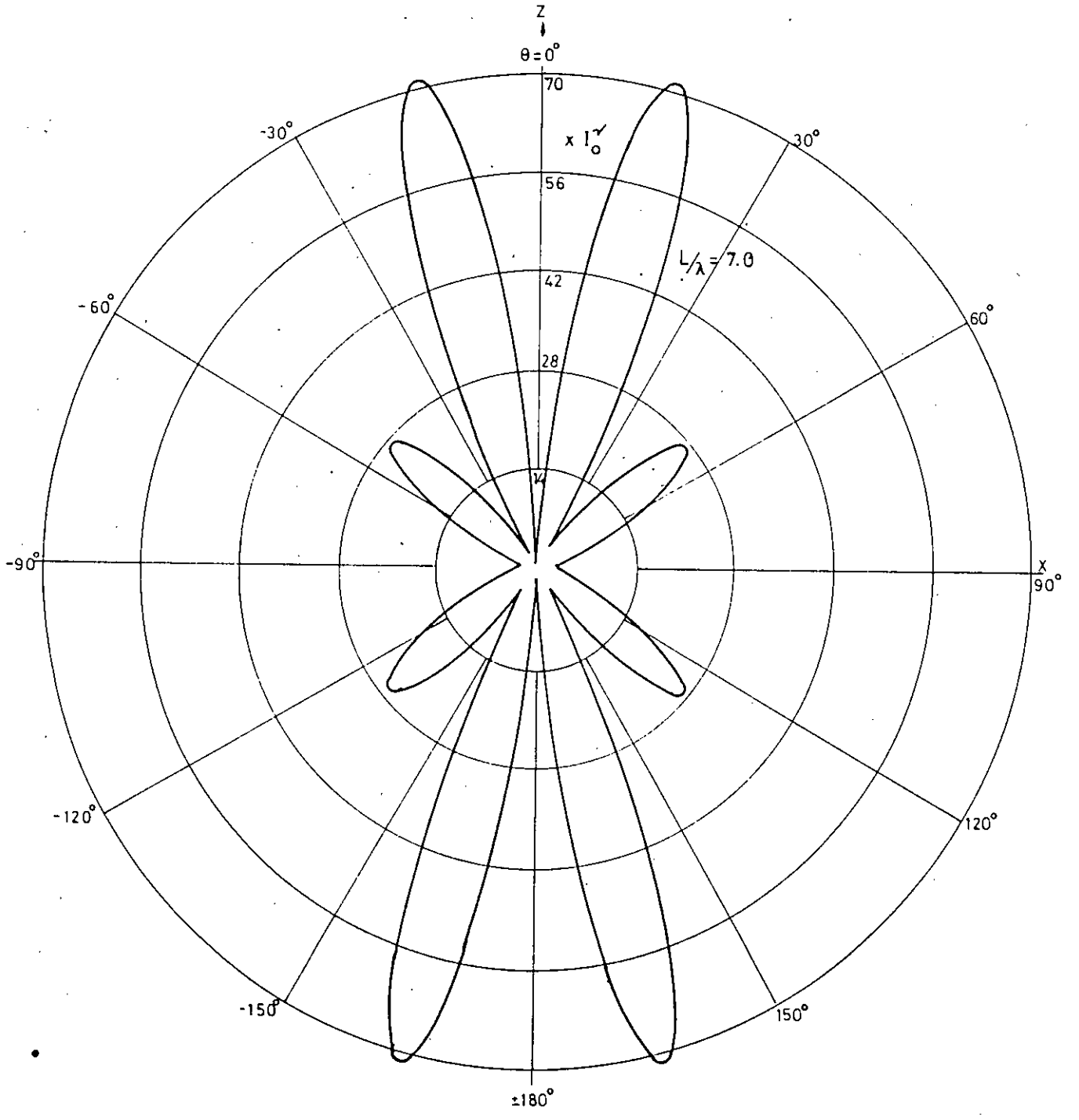

FIG. 4.8 Radiation pattern of a circular loop antenna in xz-plane for $L/\lambda = 7.0$

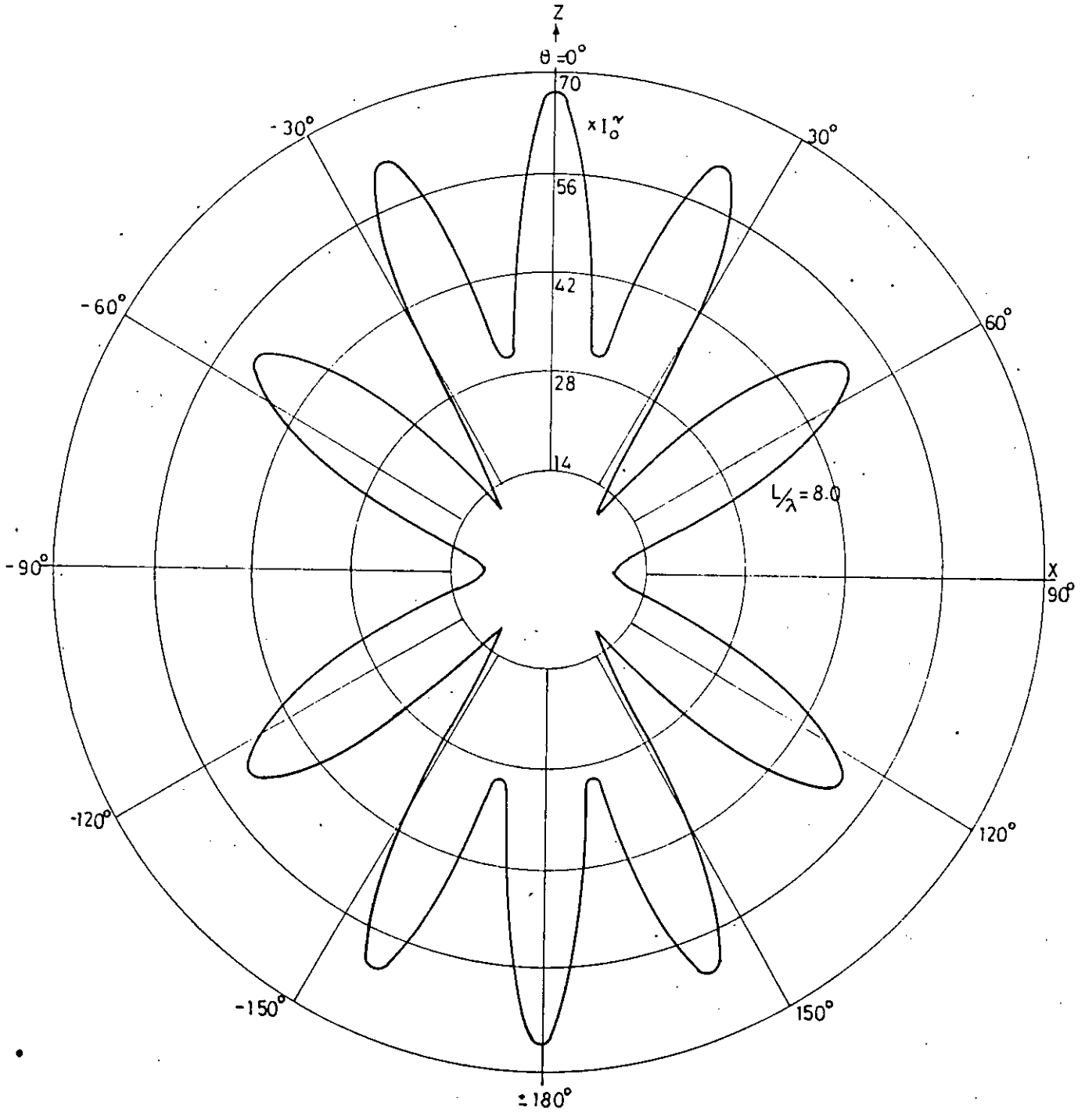

FIG. 4.9 Radiation pattern of a circular loop antenna in xz-plane for $L/\lambda = 8.0$

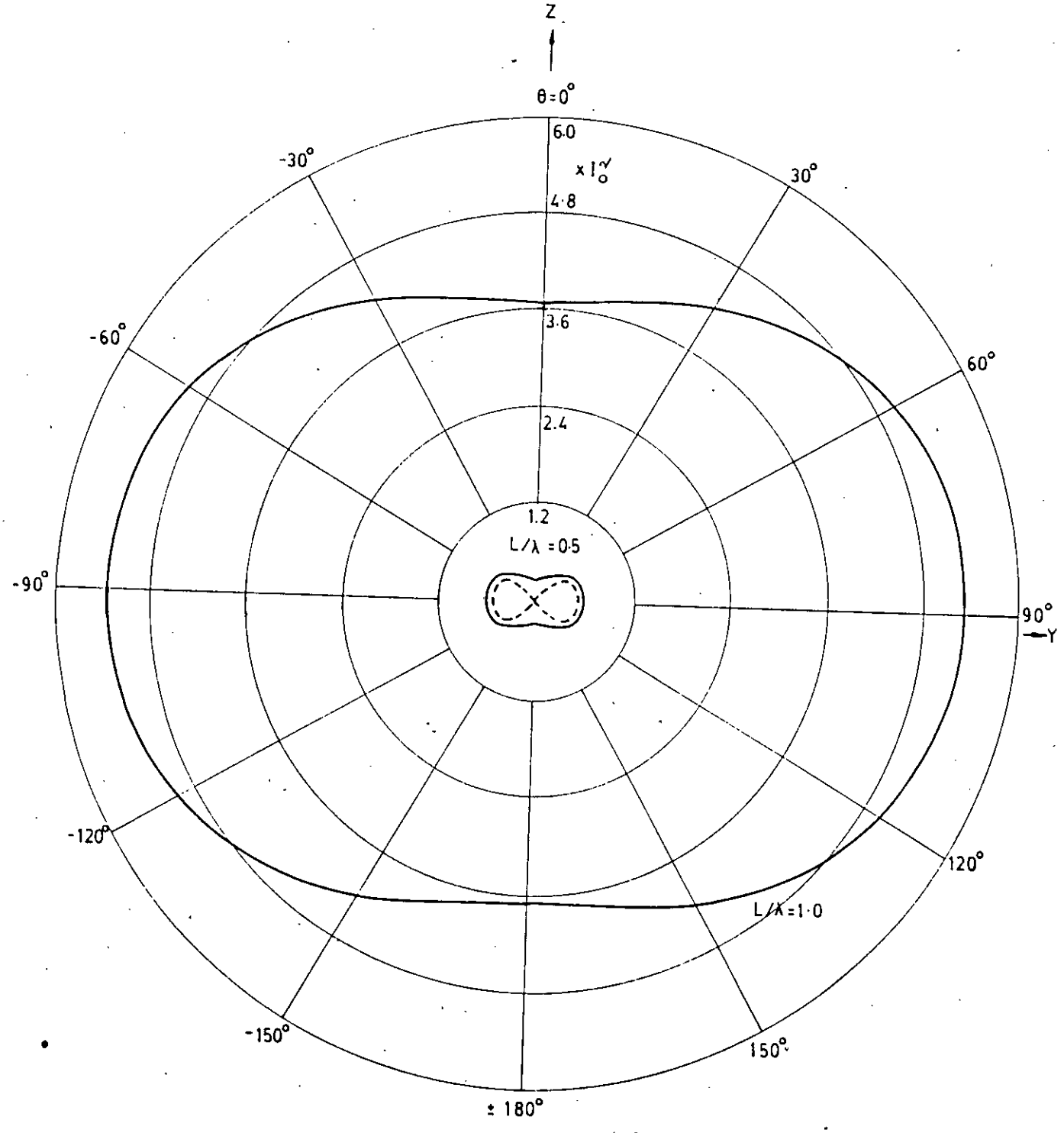

Fig. 4.10 Radiation pattern of a large circular loop antenna in yz - plane for L/λ =0.5 and 1.0

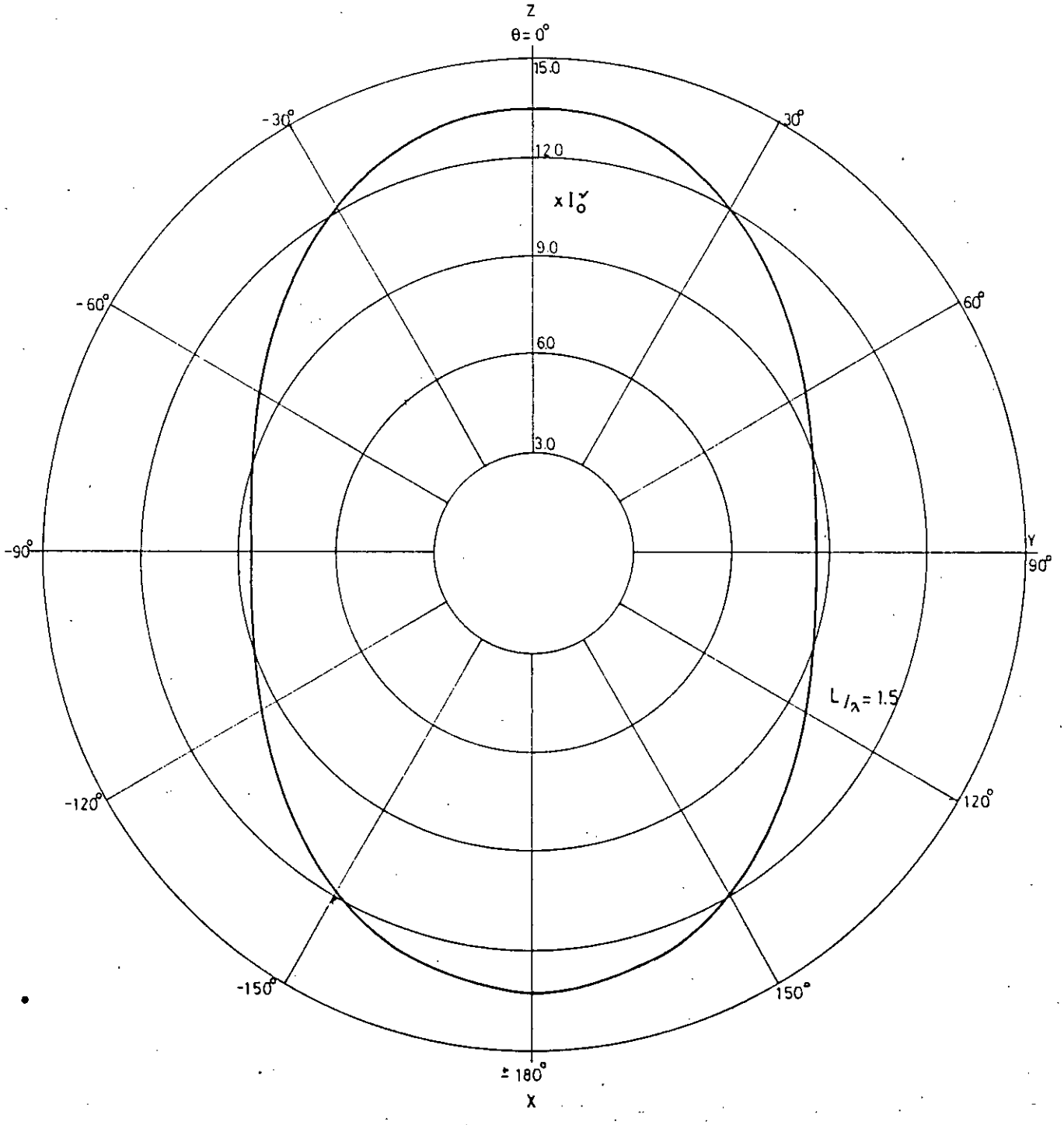

FIG. 4.11 Radiation pattern of a large circular loop antenna in YZ-plane for $L/\lambda = 1.5$

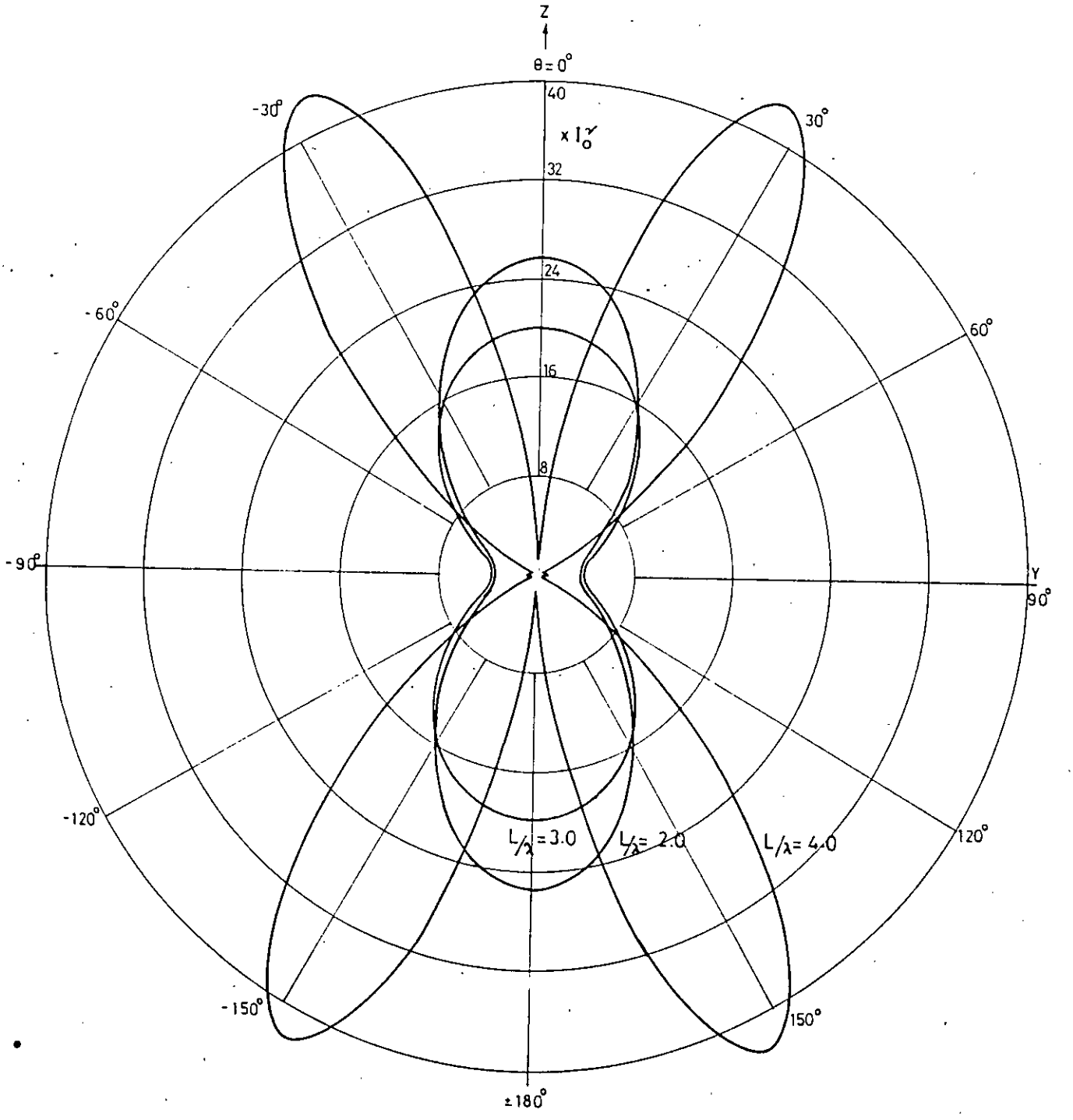

FIG. 4.12 Radiation pattern of a large circular loop antenna in yz-plane for L/λ = 2.0 3.0 and 4.0

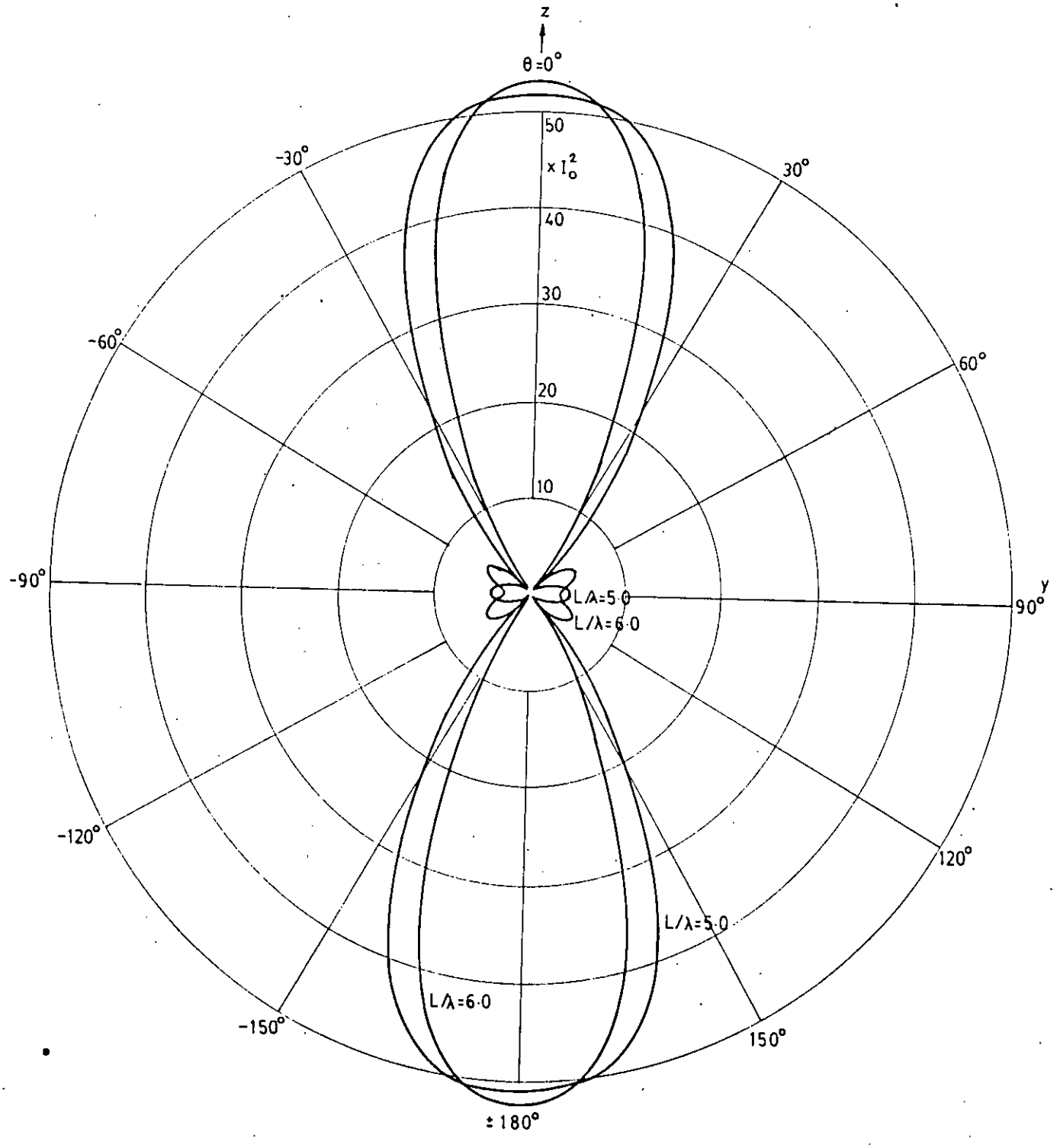

FIG. 4.13 Radiation pattern of a large circular loop antenna in yz-plane for $L/\lambda = 5.0$ and 6.0

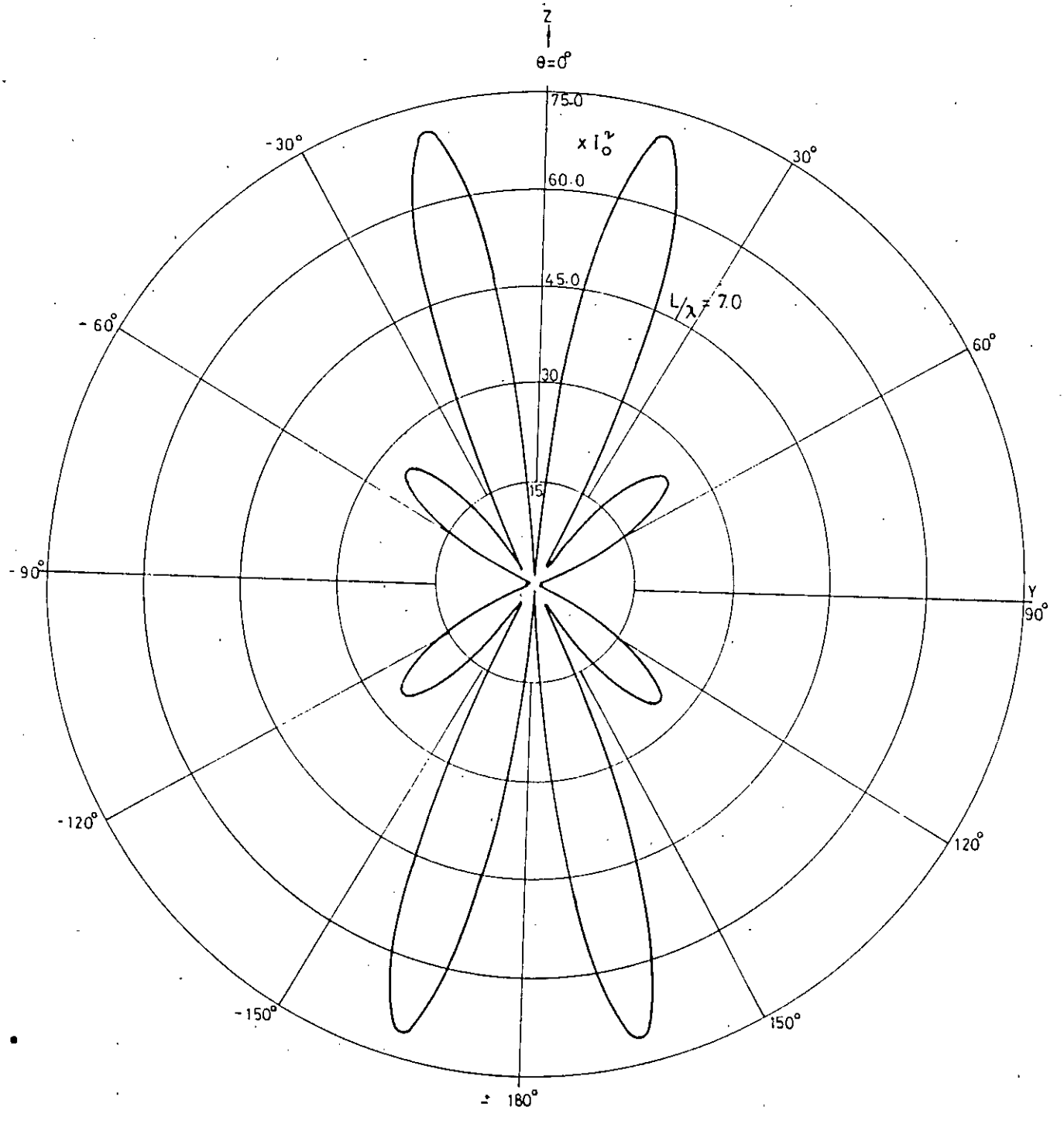

FIG. 4.14 Radiation pattern of a large circular loop antenna in yz-plane for $L/\lambda = 7.0$

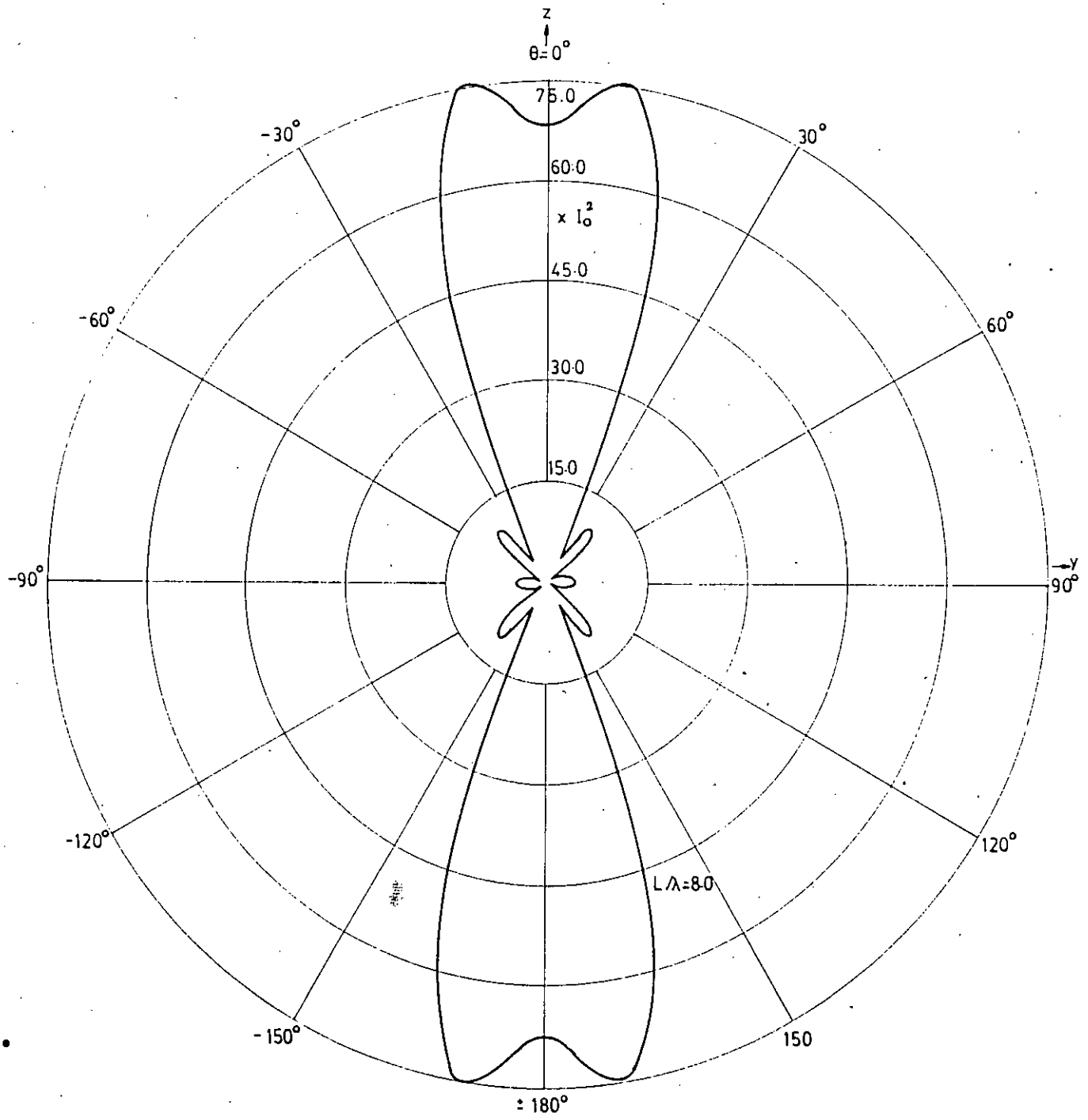

Fig. 4.15 Radiation pattern of a large circular loop antenna in yz-plane for $L/\lambda = 8.0$

In the xz- plane the radiation pattern is in the form of a dum bell for upto $L/\lambda = 1.0$ having maximum radiation intensity along the x-axis and minimum radiation intensity along the axis of the loop. The radiation pattern is elliptical for $L/\lambda = 1.5$ (Fig. 4.5). Beyond this limit the radiation pattern is splitted into several lobes exhibiting narrower maim beams with increasing number of side lobes (Figs. 4.6 - 9). Almost similar behaviour can be observed in the yz-plane pattern (Figs. 4.10 - 15). For $L/\lambda = 5.0$, 6.0 and 8.0, the sidelobes are in reduced forms in the yz-plane (Figs. 4.13-15) compared with those appearing in the xz-plane (Figs. 4.7-9).

4.4 Discussion

In the above the radiation pattern of a circular loop antenna has been calculated evaluating the far field. Schelkunoff's systemization of Poynting calculation has been adopted to obtain the far field radiation vector. The electric field in the radiation vector is found to consist of both θ -and ϕ -polarizations producing a cross-polarized field. However, along the plane of the loop only the ϕ -polarization exists. Numerical radiation pattern in the yx, yz and xz-planes are shown in Figs. 4.1-15. A circular loop antenna can be considered as an array of small electric dipoles. For small loop sizes the array produces maximum beam direction along the plane of the array and for larger loop-sizes the maximum beam direction is either along the axis of the loop or at some other direction.

CHAPTER - 5

RADIATED POWER AND RADIATION RESISTANCE OF A LARGE CIRCULAR LOOP ANTENNA

5.1 Introduction

In the previous chapter we calculated the radiation intensity of a circular loop antenna. In the present chapter we shall first calculate the radiated power integrating the radiation intensity in the entire spherical domain and then find the radiation resistance of a circular loop antenna. The results will be discussed by plotting the numerical data.

5.2 The Radiated Power

The radiated power of a circular loop antenna may be found by integrating the radiation intensity over a large spherical surface surrounding the antenna. From eqn. (A-13) of the appendix we have the time-average radiated power given by

$$W = \int_0^{2\pi} d\phi \int_0^{\pi} d\theta \; K(\theta, \phi) \sin\theta \tag{5.1}$$

Substituting the value of K (θ, ϕ) from eqn. (4.19) into eqn. (5.1), we have

$$W = 15\pi \tilde{L_o}^2 (K_o a)^2 \int_0^{2\pi} d\phi \int_0^{\pi} d\theta \; |S(\theta, \phi)|^2 \sin\theta \tag{5.2}$$

Let us designate the ϕ-integral as

$$Q(\theta) = \int_0^{2\pi} |S(\theta, \phi)|^2 d\phi \tag{5.3}$$

where S (θ, ϕ) is given by eqn. (4.20) - (4.25)

Now applying the identity,

$$\int_0^{2\pi} \cos p\alpha \cos q\alpha \, d\alpha = \begin{cases} 0 & , \text{if } p \neq q \\ \pi & , \text{if } p = q \end{cases}$$

we get

$$Q(\theta) = 2\pi \Psi(\theta) \tag{5.4}$$

where

$$\psi(\theta) = J_0^2(K_0a)\,J_1^2(K_0a\sin\theta) + \frac{2}{\pi^2}\sum_{\nu\,odd}\frac{J_\nu^2(K_0a)}{\nu^2}\left[\left\{J_{\nu-1}(K_0a\sin\theta) - J_{\nu+1}(K_0a\sin\theta)\right\}^2 + \cos^2\theta\left\{J_{\nu-1}(K_0a\sin\theta) + J_{\nu+1}(K_0a\sin\theta)\right\}^2\right] \quad (5.5)$$

Substituting the value of $Q(\theta)$ from (5.4) into (5.2) we have

$$W = 30\,\pi^2 I_0^2 (K_0a)^2 \int_0^{\pi} \psi(\theta)\sin\theta\, d\theta \quad (5.6)$$

The integral is performed numerically by the Gauss-Legendre method [27]. The radiated power as a function of Loop-size L/λ is plotted in Fig. 5.1. Anti-resonances occur at $J_0(K_0a) = 0$. i.e., at L/λ = 2.45, 5.6, 8.7. and resonances occur at L/λ = 1.55, 3.45, 4.6, 6.75, 10.0. Among them the points at L/λ = 3.45, 6.75, 10.0 correspond to the maxima of $J_2(K_0a)$ and the points L/λ = 1.55, 4.6 correspond to the intersections of $J_0(K_0a)$ and $J_1(K_0a)$.

5.3 The Radiation Resistance

The radiation resistance of an antenna system is of considerable importance to the the system engineer since it directly affects the efficiency of energy transfer from the antenna. The radiation resistance of an antenna is defined as the equivalent resistance that would dissipate an amount of power equal to total radiated power when the current through the resistance is equal to the current at the antenna input terminals. The radiation resistance of a circular loop antenna may be found by evaluating the total radiated power passing through a large spherical surface surrounding

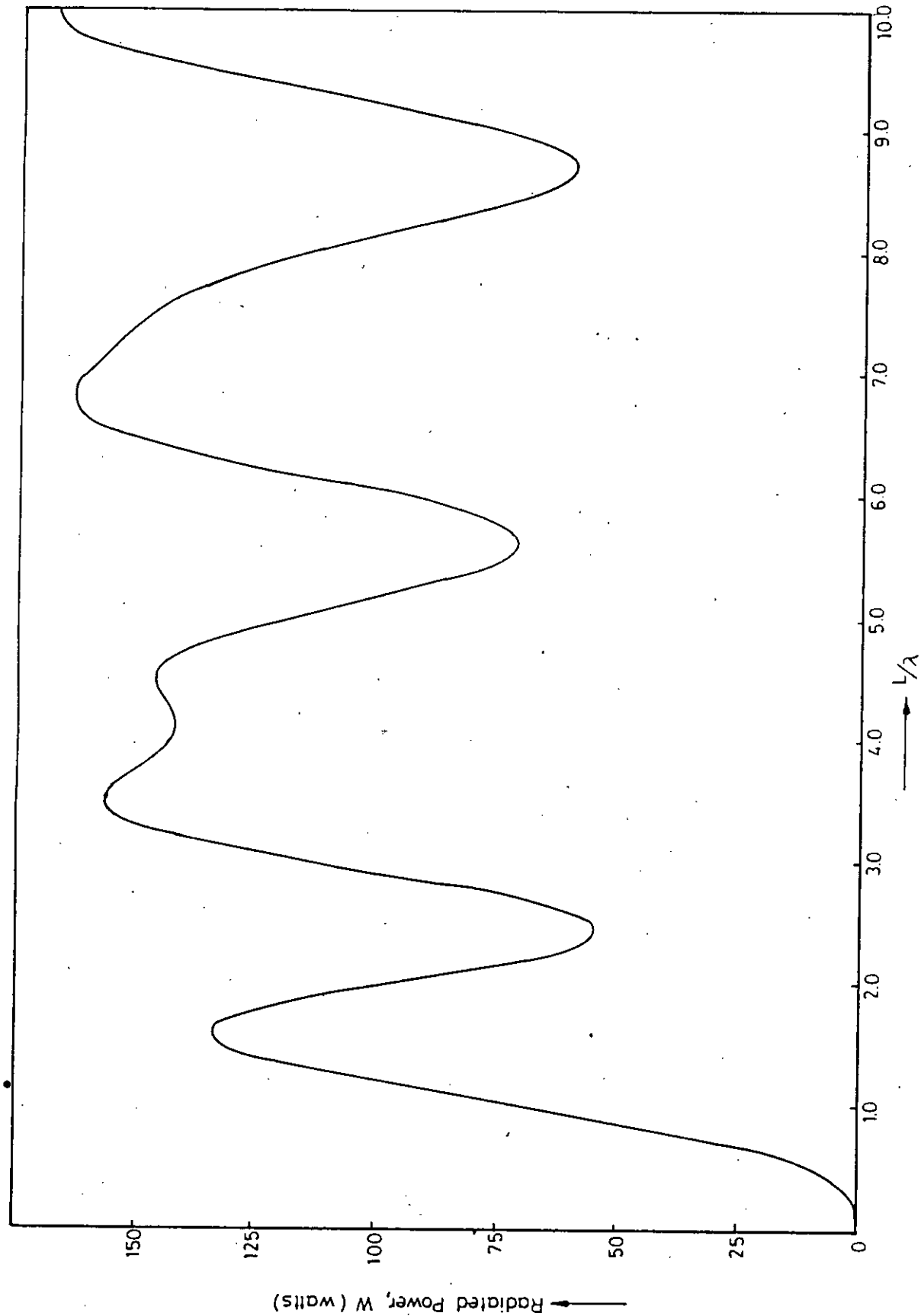

FIG. 5.1 The time average radiated power of a circular loop antenna as a function of loop size, L/λ

the antenna and dividing the radiated power by the square of the current at the feed point. Thus the radiation resistance becomes [30],

$$R_r = \frac{2W}{I^2(0)} \tag{5.7}$$

Now, substituting the values of W from eqn. (5.6) and I (0) from eqn. (3.11) into eqn. (5.7) we get

$$R_r = \frac{60\pi^2(k_0a)^2\int_0^{\pi}\psi(\theta)\sin\theta\, d\theta}{M^2} \tag{5.8}$$

where

$$M = J_0(k_0a) + 4/\pi \sum_{\nu\ odd} \frac{1}{\nu}\cdot(-1)^{(\nu-1)/2}\cdot J_\nu(k_0a) \tag{5.9}$$

The radiation resistance calculated by eqn. (5.8) is plotted in Fig. 5.2 (Solid lines) as a function loop-sizes.

It may be of interest to see the effect of non-Uniformity due to harmonics in current distribution of a circular loop antenna. Hence calculation of radiation resistance has been performed assuming a uniform current distribution just retaining the first term in eqn. (5.6) and (5.9) and plotted in fig. 5.2. Again if the first two terms are retained, the result approaches the exact value as shown in Fig. 5.2.

5.4 Discussion

In the above the radiated power and radiation resistance of a circular loop antenna have been calculated for different loop-sizes. The resonances are found to occur at L/λ =1.55, 3.45, 4.6, 6.75, 10.0 and the antiresonances at L/λ =2.45, 5.6, 8.7. Numerical plots of radiated power and radiation resistance as a function of loop-size are illustrated in Figs. 5.1 and 5.2. Loops having sizes upto L/λ =0.5 can be treated as small loops supporting approximately uniform current distribution. With a two-term approximation of the current distribution the radiation resistance approaches the exact value.

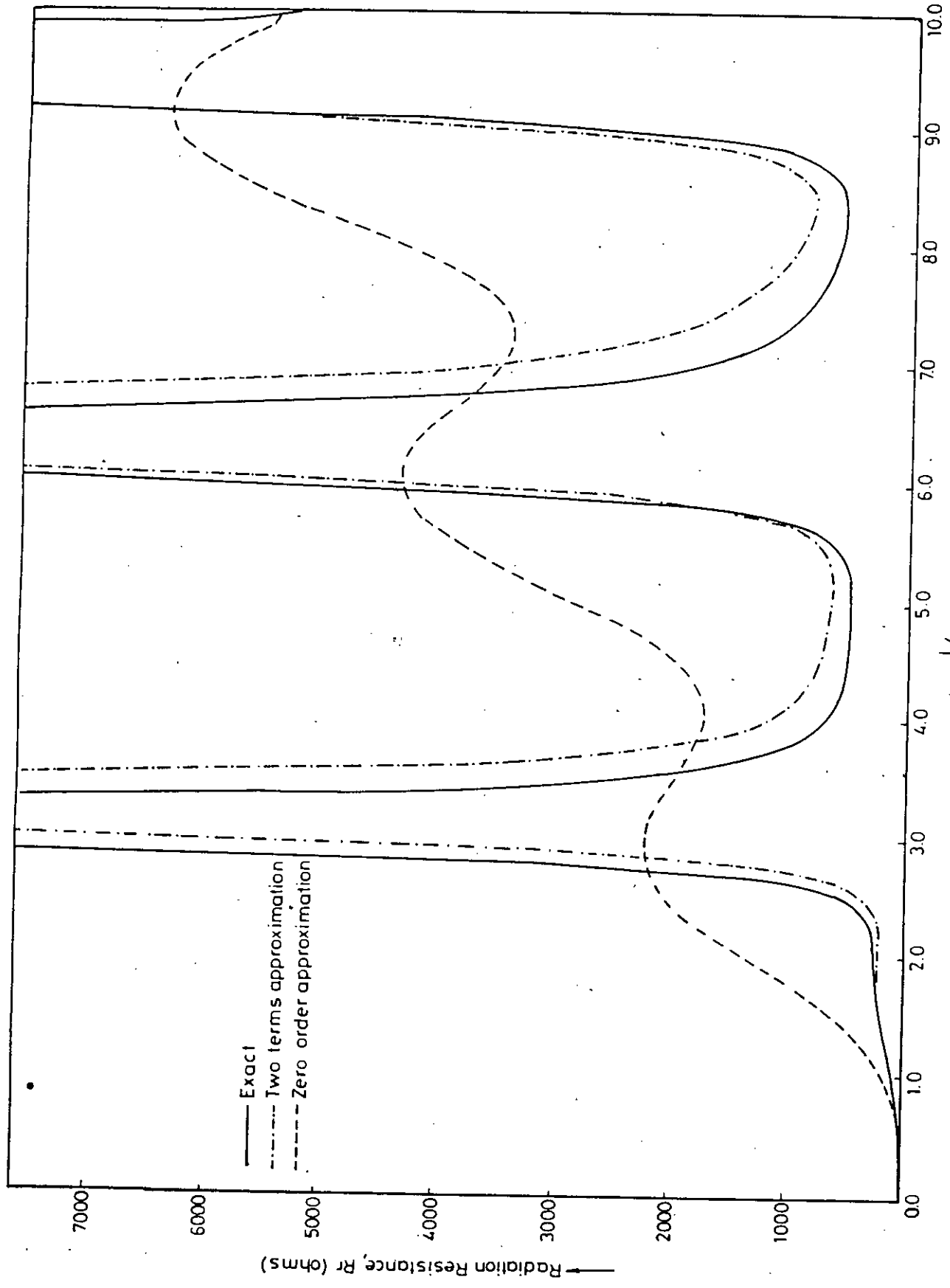

FIG. 5.2 Radiation resistance of a circular loop antenna as a function loop-size, L/λ

CHAPTER - 6

DIRECTIVE GAIN OF A LARGE CIRCULAR LOOP ANTENNA

6.1 Introduction

Using the radiation intensity and the radiated power calculated in the previous chapters we now proceed to evaluate the directive gain of a circular loop antenna. The present chapter deals with this important property of the antenna by illustrating numerical results for different loopsizes.

6.2 Directivity of the Loop Antenna

The directivity of an antenna is a measure of the directional properties or relative concentration of radiated power in different directions. Usually the directivity is specified with reference to an isotropic radiator, a hypothetical lossless antenna which radiates uuniformly in all directions. If an antenna radiates a total power W, the power density per unit solid angle would be $W/4\pi$ if the antenna radiates isotropically. The directivity of an antenna in a given direction (θ, ϕ) is given by $D(\theta, \phi)$ [31],

where

$$D(\theta, \phi) = \frac{4\pi R^2 P_R}{W} \tag{6.1}$$

and gives the power density in that direction relative to that which an isotropic radiator would produce.

The maximum directivity of an antenna occurs in the direction of the main-beam maximum and is a measure of the ability of an antenna to concentrate the radiated power in a given direction. A rough estimate of the maximum directivity of an antenna producing a main-beam with narrow beam-width can be obtained by dividing 4π by the solid angle subtended by the main-beam between half-power points. It is apparent that a highly directivity antenna will have a very sharp (narrow beam width) main-beam.

To obtain the directivity of a circular loop antenna, substitution of the value of P_R from eqn. (A-10) of the appendix with N_θ = 0 into eqn. (6.1) gives

$$D(\theta, \phi) = \frac{4\pi K(\theta, \phi)}{W} \tag{6.2}$$

Now, substituting the value K (θ, ϕ) from eqn (4.19) and W from eqn (5.6) into eqn (6.2), we have

$$D(\theta, \phi) = 2 \frac{|S(\theta, \phi)|^2}{\int_0^\pi \psi(\theta) \sin\theta \, d\theta} \tag{6.3}$$

where S (θ, ϕ) and ψ (θ))follow from (4.20) and (5.5) Plots of directional pattern D (θ, ϕ) are shown in Figs. 6.1 - 6.3. The directional pattern is very sensitive to the change of the loop-size.

6.3 Gain of the Loop Antenna

The gain of an antenna is a basic property which is frequently used as a figure of merit. Gain is closely associated with directivity which in tern is dependent upon the radiation pattern of an antenna. The gain G(θ, ϕ) of an antenna differs from the directivity by a factor which takes into account the efficiency of the antenna. Since all antennas have some dissipative loss, not all of the input power is radiated. The gain of an antenna is defined by [31],

$$G(\theta, \phi) = 4\pi \frac{\text{Power density per unit solid angle in the direction } (\theta, \phi)}{\text{total input power to antenna}} \tag{6.4}$$

and is less than the directivity by a factor equal to the efficiency. The antenna gain function G (θ, ϕ)in obviously a more useful parameter than the directivity in describing the overall performance of a practical antenna.

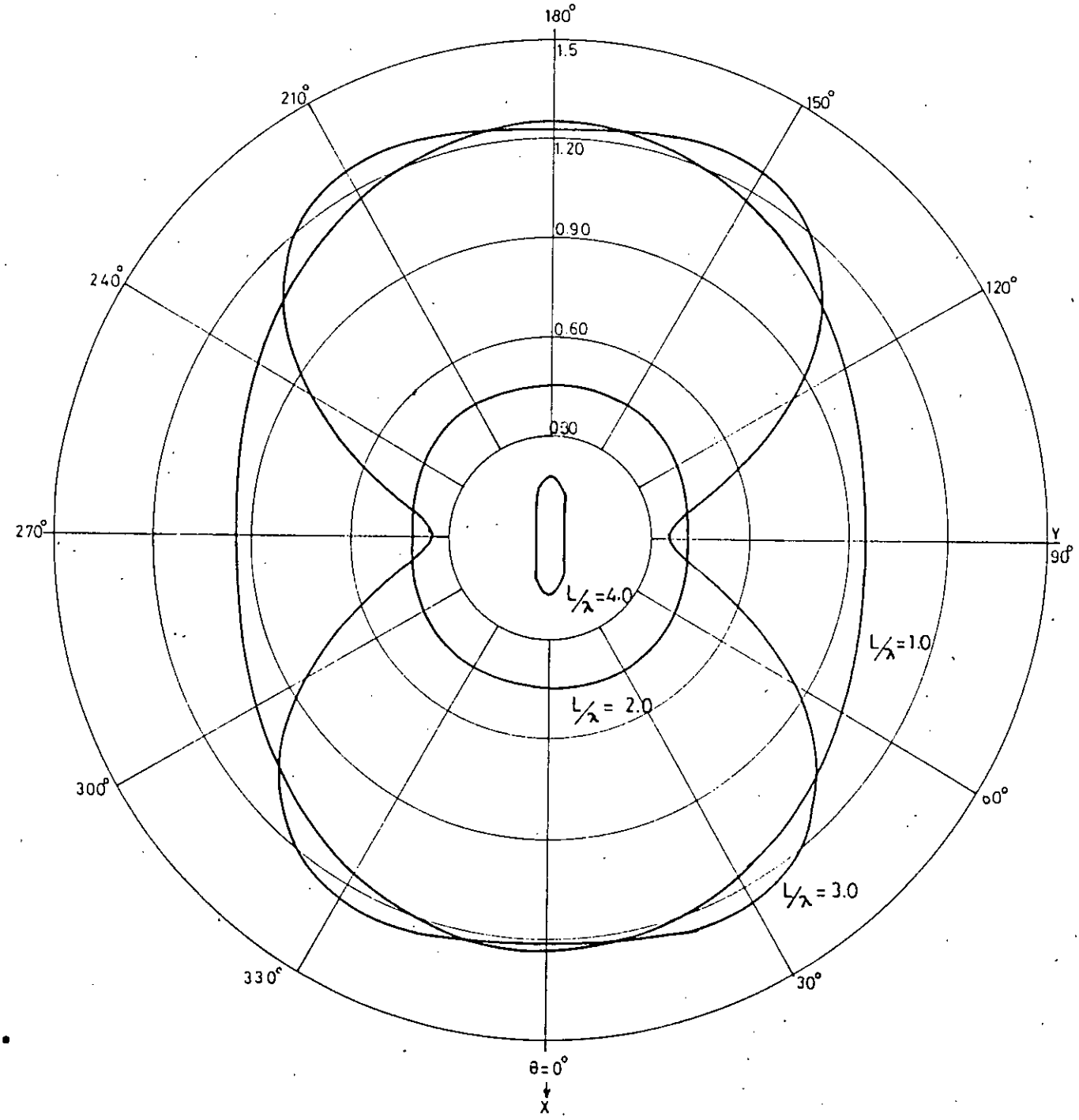

FIG. 6.1 Directivity pattern of a circular loop antenna in yx-plane for L/λ = 1.0 2.0 3.0 and 4.0

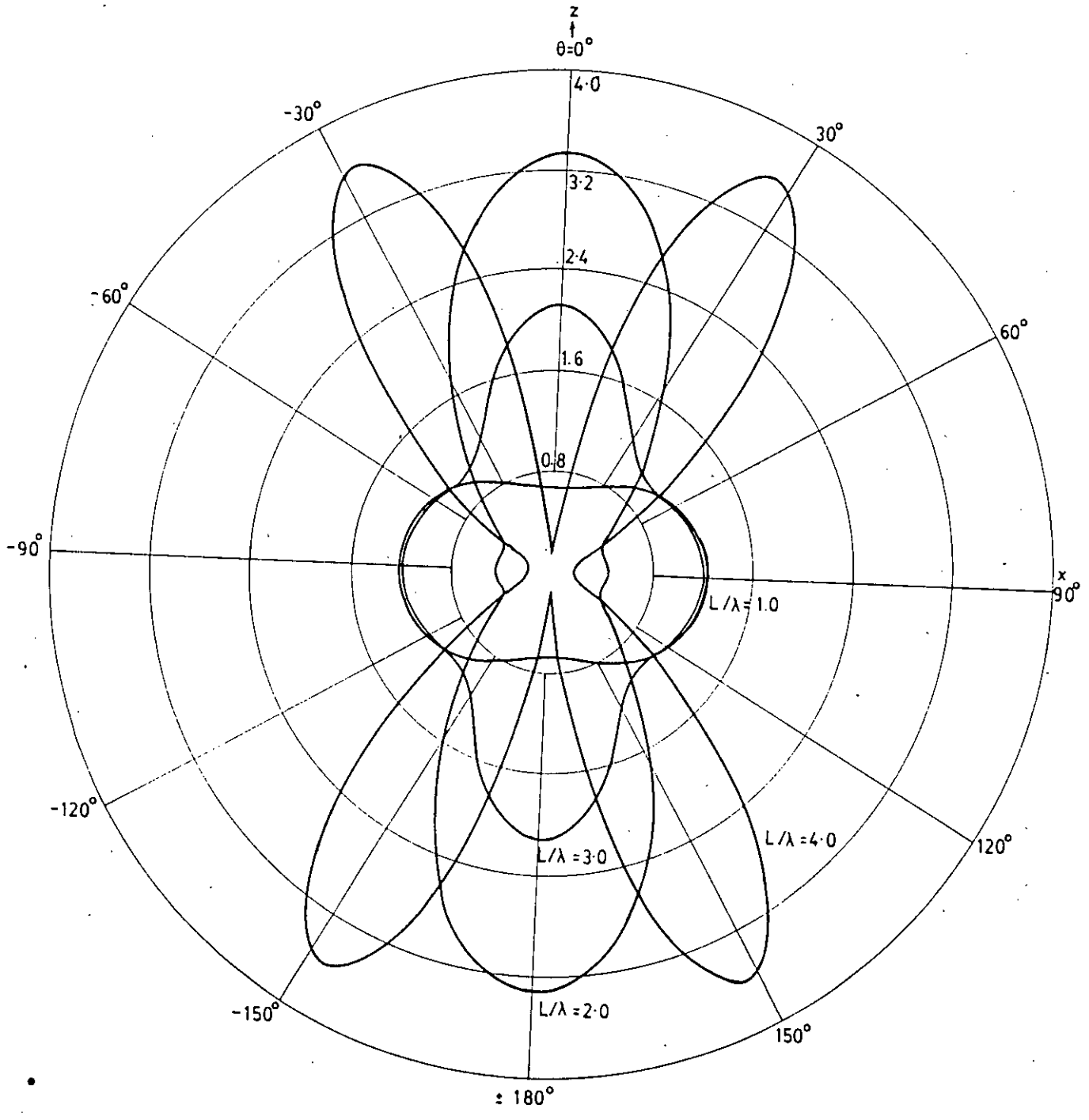

Fig. 6.2 Directively pattern of a circular loop antenna in xz-plane for L/λ = 1.0, 2.0, 3.0 and 4.0

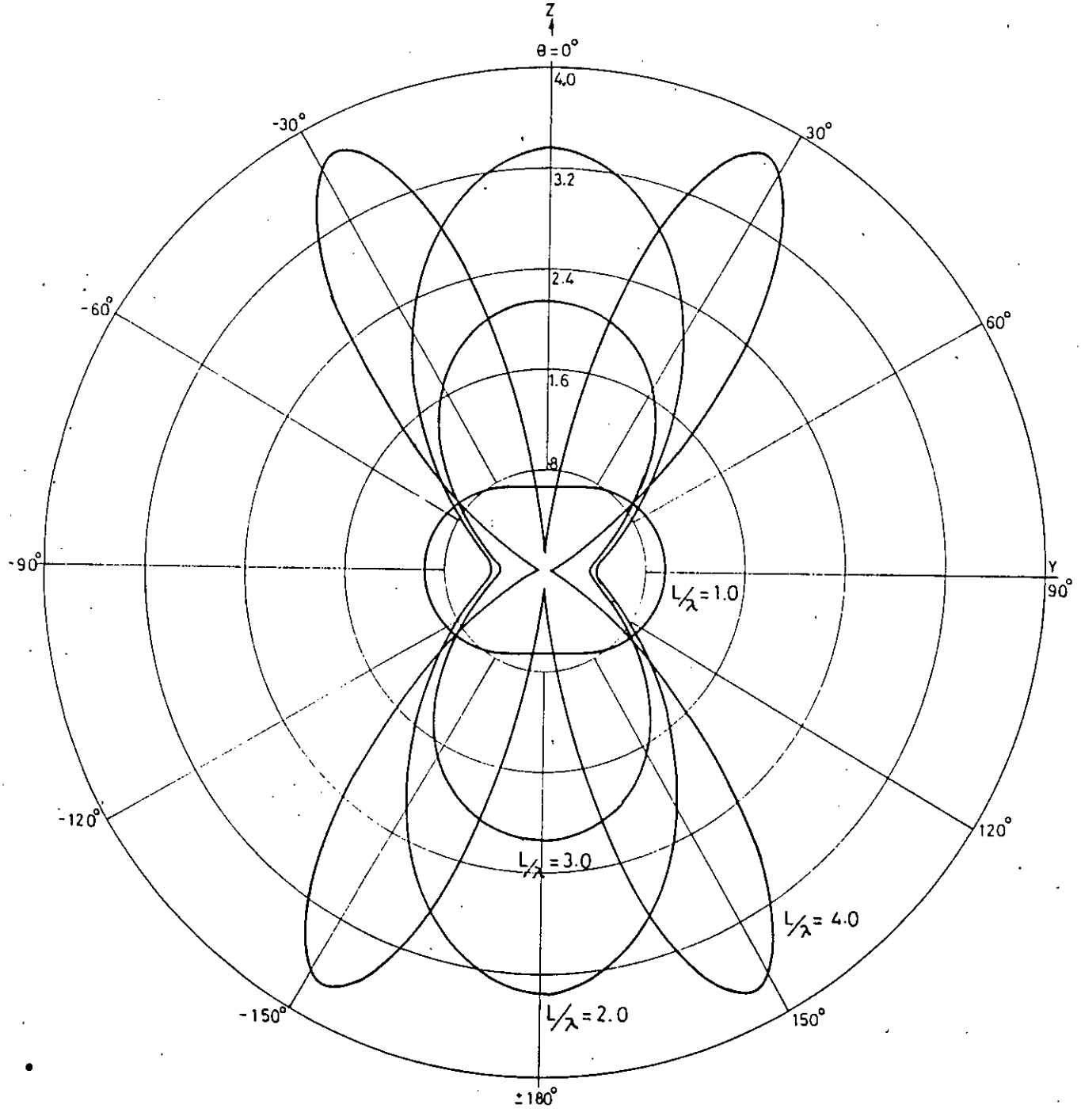

FIG. 6.3 Directivity pattern of a circular loop antenna in yz-plane for L/λ = 1.0 2.0 3.0 and 4.0

If η be the efficiency of an antenna the gain from eqn. (6.4)becomes,

$$G(\theta, \phi) = \eta\, D(\theta, \phi)$$

Assuming $\eta = 1$, $G(\theta, \phi)$ is plotted in Fig. 6.4 as a function of loop-size L/λ for x, y and z directions.

It can be observed that for loop-sizes upto $L/\lambda = 1.3$, the gain is maximum in the x-direction, i.e, along the feed point and minimum in Z-direction. For loop-sizes exceeding the limit $L/\lambda = 1.3$, gain is always maximum in Z-direction, i.e., along the axis of the loop and minimum in y-direction. Loop-sizes upto $L/\lambda = 1.3$ exhibit endfire property. The circular loop exhibits broadside propety in the ranges $1.4 < L/\lambda < 3.2$, $4.4 < L/\lambda < 6.6$, $7.4 < L/\lambda < 9.8$. Gain is very poor for ranges $3.2 < L/\lambda < 4.4$, $6.6 < L/\lambda < 7.4$. In these cases the directivity pattern is splitted into several lobes in different directions so that radiation is minimum in x, y and z-directions.

6.4 Discussion

In the above the directional pattern and gain of a circular loop antenna have been evaluated for different loop-sizes. Circular loop antennas exhibit end fire property for upto $L/\lambda = 1.3$ Loop-sizes exceeding this limit exhibit broad-side property in the ranges $1.4 < L/\lambda < 3.2$, $4.4 < L/\lambda < 6.6$, $7.4 < L/\lambda < 9.8$. Moreover, broadband and supergain properties can be observed for a very large circular loop antenna .

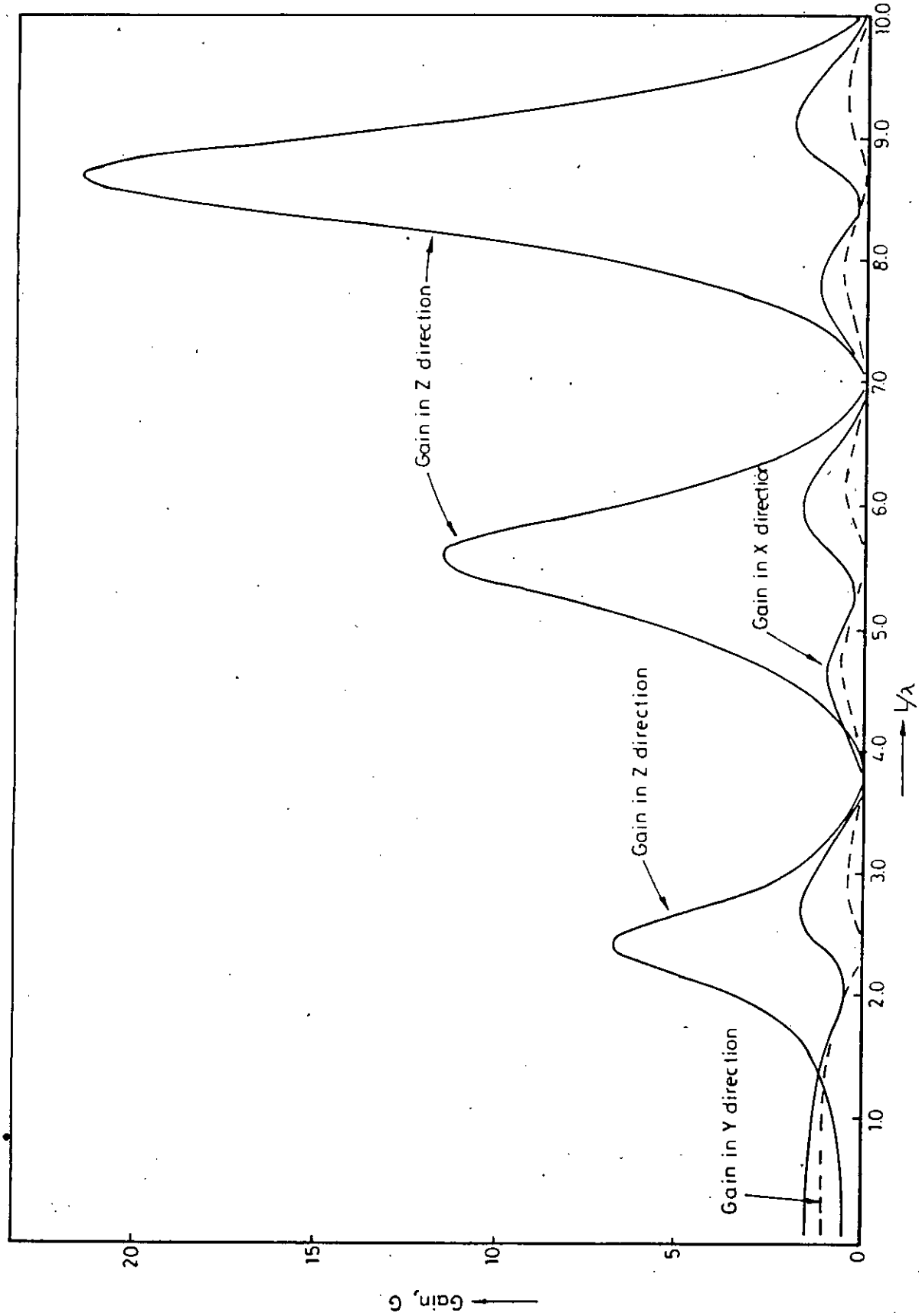

FIG. 6.4 Gain of a circular loop antenna as a function of loop size, L/λ

CHAPTER - 7

GENERAL DISCUSSION AND CONCLUSIONS

In the above an investigation has been carried out for determining the radiation characteristics of a large circular loop antenna. For this purpose the analysis has been carried out in a straight-forward manner from Maxwell's equations.

The field distribution in a region enclosed by a circular loop antenna has been obtained by assuming that the magnetic lines of forces are perpendicular to the plane of the loop and the electric field is polarized with the radial and circumferential components in the plane of the circular loop. The gap at the feed point is assumed to be very small so that there is no radial component of the electric field in the gap. The field solution is obtained in infinite series involving products of higher order Bessel and cosine harmonics.

The current distribution in the circular conducting loop has been derived by using the field solution in the loop region. The ϕ -dependence of the current is representable in a Fourier series of which each term is reduced by a Bessel's function of corresponding order accounting for the effects of loop-size on the resulting current distribution. The infinite series converges to a finite value rapidly after a few terms. For accuracy of calculations we considered upto the nineth harmonic. Numerical plots of the current distribution for different loop-sizes are illustrated in Figs. 3.2 and 3.3. Harmonic distortions in the current distribution increases with the increase of the loop-length with respect to a free-space wavelength. In general the speed of the wave is greatly reduced on the circular path of the loop.

The radiation intensity has been evaluated using the far field radiation vector. Schelkunoff's systemization of Poynting calculations have been applied to obtain the far field radiation vector. Cross-Polarized field can be observed in all planes other than the plane in which the loop lies. Numerical results have been plotted in Figs. 4.1-4.15 to obtain the radiation pattern of a circular loop

antenna. A circular loop can be treated as an array of small electric dipoles. For small loop-sizes the array produces maximum beam direction along the plane of the array and for larger loop-sizes the maximum beam direction is either along the axis of the loop or splitted into serveral beams at different directions.

The radiated power has been calculated by integrating the far field radiation intensity in the spherical domain. Numerical plot of the radiated power has been shown in Fig. 5.1. The peaks in the power curve indicate the resonances, and the antiresonances correspond to minimum radiated power. The resonances are found to occur at L/λ =1.55, 3.45, 4.6, 6.77, 10.0 and the antiresonances at L/λ = 2.45, 5.6, 8.7. The radiation resistance has been plotted in Fig. 5.2. as a function of loop-size. In order to assess the harmonic effects of the current distribution the radiation resistance has been calculated assuming a uniform current and the first two-term approximation of the current, and plotted in Fig. 5.2. It can be observed that the radiation resistance with the first two-term approximation approaches the exact value. The zero-order approximation is valid for small circular loops. Loops having circumferences upto a half-wavelength can be treated as small loops.

The directivity of a circular loop has been evaluated using the radiation intensity and the radiated power. Plots of the numerical results have been shown in Figs. 6.1-6.3. The directional pattern is highly sensitive to the operating frequency. The directional gain of the loop antenna has been calculated considering it as a lossless antenna . Numerical plots of endfire and broadside gain of the antenna are plotted in fig. 6.4 as a function of loop-size . The circular loop exhibits endfire property for upto L/λ =1.3 and boradside property in the bands $1.4 < L/\lambda < 3.2$, $4.4 < L/\lambda < 6.6$, $7.4 < L/\lambda < 9.8$. Beam-splitting in different directions is possible by changing the operating frequency of a large circular loop antenna. Also super gain broadband property can be obtained for very large loop antennas.

In conclusion it can be said that the theoretical investigations performed above should be confirmed by experiments. Also, the impedance of the antenna including the reactive part can be a subject of study in further research on a large circular loop antenna. As our analysis is limited to a thin-wire circular loop antenna, the effect of wire-thickness on the properties of the antenna may also be a subject of further investigation.

APPENDICES

Appendix-A

Systemization of Poynting Calculations

In using the Poynting integration for calculation of radiated power and radiation intensity many of the same mathematical approximation are introduced. A shortcut method has been developed by Schelkunoff [26].

In the Poynting method field is usually calculated at a great distance from the radiator. The following assumptions are carried out.

1. Differences in radius vector to different points of the radiator are absolutely unimportant in their effect on magnitude of the Green's function.

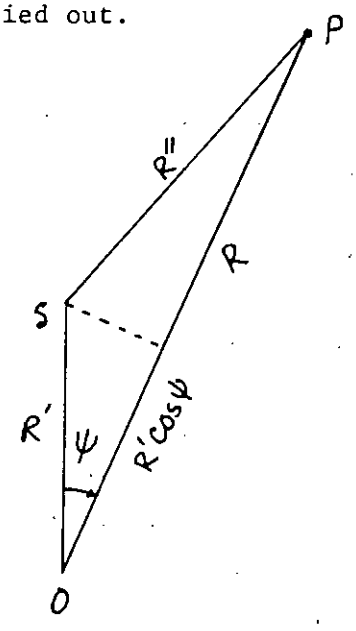

Fig. A-1 Co-ordinates of general current element at s and distant point P with respect to origin O.

2. Differences in direction of the radius vector to different points on the radiator are negligible.

3. All field components decreasing with distance faster than $1/R$ are completely negligible compared with those decreasing as $1/R$.

4 Differences in radius vector to different points on the radiator for purposes of finding phase differences are taken as $R' \cos\psi$ of Fig. A-1, where R' is the radial distance of the radiating element from the origin, ψ the angle

between R' and R, and R is the radial distance of the point at which the field is to be calculated.

Consider the vector potential at point P distant R from the origion of a radiating system made up of current elements arranged in any manner whatsoever in the element δ shown at radius R' from the origin,

$$\bar{A} = \mu_0 \int_{v'} \frac{\bar{i}_s \, e^{j\omega[t-(R''/v)]}}{4\pi R''} \, dv' \qquad \text{(A-1)}$$

where $\bar{i}_s$ is the current density in Amp/m^2, $v = \frac{1}{\sqrt{\mu_0 \epsilon_0}}$ is the speed of the electromagnetic wave, t is the instant of time, ω is the angular operating frequency and v' is the volume occupied by the source.

From the assumptions 1-3 and $e^{j\omega t}$ understood,

$$\bar{A} = \mu_0 \frac{e^{-jK_0 R}}{4\pi R} \int_{v'} \bar{i}_s \, e^{jK_0 R' \cos\psi} \, dv' \qquad \text{(A-1)}$$

The function of R is now completely outside the integral; the integral itself is only a function of the antenna configuration and the current distribution. Let us define the vector,

$$\bar{N} = \int_{v'} \bar{i}_s \, e^{jK_0 R' \cos\psi} \, dv' \qquad \text{(A-3)}$$

Then $$\bar{A} = \mu_0 \frac{e^{-jK_0 R}}{4\pi R} \bar{N} \qquad \text{(A-4)}$$

In the most general case, $\bar{A}$ and hence $\bar{N}$ may have components in any direction. In spherical coordinates employing the unit vectors, $\bar{a}_\theta$, $\bar{a}_\phi$ and we have

$$\bar{A} = \mu_0 \frac{e^{-jK_0 R}}{4\pi R} \left(\bar{a}_R N_R + \bar{a}_\theta N_\theta + \bar{a}_\phi N_\phi \right) \qquad \text{(A-5)}$$

A study of the equation $\bar{B} = \nabla \times \bar{A}$ in spherical coordinates shows that the only components which do not decrease faster than $1/R$ are

$$H_\theta = -\frac{1}{\mu_0 R}\frac{\partial}{\partial R}(RA_\phi) = \frac{jK_0}{4\pi R} e^{-jK_0R} N_\phi \qquad \text{(A-6)}$$

$$H_\phi = \frac{1}{\mu_0 R}\frac{\partial}{\partial R}(RA_\theta) = -\frac{jK_0}{4\pi R} e^{-jK_0R} N_\theta \qquad \text{(A-7)}$$

An examination of

$$\bar{E} = -\frac{j\omega}{K_0^2}\nabla(\nabla\cdot\bar{A}) - j\omega\bar{A}$$

shows that the only components of $\bar{E}$ which do not decrease faster than $1/R$ are

$$E_\theta = -\frac{j\omega\mu_0}{4\pi R} e^{-jK_0R} N_\theta \qquad \text{(A-8)}$$

$$E_\phi = -\frac{j\omega\mu_0}{4\pi R} e^{-jK_0R} N_\phi \qquad \text{(A-9)}$$

The Poynting vector $\bar{P} = \bar{E} \times \bar{H}$ has a time-average value

$$P_R = \frac{1}{2} \times \frac{\eta}{2\lambda R} \times \frac{1}{2\lambda R}\left[|N_\theta|^2 + |N_\phi|^2\right] \qquad \text{(A-10)}$$

Total time average power radiated is given by

$$W = \int_0^{\pi}\int_0^{2\pi} P_R R^2 \sin\theta \, d\theta \, d\phi$$

$$W = \frac{\eta}{8\lambda^2}\int_0^{\pi}\int_0^{2\pi}\left[|N_\theta|^2 + |N_\phi|^2\right]\sin\theta \, d\theta \, d\phi \qquad \text{(A-11)}$$

The expression is independent of R.

The Poynting vector $\bar{P}$ gives the actual power density at any point. To obtain a quantity which does not depend on distance from the radiator we define K, the radiation intensity as the power radiated in a given direction per unit solid angle. This is the time-average $\bar{P}$ on a sphere of unit radius.

$$K = \frac{\eta}{8\lambda^2}\left[|N_\theta|^2 + |N_\phi|^2\right] \tag{A-12}$$

and

$$W = \int_0^{\pi}\int_0^{2\pi} K \sin\theta \, d\theta \, d\phi \tag{A-13}$$

A plot of K against direction may then define the radiation Pattern. It should be recognized that this is a power radiation pattern and not a field strength radiation pattern.

The angle ψ appearing in the expression of $\bar{N}$ can be found as follows. If θ, ϕ are the angular co-ordinates of the distant point P, and θ' are ϕ' angular co-ordinates in the source region, then

$$\cos\psi = \cos\theta\cos\theta' + \sin\theta\sin\theta'\cos(\phi - \phi') \tag{A-14}$$

Appendix-B

Computer Programs

FLOW CHART FOR CALCULATION OF CURRENT AND RADIATION INTENSITY

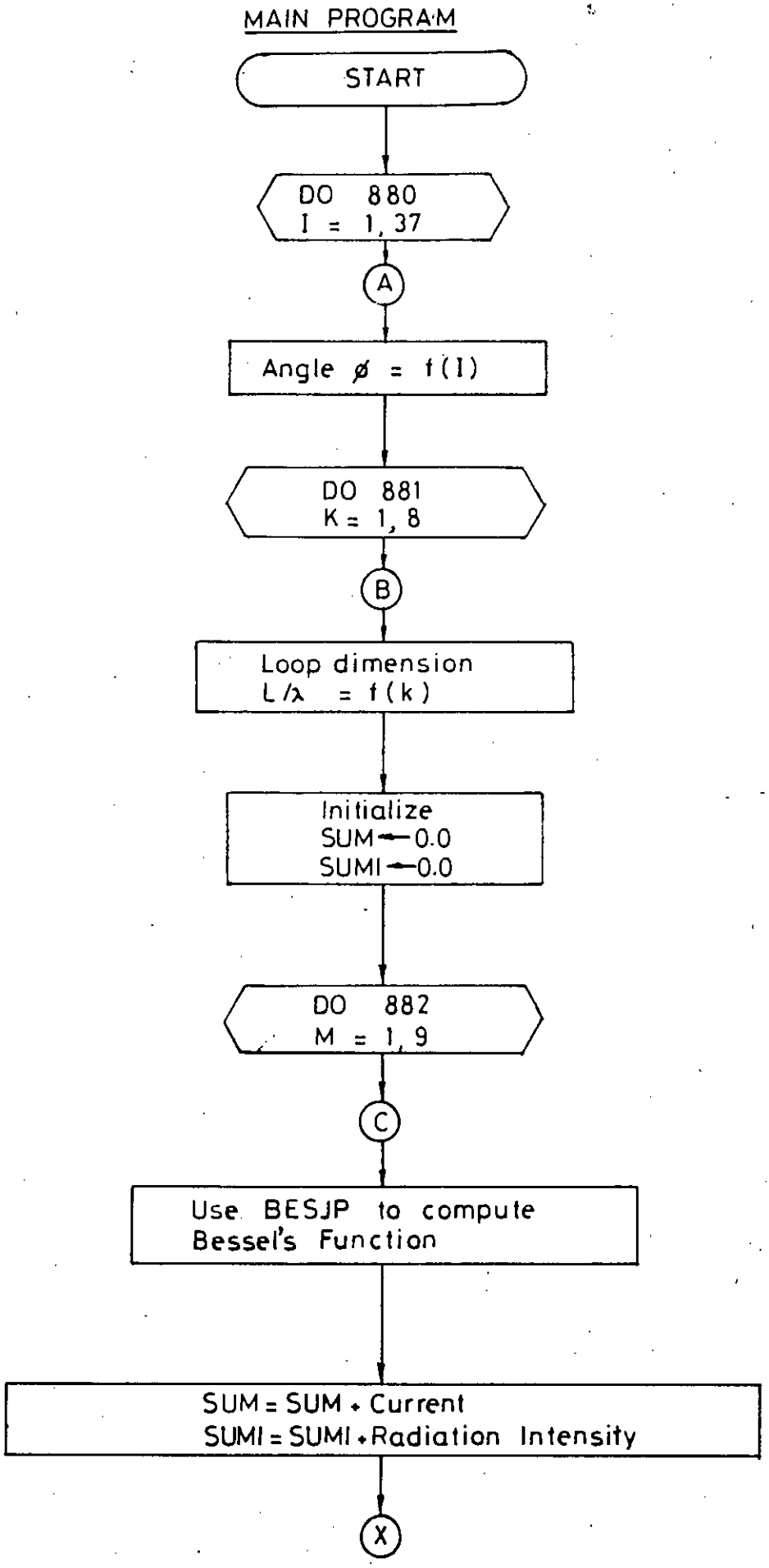

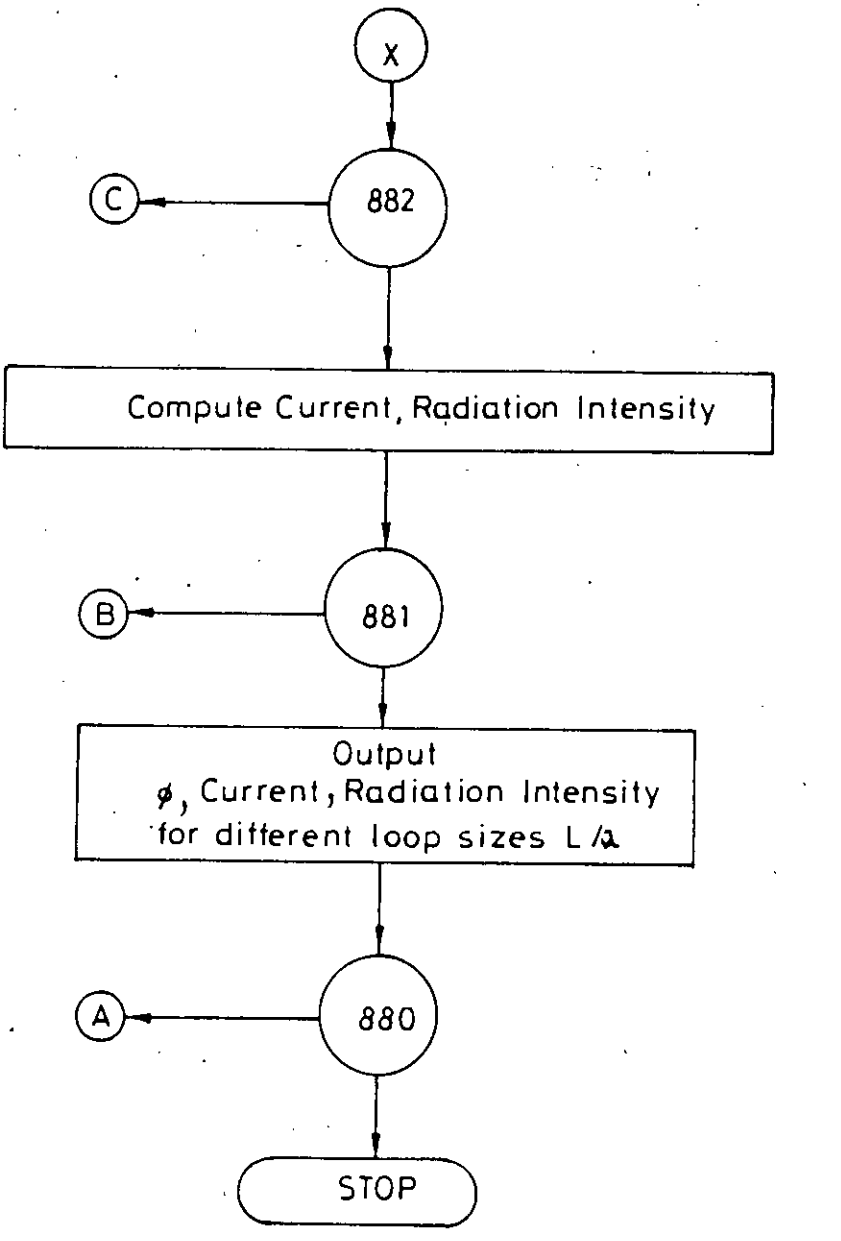
X
C
882
Compute Current, Radiation Intensity
B
881
Output
φ, Current, Radiation Intensity
for different loop sizes L/λ
A
880
STOP

SUBROUTINE

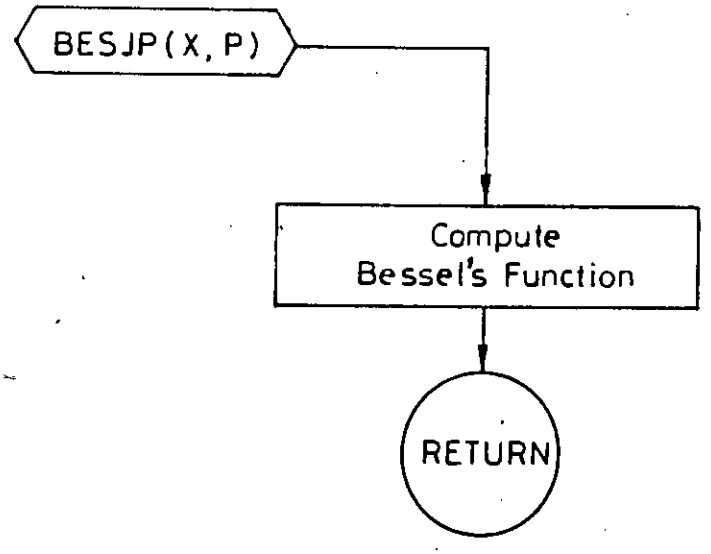
BESJP(X, P)
Compute
Bessel's Function
RETURN

```
C
C-----------------------------------------------------------------------
C     PROGRAM FOR CURRENT DISTRIBUTION IN A LARGE CIRCULAR LOOP
C     ANTENNA FOR L/LAMDA=0.5 TO 4.0
C-----------------------------------------------------------------------
C
C
      DIMENSION AMP(20)
      OPEN(UNIT=9,FILE='OUTPUT',STATUS='NEW')
      WRITE(9,189)
  189 FORMAT(1X//5X,'DATA FOR CURRENT DISTRIBUTION IN A LARGE
     +CIRCULAR LOOP ANTENNA'//)
      WRITE(9,400)
  400 FORMAT(/1X,'phy',3X,'I(L/LAM=0.5)',3X,'I(L/LAM=1.0)',3X,
     +'I(L/LAM=1.5)',3X,'I(L/LAM=2.0)',2X,'I(L/LAM=2.5)',2X,'I(L/LAM=
     +3.0)',2X,'I(L/LAM=3.5)',2X,'I(L/LAM=4.0)'/)
      PI=2.0*ASIN(1.0)
      DO 880 J=1,37
      Z=FLOAT(J-1)*10.0
      RD=PI/180.
      PHY=Z*RD
      DO 881 I=1,8
      RKA=0.5*FLOAT(I)
      R1=BESJP(RKA,0.0)
      SUM=0.0
      DO 882 K=1,9
      RJ=FLOAT(K)
      RR=BESJP(RKA,RJ)
      SUM=SUM+SIN(PI/2.0*RJ)*RR*COS(RJ*PHY)/RJ
  882 CONTINUE
      AMP(I)=SUM*4.0/PI+R1
  881 CONTINUE
      WRITE(6,*) Z,(AMP(I),I=1,8)
      WRITE(9,883) Z,(AMP(I),I=1,8)
  883 FORMAT(2X,F6.1,8(2X,E13.6)/)
  880 CONTINUE
      STOP
      END
      DOUBLE PRECISION FUNCTION BESJP(X,P)
C
C-----------------------------------------------------------------------
C     SUBROUTINE BESSEL(BESJP,X,P)
C-----------------------------------------------------------------------
C
C     COMPUTATION OF BESSEL FUNCTIONJ(X,J) OF THE ORDER OF P
C     LIMITATION X.GE.0.AND.P.GT.(-1)
C     RETERNS THE VALUE ZERO IF X.LT.0.OR.P.LT.(-1).OR.IF(X.EQ.0.
C     AND P.LT.0).OR.WHEN THE VALUE OF THE BESSEL FUNCTION WOULD CAUSE
C     AN UNDER FLOW.
C
      DOUBLE PRECISION A,A1 AK,AL,ALOGUF,BL,Y2,DABS,DCOS,DEXP,DLOG,
     +DSIN,DSQRT,EMPACH,FF,FI,P,PP,PN,QN,S,SIGN,U,UB,UU,U1,V,X,XB,
     +XX,Y,Y1,PI
      INTEGER I,K,L,NP,NU,NUB,NUM
C     THE CONSTANTS DEFINED IN THE FOLLOWING DATA STATEMENT ARE MACHINE
```

```
C      DEPENDENT
C      ALOGUF IS THE NATURAL LOGARITHM OF THE LAGEST MACHINE NUMBER.
C      EMPACH IS THE SMALLEST POSITIVE NUMBER SO THAT (1+EPMACH) > 1.
       DATA ALOGUF/1.70D+02/
       DATA EMPACH/1.0D-16/
       DATA PI/3.14159265358979323846264338327950288D+00/
       BESJP=0.0D+00
       IF(X.EQ.0.0D+00.AND.P.EQ.0.0D+00)BESJP=1.0D+00
       IF(X.LE.0.0D+00.OR.P.LE.(-1.0D+00))GO TO 110
       XB=(-6.0D-01)*(DLOG(EMPACH))
       IF(X.GE.XB.AND.P.LT.X)GO TO 60
       NP=X-P
       PP=NP
       IF(NP.GT.0)U=P+PP+1.0D+00
       IF(NP.LE.0)U=P
C      COMPUTATION OF THE LOGARITHM OF THE GAMMA FUNCTION
       UU=U
       AL=0.0D+00
       NUB=10
       IF(EMPACH.LT.1.0D-17)NUB=50
       UB=NUB
       IF(U.GE.UB)GO TO 20
       NU=U
       L=NUB-NU
       BL=L
       UU=U+BL
       S=1.0D+00
       DO 10 K=1,L
       AK=K
       S=S*(U+AK)
10     CONTINUE
       AL=DLOG(S)
20     A=2.5D-01*X*X/(U+1.0D+00)
       XX=1.0D+00/(UU+1.0D+00)**2
       F1=(((((XX/1.56D+02-6.91D+02/3.60360D+05)*XX+1.0D+00/1.188D+03)
      +*XX-1.0D+00/1.680D+03)*XX+1.0D+00/1.260D+03)*XX-1.0D+00/3.6D+02)
      +*XX+1.0D+00/1.2D+01)/(UU+1.0D+00)-AL
       FF=-F1-A+U*DLOG(5.0D-01*X)+UU*(1.0D+00-DLOG(UU+1.0D+00))+1.0D+00
      +-5.0D-01*DLOG(2.0D+00*PI*(UU+1.0D+00))
       IF(-FF.GT.(ALOGUF-1.0D+01))GO TO 110
       FF=DEXP(FF)
C      EVALUATION OF SERIES EXPANSION
       V=1.0D+00
       Y1=0.0D+00
       BESJP=1.0D+00
       S=U-A
       DO 30 I=2,200
       AI=I
       Y2=A*(Y1*(AI+AI-2.0D+00)-V*A)/(AI*(AI+U))
       BESJP=BESJP+Y2
       S=S+(U-A+AI)*Y2
       IF(X.LT.1.0D-01.AND.DABS(Y2).LT.(1.0D-02*EMPACH))GO TO 40
       IF((1.0D+01/EMPACH)*(U-A+AI)*(DABS(Y1)+DABS(Y2)).LT.DABS(S))GO TO
      +40
       V=Y1
```

```
      Y1=Y2
30    CONTINUE
40    BESJP=BESJP*FF
      IF(NP.LE.0)GO TO 110
C     START OF BACKWARD RECURSION(WHEN X.LT.XB.AND.P.LT.X)
      XX=2.0D+00/X
      V=S*XX*FF
      DO 50 K=1,NP
      AK=K
      Y=XX*(U-AK)*V-BESJP
      BESJP=V
      V=Y
50    CONTINUE
      BESJP=V
      GO TO 110
C     COMPUTATION WHEN X.GE.XB.AND.P.LT.X
60    NUM=1
      IF(P.GT.2.0D+00)NUM=2
      NP=P
      PP=NP
      UU=P-PP+1.0D+00
      IF(NUM.EQ.1)UU=P
      DO 90 K=1,NUM
      AK=K
      U=UU+1.0D+00-AK
C     HANKEL'S ASYMPTOTIC EXPANSION OF BESSEL FUNCTION
      V=1.0D+00
      U1=4.0D+00*U*U
      XX=8.0D+00*X
      PN=1.0D+00
      QN=0.0D+00
      SIGN=1.0D+00
      AI=-1.0D+00
      DO 70 I=1,100
      AI=AI+2.0D+00
      V=V*(U1-AK*AK)/(AI*XX)
      IF(DABS(V).LT.EMPACH)GO TO 80
      SIGN=-SIGN
70    CONTINUE
80    FI=X-(5.0D-01*U+2.5D-01)*PI
      Y1=DSQRT(2.0D+00/(PI*X))*(PN*X)*(PN*DCOS(FI)-QN*DSIN(FI))
      IF(NUM.EQ.1)Y2=Y1
90    CONTINUE
      BESJP=Y2
      IF(NUM.EQ.1)GO TO 110
C     START OF FORWARD RECURSION(WHEN X.GT.2.AND.P.LT.X)
      XX=2.0D+00/X
      DO 100 K=2,NP
      BESJP=XX*UU*Y2-Y1
      UU=UU+1.0D+00
      Y1=Y2
      Y2=BESJP
100   CONTINUE
110   RETURN
      END
```

DATA FOR CURRENT DISTRIBUTION IN A LARGE CIRCULAR LOOP ANTENNA

PHY	I(L/LAM=0.5)	I(L/LAM=1.0)	I(L/LAM=1.5)	I(L/LAM=2.0)	I(L/LAM=2.5)	I(L/LAM=3.0)	I(L/LAM=3.5)	I(L/LAM=4.0)
0.0	0.124585E+01	0.131725E+01	0.119679E+01	0.905235E+00	0.497435E+00	0.509869E-01	-0.350061E+00	-0.632801E+00
10.0	0.124131E+01	0.130982E+01	0.118931E+01	0.900791E+00	0.498452E+00	0.583808E-01	-0.337281E+00	-0.617395E+00
20.0	0.122779E+01	0.128753E+01	0.116636E+01	0.886265E+00	0.499645E+00	0.784715E-01	-0.300498E+00	-0.571211E+00
30.0	0.120561E+01	0.125037E+01	0.112665E+01	0.858295E+00	0.495562E+00	0.104726E+00	-0.245325E+00	-0.496711E+00
40.0	0.117531E+01	0.119849E+01	0.106852E+01	0.812076E+00	0.477736E+00	0.125872E+00	-0.183478E+00	-0.402234E+00
50.0	0.113769E+01	0.113251E+01	0.990701E+00	0.742644E+00	0.436223E+00	0.126834E+00	-0.133750E+00	-0.307313E+00
60.0	0.109379E+01	0.105368E+01	0.893122E+00	0.646650E+00	0.362414E+00	0.922048E-01	-0.118935E+00	-0.241319E+00
70.0	0.104491E+01	0.964081E+00	0.777656E+00	0.524219E+00	0.252681E+00	0.122849E-01	-0.157183E+00	-0.232900E+00
80.0	0.992579E+00	0.866691E+00	0.648477E+00	0.380168E+00	0.111425E+00	-0.110661E+00	-0.250790E+00	-0.291973E+00
90.0	0.938469E+00	0.765198E+00	0.511828E+00	0.223891E+00	-0.483829E-01	-0.260051E+00	-0.380127E+00	-0.397149E+00
100.0	0.884359E+00	0.663704E+00	0.375179E+00	0.676140E-01	-0.208192E+00	-0.409441E+00	-0.509464E+00	-0.502325E+00
110.0	0.832024E+00	0.566314E+00	0.246000E+00	-0.764363E-01	-0.349448E+00	-0.532388E+00	-0.603071E+00	-0.561399E+00
120.0	0.783148E+00	0.476718E+00	0.130534E+00	-0.198868E+00	-0.459181E+00	-0.612308E+00	-0.641320E+00	-0.552981E+00
130.0	0.739250E+00	0.397882E+00	0.329539E-01	-0.294862E+00	-0.532991E+00	-0.646938E+00	-0.626505E+00	-0.486987E+00
140.0	0.701629E+00	0.331900E+00	-0.448653E-01	-0.364295E+00	-0.574504E+00	-0.645976E+00	-0.576777E+00	-0.392066E+00
150.0	0.671332E+00	0.280028E+00	-0.102992E+00	-0.410514E+00	-0.592330E+00	-0.624830E+00	-0.514930E+00	-0.297589E+00
160.0	0.649151E+00	0.242860E+00	-0.142704E+00	-0.438484E+00	-0.596413E+00	-0.598575E+00	-0.459757E+00	-0.222999E+00
170.0	0.635631E+00	0.220570E+00	-0.165652E+00	-0.453010E+00	-0.595220E+00	-0.578484E+00	-0.422974E+00	-0.176905E+00
180.0	0.631090E+00	0.213147E+00	-0.173139E+00	-0.457454E+00	-0.594203E+00	-0.571090E+00	-0.410193E+00	-0.161499E+00
190.0	0.635631E+00	0.220569E+00	-0.165653E+00	-0.453010E+00	-0.595220E+00	-0.578484E+00	-0.422974E+00	-0.176904E+00
200.0	0.649151E+00	0.242860E+00	-0.142705E+00	-0.438484E+00	-0.596413E+00	-0.598575E+00	-0.459756E+00	-0.222998E+00
210.0	0.671332E+00	0.280027E+00	-0.102993E+00	-0.410515E+00	-0.592330E+00	-0.624829E+00	-0.514929E+00	-0.297587E+00
220.0	0.701628E+00	0.331899E+00	-0.448666E-01	-0.364296E+00	-0.574504E+00	-0.645976E+00	-0.576775E+00	-0.392064E+00
230.0	0.739249E+00	0.397881E+00	0.329524E-01	-0.294864E+00	-0.532992E+00	-0.646938E+00	-0.626504E+00	-0.486985E+00
240.0	0.783147E+00	0.476717E+00	0.130533E+00	-0.198870E+00	-0.459183E+00	-0.612309E+00	-0.641320E+00	-0.552980E+00
250.0	0.832023E+00	0.566313E+00	0.245998E+00	-0.764388E-01	-0.349450E+00	-0.532389E+00	-0.603072E+00	-0.561399E+00
260.0	0.884358E+00	0.663703E+00	0.375176E+00	0.676113E-01	-0.208194E+00	-0.409444E+00	-0.509466E+00	-0.502327E+00
270.0	0.938468E+00	0.765196E+00	0.511825E+00	0.223888E+00	-0.483861E-01	-0.260054E+00	-0.380129E+00	-0.397151E+00
280.0	0.992578E+00	0.866690E+00	0.648475E+00	0.380166E+00	0.111423E+00	-0.110663E+00	-0.250792E+00	-0.291975E+00
290.0	0.104491E+01	0.964080E+00	0.777654E+00	0.524216E+00	0.252679E+00	0.122831E-01	-0.157184E+00	-0.232901E+00
300.0	0.109379E+01	0.105367E+01	0.893120E+00	0.646648E+00	0.362413E+00	0.922042E-01	-0.118935E+00	-0.241318E+00
310.0	0.113769E+01	0.113251E+01	0.990700E+00	0.742643E+00	0.436223E+00	0.126834E+00	-0.133749E+00	-0.307311E+00
320.0	0.117531E+01	0.119849E+01	0.106852E+01	0.812076E+00	0.477737E+00	0.125874E+00	-0.183475E+00	-0.402231E+00
330.0	0.120561E+01	0.125037E+01	0.112565E+01	0.858295E+00	0.495562E+00	0.104727E+00	-0.245323E+00	-0.496709E+00
340.0	0.122779E+01	0.128753E+01	0.116636E+01	0.886265E+00	0.499646E+00	0.784734E-01	-0.300496E+00	-0.571308E+00
350.0	0.124131E+01	0.130982E+01	0.118931E+01	0.900791E+00	0.498453E+00	0.583814E-01	-0.337280E+00	-0.617394E+00
360.0	0.124585E+01	0.131725E+01	0.119679E+01	0.905235E+00	0.497435E+00	0.509869E-01	-0.350061E+00	-0.632801E+00

```
C
C
C-----------------------------------------------------------------------
C     PROGRAM FOR RADIATION INTENSITY OF A LARGE CIRCULAR LOOP
C     ANTENNA IN X-Y PLANE FOR L/LAMDA=0.5 TO 4.0
C-----------------------------------------------------------------------
C
C
      DIMENSION RI(20)
      OPEN(UNIT=9,FILE='OUTPUT',STATUS='NEW')
      WRITE(9,212)
 212  FORMAT(5X,'DATA FOR RADIATION INTENSITY OF A LARGE CIRCULAR LOOP
     +ANTENNA IN X-Y PLANE'/)
      WRITE(9,400)
400   FORMAT(/1X,'PHY  ',3X,'I(L/LAM=0.5)',3X,'I(L/LAM=1.0)',3X,
     +'I(L/LAM=1.5)',3X,'I(L/LAM=2.0)',2X,'I(L/LAM=2.5)',2X,'I(L/LAM=3
     +.0)',2X,'I(L/LAM=3.5)',3X,'I(L/LAM=4.0)'/)
      PI=2.0*ASIN(1.0)
      THETA=PI/2.0
      DO 880 J=1,73
      Z=FLOAT(J-1)*5.0
      RD=PI/180.
      PHY=Z*RD
      DO 881 I=1,8
      RKA=0.5*FLOAT(I)
      RKA1=RKA*SIN(THETA)
      R0=BESJP(RKA,0.0)
      R1=BESJP(RKA1,1.0)
      GM=R0*R1
      SUM=0.0
      DO 882 K=1,9,2
      BJ=FLOAT(K-1)
      BJ1=FLOAT(K+1)
      RJ=FLOAT(K)
      CO=COS(RJ*PHY)
      RR=BESJP(RKA,RJ)
      RR1=BESJP(RKA1,BJ1)
      RR2=BESJP(RKA1,BJ)
      FTH=(-1)**K*RR1+(-1)**(K-1)*RR2
      Y1=RR*FTH*CO/RJ
      SUM=SUM+Y1
 882  CONTINUE
      STP2=GM*GM+4.0*SUM*SUM/(PI*PI)
      RI(I)=15.0*PI*RKA*RKA*STP2
 881  CONTINUE
      WRITE(6,*) Z,(RI(I),I=1,8)
      WRITE(9,883) Z,(RI(I),I=1,8)
 883  FORMAT(1X,F5.1,8(2X,E13.6)/)
 880  CONTINUE
      STOP
      END
```

```
      DOUBLE PRECISION FUNCTION BESJP(X,P)
C-----------------------------------------------------------------------
C     SUBROUTINE BESSEL(BESJP,X,P)
C-----------------------------------------------------------------------
C     COMPUTATION OF BESSEL FUNCTIONJ(X,J) OF THE ORDER OF P
C     LIMITATION X.GE.0.AND.P.GT.(-1)
C     RETERNS THE VALUE ZERO IF X.LT.0.OR.P.LT.(-1).OR.IF(X.EQ.0.
C     AND P.LT.0).OR.WHEN THE VALUE OF THE BESSEL FUNCTION WOULD CAUSE
C     AN UNDER FLOW.
C
      DOUBLE PRECISION A,A1 AK,AL,ALOGUF,BL,Y2,DABS,DCOS,DEXP,DLOG,
     +DSIN,DSQRT,EMPACH,FF,FI,P,PP,PN,QN,S,SIGN,U,UB,UU,U1,V,X,XB,
     +XX,Y,Y1,PI
      INTEGER I,K,L,NP,NU,NUB,NUM
C     THE CONSTANTS DEFINED IN THE FOLLOWING DATA STATEMENT ARE MACHINE
C     DEPENDENT
C     ALOGUF IS THE NATURAL LOGARITHM OF THE LAGEST MACHINE NUMBER.
C     EMPACH IS THE SMALLEST POSITIVE NUMBER SO THAT (1+EPMACH) > 1.
      DATA ALOGUF/1.70D+02/
      DATA EMPACH/1.0D-16/
      DATA PI/3.14159265358979323846264338327950288D+00/
      BESJP=0.0D+00
      IF(X.EQ.0.0D+00.AND.P.EQ.0.0D+00)BESJP=1.0D+00
      IF(X.LE.0.0D+00.OR.P.LE.(-1.0D+00))GO TO 110
      XB=(-6.0D-01)*(DLOG(EMPACH))
      IF(X.GE.XB.AND.P.LT.X)GO TO 60
      NP=X-P
      PP=NP
      IF(NP.GT.0)U=P+PP+1.0D+00
      IF(NP.LE.0)U=P
C     COMPUTATION OF THE LOGARITHM OF THE GAMMA FUNCTION
      UU=U
      AL=0.0D+00
      NUB=10
      IF(EMPACH.LT.1.0D-17)NUB=50
      UB=NUB
      IF(U.GE.UB)GO TO 20
      NU=U
      L=NUB-NU
      BL=L
      UU=U+BL
      S=1.0D+00
      DO 10 K=1,L
      AK=K
      S=S*(U+AK)
10    CONTINUE
      AL=DLOG(S)
20    A=2.5D-01*X*X/(U+1.0D+00)
      XX=1.0D+00/(UU+1.0D+00)**2
      F1=(((((XX/1.56D+02-6.91D+02/3.60360D+05)*XX+1.0D+00/1.188D+03)
     +*XX-1.0D+00/1.680D+03)*XX+1.0D+00/1.260D+03)*XX-1.0D+00/3.6D+02)
```

```
     +*XX+1.0D+00/1.2D+01)/(UU+1.0D+00)-AL
      FF=-F1-A+U*DLOG(5.0D-01*X)+UU*(1.0D+00-DLOG(UU+1.0D+00))+1.0D+00
     +-5.0D-01*DLOG(2.0D+00*PI*(UU+1.0D+00))
      IF(-FF.GT.(ALOGUF-1.0D+01))GO TO 110
      FF=DEXP(FF)
C     EVALUATION OF SERIES EXPANSION
      V=1.0D+00
      Y1=0.0D+00
      BESJP=1.0D+00
      S=U-A
      DO 30 I=2,200
      AI=I
      Y2=A*(Y1*(AI+AI-2.0D+00)-V*A)/(AI*(AI+U))
      BESJP=BESJP+Y2
      S=S+(U-A+AI)*Y2
      IF(X.LT.1.0D-01.AND.DABS(Y2).LT.(1.0D-02*EMPACH))GO TO 40
      IF((1.0D+01/EMPACH)*(U-A+AI)*(DABS(Y1)+DABS(Y2)).LT.DABS(S))GO TO
     +40
      V=Y1
      Y1=Y2
30    CONTINUE
40    BESJP=BESJP*FF
      IF(NP.LE.0)GO TO 110
C     START OF BACKWARD RECURSION(WHEN X.LT.XB.AND.P.LT.X)
      XX=2.0D+00/X
      V=S*XX*FF
      DO 50 K=1,NP
      AK=K
      Y=XX*(U-AK)*V-BESJP
      BESJP=V
      V=Y
50    CONTINUE
      BESJP=V
      GO TO 110
C     COMPUTATION WHEN X.GE.XB.AND.P.LT.X
60    NUM=1
      IF(P.GT.2.0D+00)NUM=2
      NP=P
      PP=NP
      UU=P-PP+1.0D+00
      IF(NUM.EQ.1)UU=P
      DO 90 K=1,NUM
      AK=K
      U=UU+1.0D+00-AK
C     HANKEL'S ASYMPTOTIC EXPANSION OF BESSEL FUNCTION
      V=1.0D+00
      U1=4.0D+00*U*U
      XX=8.0D+00*X
      PN=1.0D+00
      QN=0.0D+00
      SIGN=1.0D+00
```

```
      AI=-1.0D+00
      DO 70 I=1,100
      AI=AI+2.0D+00
      V=V*(U1-AK*AK)/(AI*XX)
      IF(DABS(V).LT.EMPACH)GO TO 80
      SIGN=-SIGN
70    CONTINUE
80    FI=X-(5.0D-01*U+2.5D-01)*PI
      Y1=DSQRT(2.0D+00/(PI*X))*(PN*X)*(PN*DCOS(FI)-QN*DSIN(FI))
      IF(NUM.EQ.1)Y2=Y1
90    CONTINUE
      BESJP=Y2
      IF(NUM.EQ.1)GO TO 110
C     START OF FORWARD RECURSION(WHEN X.GT.2.AND.P.LT.X)
      XX=2.0D+00/X
      DO 100 K=2,NP
      BESJP=XX*UU*Y2-Y1
      UU=UU+1.0D+00
      Y1=Y2
      Y2=BESJP
100   CONTINUE
110   RETURN
      END
```

DATA FOR RADIATION INTENSITY OF A LARGE CIRCULAR LOOP ANTENNA IN X-Y PLANE

PHY	I(L/LAM=0.5)	I(L/LAM=1.0)	I(L/LAM=1.5)	I(L/LAM=2.0)	I(L/LAM=2.5)	I(L/LAM=3.0)	I(L/LAM=3.5)	I(L/LAM=4.0)
0.0	0.840030E+00	0.691507E+01	0.975424E+01	0.342342E+01	0.587618E+01	0.112774E+02	0.305469E+01	0.194864E+01
5.0	0.838273E+00	0.690289E+01	0.974396E+01	0.342517E+01	0.587649E+01	0.113055E+02	0.309034E+01	0.189937E+01
10.0	0.833057E+00	0.686673E+01	0.971361E+01	0.343016E+01	0.587431E+01	0.113827E+02	0.319500E+01	0.176231E+01
15.0	0.824540E+00	0.680776E+01	0.966461E+01	0.343762E+01	0.586049E+01	0.114890E+02	0.336075E+01	0.156592E+01
20.0	0.812982E+00	0.672786E+01	0.959924E+01	0.344630E+01	0.582077E+01	0.115920E+02	0.357200E+01	0.134678E+01
25.0	0.798733E+00	0.662959E+01	0.952042E+01	0.345445E+01	0.573723E+01	0.116501E+02	0.380385E+01	0.113842E+01
30.0	0.782230E+00	0.651605E+01	0.943153E+01	0.345999E+01	0.559051E+01	0.116162E+02	0.402276E+01	0.963413E+00
35.0	0.763974E+00	0.639082E+01	0.933616E+01	0.346065E+01	0.536256E+01	0.114444E+02	0.419052E+01	0.830780E+00
40.0	0.744518E+00	0.625779E+01	0.923793E+01	0.345430E+01	0.503982E+01	0.110964E+02	0.427074E+01	0.738536E+00
45.0	0.724458E+00	0.612106E+01	0.914024E+01	0.343931E+01	0.461632E+01	0.105498E+02	0.423644E+01	0.678551E+00
50.0	0.704400E+00	0.598482E+01	0.904618E+01	0.341488E+01	0.409636E+01	0.980355E+01	0.407619E+01	0.641070E+00
55.0	0.684955E+00	0.585318E+01	0.895839E+01	0.338135E+01	0.349597E+01	0.888159E+01	0.379727E+01	0.617330E+00
60.0	0.666713E+00	0.573008E+01	0.887902E+01	0.334038E+01	0.284305E+01	0.783322E+01	0.342479E+01	0.600407E+00
65.0	0.650227E+00	0.561916E+01	0.880974E+01	0.329489E+01	0.217568E+01	0.672906E+01	0.299757E+01	0.585328E+00
70.0	0.635998E+00	0.552367E+01	0.875180E+01	0.324878E+01	0.153888E+01	0.565405E+01	0.256188E+01	0.569272E+00
75.0	0.624457E+00	0.544639E+01	0.870605E+01	0.320651E+01	0.980014E+00	0.469794E+01	0.216473E+01	0.551917E+00
80.0	0.615955E+00	0.538955E+01	0.867304E+01	0.317248E+01	0.543531E+00	0.394478E+01	0.184807E+01	0.535375E+00
85.0	0.610748E+00	0.535479E+01	0.865313E+01	0.315039E+01	0.265728E+00	0.346301E+01	0.164442E+01	0.523210E+00
90.0	0.608995E+00	0.534309E+01	0.864648E+01	0.314274E+01	0.170372E+00	0.329726E+01	0.157422E+01	0.518712E+00
95.0	0.610748E+00	0.535479E+01	0.865313E+01	0.315039E+01	0.265725E+00	0.346301E+01	0.164442E+01	0.523210E+00
100.0	0.615955E+00	0.538955E+01	0.867304E+01	0.317248E+01	0.543521E+00	0.394476E+01	0.184806E+01	0.535374E+00
105.0	0.624457E+00	0.544639E+01	0.870605E+01	0.320651E+01	0.980006E+00	0.469792E+01	0.216473E+01	0.551917E+00
110.0	0.635998E+00	0.552367E+01	0.875180E+01	0.324878E+01	0.153886E+01	0.565403E+01	0.256187E+01	0.569272E+00
115.0	0.650227E+00	0.561916E+01	0.880974E+01	0.329489E+01	0.217566E+01	0.672904E+01	0.299756E+01	0.585328E+00
120.0	0.666712E+00	0.573008E+01	0.887901E+01	0.334038E+01	0.284303E+01	0.783319E+01	0.342478E+01	0.600407E+00
125.0	0.684954E+00	0.585318E+01	0.895839E+01	0.338135E+01	0.349596E+01	0.888157E+01	0.379727E+01	0.617330E+00
130.0	0.704400E+00	0.598482E+01	0.904618E+01	0.341488E+01	0.409635E+01	0.980353E+01	0.407619E+01	0.641070E+00
135.0	0.724457E+00	0.612106E+01	0.914024E+01	0.343931E+01	0.461632E+01	0.105498E+02	0.423643E+01	0.678550E+00
140.0	0.744518E+00	0.625778E+01	0.923793E+01	0.345430E+01	0.503981E+01	0.110964E+02	0.427075E+01	0.738534E+00
145.0	0.763973E+00	0.639081E+01	0.933616E+01	0.346065E+01	0.536256E+01	0.114444E+02	0.419052E+01	0.830779E+00
150.0	0.782229E+00	0.651605E+01	0.943152E+01	0.345999E+01	0.559050E+01	0.116162E+02	0.402277E+01	0.963410E+00
155.0	0.798733E+00	0.662959E+01	0.952042E+01	0.345445E+01	0.573723E+01	0.116501E+02	0.380385E+01	0.113842E+01
160.0	0.812981E+00	0.672786E+01	0.959924E+01	0.344630E+01	0.582076E+01	0.115920E+02	0.357201E+01	0.134677E+01
165.0	0.824540E+00	0.680776E+01	0.966461E+01	0.343762E+01	0.586049E+01	0.114890E+02	0.336075E+01	0.156592E+01
170.0	0.833057E+00	0.686673E+01	0.971360E+01	0.343016E+01	0.587431E+01	0.113827E+02	0.319500E+01	0.176230E+01

175.0	0.838273E+00	0.690289E+01	0.974396E+01	0.342517E+01	0.587649E+01	0.113055E+02	0.309034E+01	0.189937E+01
180.0	0.840030E+00	0.691507E+01	0.975424E+01	0.342342E+01	0.587618E+01	0.112774E+02	0.305469E+01	0.194864E+01
185.0	0.838273E+00	0.690289E+01	0.974396E+01	0.342517E+01	0.587649E+01	0.113055E+02	0.309034E+01	0.189937E+01
190.0	0.833057E+00	0.686673E+01	0.971361E+01	0.343016E+01	0.587431E+01	0.113827E+02	0.319500E+01	0.176231E+01
195.0	0.824540E+00	0.680776E+01	0.966461E+01	0.343762E+01	0.586048E+01	0.114890E+02	0.336075E+01	0.156593E+01
200.0	0.812982E+00	0.672786E+01	0.959924E+01	0.344630E+01	0.582077E+01	0.115920E+02	0.357200E+01	0.134678E+01
205.0	0.798733E+00	0.662959E+01	0.952042E+01	0.345445E+01	0.573723E+01	0.116501E+02	0.380384E+01	0.113843E+01
210.0	0.782230E+00	0.651606E+01	0.943153E+01	0.345998E+01	0.559051E+01	0.116162E+02	0.402276E+01	0.963416E+00
215.0	0.763974E+00	0.639082E+01	0.933616E+01	0.346065E+01	0.536257E+01	0.114444E+02	0.419052E+01	0.830782E+00
220.0	0.744518E+00	0.625779E+01	0.923793E+01	0.345430E+01	0.503982E+01	0.110964E+02	0.427074E+01	0.738537E+00
225.0	0.724458E+00	0.612107E+01	0.914025E+01	0.343931E+01	0.461633E+01	0.105499E+02	0.423644E+01	0.678551E+00
230.0	0.704400E+00	0.598483E+01	0.904618E+01	0.341488E+01	0.409636E+01	0.980356E+01	0.407620E+01	0.641071E+00
235.0	0.684955E+00	0.585319E+01	0.895839E+01	0.338135E+01	0.349598E+01	0.888161E+01	0.379728E+01	0.617330E+00
240.0	0.666713E+00	0.573008E+01	0.887902E+01	0.334038E+01	0.284305E+01	0.783323E+01	0.342480E+01	0.600407E+00
245.0	0.650227E+00	0.561916E+01	0.880974E+01	0.329489E+01	0.217569E+01	0.672908E+01	0.299758E+01	0.585328E+00
250.0	0.635998E+00	0.552367E+01	0.875180E+01	0.324878E+01	0.153889E+01	0.565406E+01	0.256188E+01	0.569272E+00
255.0	0.624458E+00	0.544639E+01	0.870605E+01	0.320651E+01	0.980024E+00	0.469795E+01	0.216474E+01	0.551918E+00
260.0	0.615955E+00	0.538955E+01	0.867304E+01	0.317248E+01	0.543534E+00	0.394479E+01	0.184807E+01	0.535375E+00
265.0	0.610748E+00	0.535479E+01	0.865313E+01	0.315039E+01	0.265731E+00	0.346302E+01	0.164442E+01	0.523210E+00
270.0	0.608995E+00	0.534309E+01	0.864648E+01	0.314274E+01	0.170372E+00	0.329726E+01	0.157422E+01	0.518712E+00
275.0	0.610748E+00	0.535479E+01	0.865313E+01	0.315039E+01	0.265721E+00	0.346300E+01	0.164442E+01	0.523210E+00
280.0	0.615955E+00	0.538955E+01	0.867304E+01	0.317248E+01	0.543518E+00	0.394476E+01	0.184806E+01	0.535374E+00
285.0	0.624457E+00	0.544639E+01	0.870605E+01	0.320651E+01	0.979996E+00	0.469790E+01	0.216472E+01	0.551917E+00
290.0	0.635998E+00	0.552367E+01	0.875180E+01	0.324878E+01	0.153886E+01	0.565402E+01	0.256186E+01	0.569272E+00
295.0	0.650226E+00	0.561915E+01	0.880974E+01	0.329489E+01	0.217565E+01	0.672902E+01	0.299755E+01	0.585328E+00
300.0	0.666712E+00	0.573008E+01	0.887901E+01	0.334038E+01	0.284303E+01	0.783318E+01	0.342478E+01	0.600407E+00
305.0	0.684954E+00	0.585318E+01	0.895839E+01	0.338135E+01	0.349595E+01	0.888156E+01	0.379726E+01	0.617329E+00
310.0	0.704399E+00	0.598482E+01	0.904618E+01	0.341488E+01	0.409635E+01	0.980352E+01	0.407618E+01	0.641070E+00
315.0	0.724457E+00	0.612106E+01	0.914024E+01	0.343931E+01	0.461631E+01	0.105498E+02	0.423644E+01	0.678549E+00
320.0	0.744518E+00	0.625778E+01	0.923793E+01	0.345430E+01	0.503982E+01	0.110964E+02	0.427076E+01	0.738532E+00
325.0	0.763973E+00	0.639081E+01	0.933616E+01	0.346065E+01	0.536255E+01	0.114443E+02	0.419053E+01	0.830776E+00
330.0	0.782229E+00	0.651605E+01	0.943152E+01	0.345999E+01	0.559051E+01	0.116162E+02	0.402278E+01	0.963406E+00
335.0	0.798733E+00	0.662959E+01	0.952042E+01	0.345445E+01	0.573724E+01	0.116501E+02	0.380387E+01	0.113841E+01
340.0	0.812981E+00	0.672786E+01	0.959924E+01	0.344630E+01	0.582078E+01	0.115921E+02	0.357202E+01	0.134677E+01
345.0	0.824539E+00	0.680775E+01	0.966461E+01	0.343762E+01	0.586049E+01	0.114890E+02	0.336076E+01	0.156592E+01
350.0	0.833057E+00	0.686673E+01	0.971360E+01	0.343016E+01	0.587432E+01	0.113827E+02	0.319501E+01	0.176230E+01
355.0	0.838273E+00	0.690289E+01	0.974396E+01	0.342517E+01	0.587650E+01	0.113055E+02	0.309035E+01	0.189936E+01
360.0	0.840030E+00	0.691507E+01	0.975424E+01	0.342342E+01	0.587618E+01	0.112774E+02	0.305469E+01	0.194864E+01

DATA FOR RADIATION INTENSITY OF A LARGE CIRCULAR LOOP ANTENNA IN Z-X PLANE

THETA	I(L/LAM=0.5)	I(L/LAM=1.0)	I(L/LAM=1.5)	I(L/LAM=2.0)	I(L/LAM=2.5)	I(L/LAM=3.0)	I(L/LAM=3.5)	I(L/LAM=4.0)
5.0	0.284767E+00	0.372969E+01	0.133263E+02	0.249204E+02	0.285159E+02	0.193461E+02	0.610295E+01	0.463858E+01
10.0	0.298180E+00	0.382218E+01	0.131791E+02	0.235116E+02	0.257397E+02	0.181867E+02	0.106484E+02	0.133521E+02
15.0	0.320000E+00	0.397098E+01	0.129471E+02	0.213477E+02	0.216161E+02	0.165075E+02	0.166984E+02	0.244020E+02
20.0	0.349454E+00	0.416860E+01	0.126486E+02	0.186690E+02	0.167738E+02	0.146116E+02	0.225643E+02	0.341691E+02
25.0	0.385511E+00	0.440549E+01	0.123053E+02	0.157496E+02	0.118822E+02	0.128007E+02	0.267923E+02	0.398892E+02
30.0	0.426934E+00	0.467076E+01	0.119401E+02	0.128538E+02	0.752002E+01	0.113073E+02	0.285670E+02	0.404832E+02
35.0	0.472332E+00	0.495305E+01	0.115744E+02	0.102008E+02	0.408517E+01	0.102574E+02	0.278230E+02	0.365614E+02
40.0	0.520219E+00	0.524128E+01	0.112260E+02	0.794209E+01	0.176054E+01	0.966904E+01	0.250885E+02	0.297997E+02
45.0	0.569071E+00	0.552522E+01	0.109085E+02	0.615500E+01	0.531833E+00	0.947770E+01	0.211873E+02	0.221221E+02
50.0	0.617385E+00	0.579600E+01	0.106301E+02	0.484940E+01	0.240070E+00	0.957420E+01	0.169445E+02	0.150675E+02
55.0	0.663720E+00	0.604633E+01	0.103948E+02	0.398279E+01	0.646816E+00	0.984062E+01	0.129918E+02	0.950975E+01
60.0	0.706740E+00	0.627054E+01	0.102026E+02	0.347937E+01	0.149351E+01	0.101757E+02	0.969498E+01	0.568932E+01
65.0	0.745248E+00	0.646453E+01	0.100510E+02	0.324815E+01	0.254419E+01	0.105068E+02	0.717920E+01	0.341350E+01
70.0	0.778202E+00	0.662552E+01	0.993588E+01	0.319779E+01	0.360844E+01	0.107914E+02	0.540246E+01	0.228558E+01
75.0	0.804740E+00	0.675179E+01	0.985257E+01	0.324673E+01	0.454777E+01	0.110107E+02	0.423689E+01	0.187944E+01
80.0	0.824182E+00	0.684240E+01	0.979667E+01	0.332912E+01	0.527067E+01	0.111619E+02	0.353410E+01	0.183795E+01
85.0	0.836044E+00	0.689689E+01	0.976465E+01	0.339748E+01	0.572270E+01	0.112491E+02	0.316747E+01	0.190929E+01
90.0	0.840030E+00	0.691507E+01	0.975424E+01	0.342342E+01	0.587618E+01	0.112774E+02	0.305468E+01	0.194865E+01
95.0	0.836044E+00	0.689689E+01	0.976465E+01	0.339748E+01	0.572270E+01	0.112491E+02	0.316747E+01	0.190929E+01
100.0	0.824183E+00	0.684241E+01	0.979667E+01	0.332912E+01	0.527069E+01	0.111619E+02	0.353409E+01	0.183795E+01
105.0	0.804741E+00	0.675180E+01	0.985257E+01	0.324673E+01	0.454778E+01	0.110107E+02	0.423686E+01	0.187943E+01
110.0	0.778203E+00	0.662552E+01	0.993587E+01	0.319779E+01	0.360848E+01	0.107914E+02	0.540242E+01	0.228556E+01
115.0	0.745248E+00	0.646453E+01	0.100510E+02	0.324814E+01	0.254421E+01	0.105068E+02	0.717916E+01	0.341347E+01
120.0	0.706741E+00	0.627054E+01	0.102026E+02	0.347935E+01	0.149354E+01	0.101757E+02	0.969489E+01	0.568924E+01
125.0	0.663721E+00	0.604633E+01	0.103948E+02	0.398278E+01	0.646826E+00	0.984062E+01	0.129917E+02	0.950968E+01
130.0	0.617386E+00	0.579601E+01	0.106301E+02	0.484938E+01	0.240073E+00	0.957421E+01	0.169444E+02	0.150673E+02
135.0	0.569072E+00	0.552522E+01	0.109085E+02	0.615499E+01	0.531824E+00	0.947770E+01	0.211872E+02	0.221220E+02
140.0	0.520220E+00	0.524129E+01	0.112260E+02	0.794205E+01	0.176051E+01	0.966903E+01	0.250885E+02	0.297996E+02
145.0	0.472333E+00	0.495306E+01	0.115744E+02	0.102008E+02	0.408513E+01	0.102574E+02	0.278230E+02	0.365613E+02
150.0	0.426935E+00	0.467076E+01	0.119401E+02	0.128538E+02	0.751994E+01	0.113073E+02	0.285670E+02	0.404832E+02
155.0	0.385512E+00	0.440549E+01	0.123053E+02	0.157495E+02	0.118822E+02	0.128007E+02	0.267923E+02	0.398893E+02
160.0	0.349455E+00	0.416861E+01	0.126485E+02	0.186689E+02	0.167738E+02	0.146116E+02	0.225644E+02	0.341693E+02
165.0	0.320000E+00	0.397098E+01	0.129471E+02	0.213476E+02	0.216161E+02	0.165074E+02	0.166985E+02	0.244021E+02
170.0	0.298180E+00	0.382218E+01	0.131791E+02	0.235116E+02	0.257397E+02	0.181867E+02	0.106485E+02	0.133523E+02
175.0	0.284767E+00	0.372970E+01	0.133263E+02	0.249204E+02	0.285159E+02	0.193460E+02	0.610299E+01	0.463867E+01
180.0	0.280242E+00	0.369832E+01	0.133768E+02	0.254095E+02	0.294956E+02	0.197603E+02	0.441538E+01	0.133283E+01

DATA FOR RADIATION INTENSITY OF A LARGE CIRCULAR LOOP ANTENNA IN Y-Z PLANE

THETA	I(L/LAM=0.5)	I(L/LAM=1.0)	I(L/LAM=1.5)	I(L/LAM=2.0)	I(L/LAM=2.5)	I(L/LAM=3.0)	I(L/LAM=3.5)	I(L/LAM=4.0)
5.0	0.282904E+00	0.371546E+01	0.133347E+02	0.250826E+02	0.288839E+02	0.196589E+02	0.608315E+01	0.487470E+01
10.0	0.290795E+00	0.376589E+01	0.132102E+02	0.241319E+02	0.271270E+02	0.193447E+02	0.105818E+02	0.141720E+02
15.0	0.303631E+00	0.384675E+01	0.130089E+02	0.226423E+02	0.244420E+02	0.187937E+02	0.165882E+02	0.258468E+02
20.0	0.320955E+00	0.395357E+01	0.127395E+02	0.207405E+02	0.211398E+02	0.179823E+02	0.224421E+02	0.359524E+02
25.0	0.342159E+00	0.408073E+01	0.124133E+02	0.185757E+02	0.175641E+02	0.169044E+02	0.266993E+02	0.415327E+02
30.0	0.366511E+00	0.422188E+01	0.120435E+02	0.162991E+02	0.140328E+02	0.155837E+02	0.285287E+02	0.415219E+02
35.0	0.393194E+00	0.437054E+01	0.116443E+02	0.140469E+02	0.107940E+02	0.140751E+02	0.278312E+02	0.367107E+02
40.0	0.421330E+00	0.452052E+01	0.112301E+02	0.119274E+02	0.800510E+01	0.124582E+02	0.250987E+02	0.290199E+02
45.0	0.450024E+00	0.466631E+01	0.108149E+02	0.100161E+02	0.573359E+01	0.108229E+02	0.211313E+02	0.205781E+02
50.0	0.478393E+00	0.480333E+01	0.104115E+02	0.835546E+01	0.397383E+01	0.925416E+01	0.167503E+02	0.130321E+02
55.0	0.505590E+00	0.492806E+01	0.100315E+02	0.696004E+01	0.267115E+01	0.782109E+01	0.126014E+02	0.726284E+01
60.0	0.530834E+00	0.503803E+01	0.968459E+01	0.582327E+01	0.174614E+01	0.657038E+01	0.907592E+01	0.345076E+01
65.0	0.553423E+00	0.513169E+01	0.937898E+01	0.492529E+01	0.111414E+01	0.552623E+01	0.632691E+01	0.131708E+01
70.0	0.572749E+00	0.520827E+01	0.912112E+01	0.423993E+01	0.698072E+00	0.469433E+01	0.433639E+01	0.385104E+00
75.0	0.588309E+00	0.526755E+01	0.891592E+01	0.374010E+01	0.435010E+00	0.406796E+01	0.299351E+01	0.170286E+00
80.0	0.599706E+00	0.530963E+01	0.876699E+01	0.340180E+01	0.278111E+00	0.363446E+01	0.215990E+01	0.280562E+00
85.0	0.606658E+00	0.533474E+01	0.867671E+01	0.320653E+01	0.195863E+00	0.338071E+01	0.171367E+01	0.447122E+00
90.0	0.608995E+00	0.534309E+01	0.864648E+01	0.314274E+01	0.170372E+00	0.329726E+01	0.157422E+01	0.518712E+00
95.0	0.606658E+00	0.533474E+01	0.867670E+01	0.320652E+01	0.195862E+00	0.338071E+01	0.171366E+01	0.447122E+00
100.0	0.599706E+00	0.530963E+01	0.876699E+01	0.340179E+01	0.278108E+00	0.363444E+01	0.215988E+01	0.280567E+00
105.0	0.588309E+00	0.526756E+01	0.891592E+01	0.374009E+01	0.435006E+00	0.406795E+01	0.299348E+01	0.170285E+00
110.0	0.572749E+00	0.520828E+01	0.912111E+01	0.423991E+01	0.698062E+00	0.469431E+01	0.433635E+01	0.385091E+00
115.0	0.553423E+00	0.513169E+01	0.937897E+01	0.492527E+01	0.111413E+01	0.552621E+01	0.632685E+01	0.131706E+01
120.0	0.530835E+00	0.503803E+01	0.968458E+01	0.582323E+01	0.174612E+01	0.657034E+01	0.907582E+01	0.345068E+01
125.0	0.505591E+00	0.492806E+01	0.100315E+02	0.696002E+01	0.267113E+01	0.782106E+01	0.126013E+02	0.726278E+01
130.0	0.478393E+00	0.480333E+01	0.104115E+02	0.835543E+01	0.397380E+01	0.925412E+01	0.167502E+02	0.130319E+02
135.0	0.450025E+00	0.466631E+01	0.108149E+02	0.100160E+02	0.573357E+01	0.108228E+02	0.211313E+02	0.205780E+02
140.0	0.421330E+00	0.452052E+01	0.112301E+02	0.119274E+02	0.800505E+01	0.124582E+02	0.250986E+02	0.290197E+02
145.0	0.393194E+00	0.437054E+01	0.116443E+02	0.140469E+02	0.107940E+02	0.140751E+02	0.278312E+02	0.367106E+02
150.0	0.366512E+00	0.422188E+01	0.120435E+02	0.162991E+02	0.140328E+02	0.155836E+02	0.285287E+02	0.415218E+02
155.0	0.342159E+00	0.408073E+01	0.124133E+02	0.185757E+02	0.175641E+02	0.169044E+02	0.266993E+02	0.415327E+02
160.0	0.320955E+00	0.395358E+01	0.127395E+02	0.207405E+02	0.211397E+02	0.179822E+02	0.224422E+02	0.359526E+02
165.0	0.303632E+00	0.384675E+01	0.130089E+02	0.226423E+02	0.244419E+02	0.187937E+02	0.165883E+02	0.258469E+02
170.0	0.290796E+00	0.376589E+01	0.132102E+02	0.241318E+02	0.271269E+02	0.193447E+02	0.105819E+02	0.141722E+02
175.0	0.282905E+00	0.371546E+01	0.133347E+02	0.250826E+02	0.288839E+02	0.196589E+02	0.608319E+01	0.487479E+01
180.0	0.280242E+00	0.369832E+01	0.133768E+02	0.254095E+02	0.294956E+02	0.197603E+02	0.441538E+01	0.133283E+01

FLOW CHART FOR COMPUTING RADIATED POWER, RADIATION RESISTANCE AND GAIN

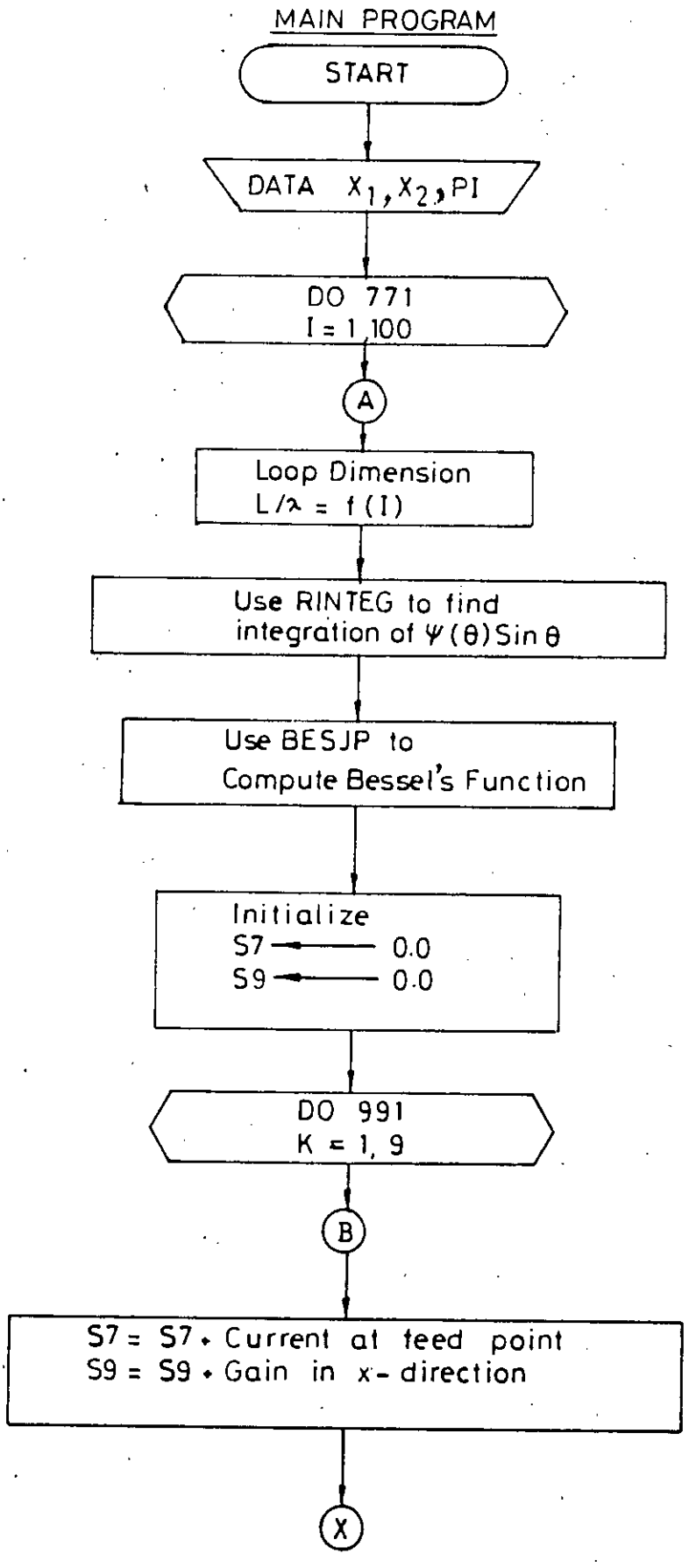

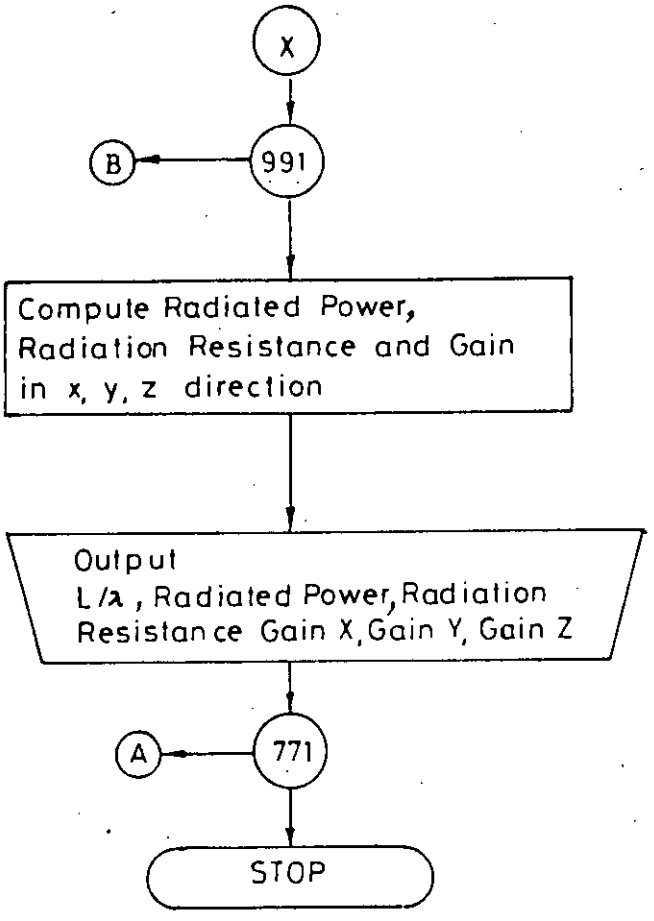
X
B
991
Compute Radiated Power,
Radiation Resistance and Gain
in x, y, z direction
Output
L/λ , Radiated Power, Radiation
Resistance Gain X, Gain Y, Gain Z
A
771
STOP

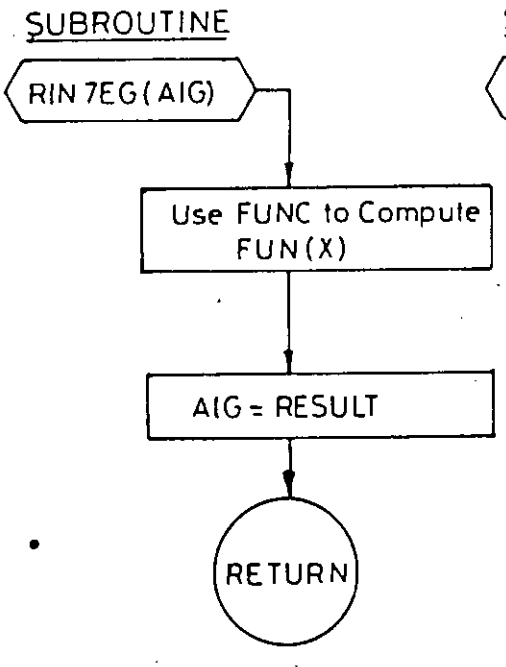
SUBROUTINE
RIN7EG(AIG)
Use FUNC to Compute
FUN(X)
AIG = RESULT
RETURN

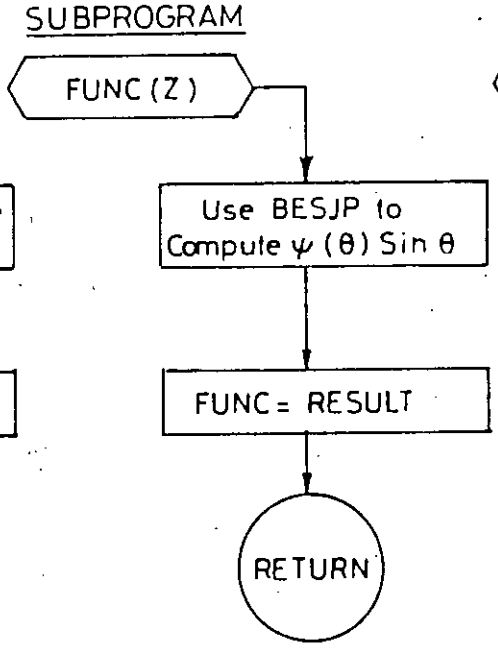
SUBPROGRAM
FUNC(Z)
Use BESJP to
Compute ψ(θ) Sin θ
FUNC = RESULT
RETURN

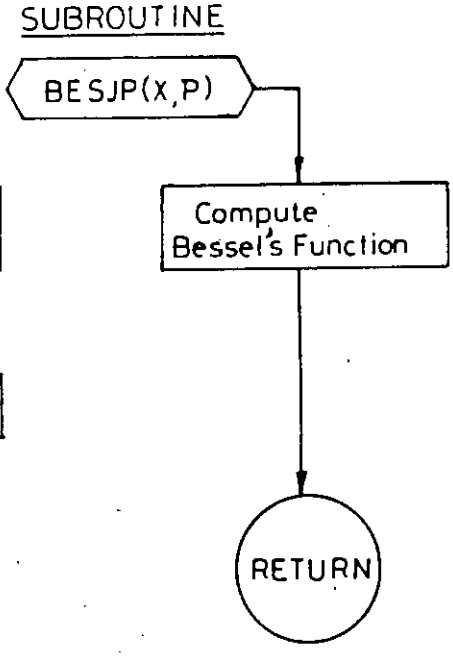
SUBROUTINE
BESJP(X,P)
Compute
Bessel's Function
RETURN

```
C
C
C-----------------------------------------------------------------------
C     PROGRAM FOR RADIATED POWER, RESISTANCE AND GAIN
C     IN X,Y,Z-DIRECTION OF A LARGE CIRCULAR LOOP ANTENNA
C-----------------------------------------------------------------------
C
C
      EXTERNAL FUNC
      COMMON RKA
      OPEN(UNIT=9,FILE='OUTPUT',STATUS='NEW')
      X1=0.0
      X2=2.0*ASIN(1.0)
      PI=2.0*ASIN(1.0)
      WRITE(9,770)
 770  FORMAT(5X,'DATA FOR RADIATED POWER, RADIATION RESISTANCE AND
     +GAIN IN X,Y,Z-DIRECTION '/)
      WRITE(9,400)
 400  FORMAT(2X,'L/LAMDA',2X,'RAD. POWER',2X,'RAD. RESIST.',5X,
     +'GAIN-X',5X,'GAIN-Y',5X,'GAIN-Z'//)
      DO 771 II=1,100
      RKA=FLOAT(II)*0.1
      THETA=PI/2.0
      PHY=0.0
      PHY1=PI/2.0
      CALL RINTEG(FUNC,X1,X2,AIG)
      W=AIG
      W1=RKA*RKA*W
      R0=BESJP(RKA,0.0)
      R1=BESJP(RKA,1.0)
      GM1=R0*R1
      S7=0.0
      S9=0.0
      DO 991 JJ1=1,9,2
      K7=(JJ1-1)/2
      PJ=FLOAT(JJ1)
      PJ1=FLOAT(JJ1+1)
      PJ2=FLOAT(JJ1-1)
      BF=BESJP(RKA,PJ)
      BF1=BESJP(RKA,PJ1)
      BF2=BESJP(RKA,PJ2)
      FNU1=BF1-BF2
      S7=S7+BF*FNU1/PJ
      S9=S9+(-1)**K7*BF/PJ
 991  CONTINUE
      BK=R0+4.0*S9/PI
      RIZERO=BK*BK
      RP=30.0*PI*PI*W1
      RESIST=60.0*PI*PI*W1/RIZERO
      STP=GM1*GM1+4.0*S7*S7/(PI*PI)
      STP1=GM1*GM1
      STP2=4.0*R1*R1/(PI*PI)
      GX=2.0*STP/W
```

```
      GY=2.0*STP1/W
      GZ=2.0*STP2/W
      WRITE(6,*) RKA,RP,RESIST,GX,GY,GZ
      WRITE(9,780) RKA,RP,RESIST,GX,GY,GZ
 780  FORMAT(2X,F6.2,5(2X,E13.6)/)
 771  CONTINUE
      STOP
      END
C-----------------------------------------------------------------------
C     SUBROUTINE FOR INTEGRATION
C-----------------------------------------------------------------------
      SUBROUTINE RINTEG(FUN,X11,X22,AIG)
      DIMENSION R64(64),W64(64),W32(32)
      DATA R64
     1/.9999824304,.9998728881,.9995987997,.9990981250,.9983166353
     2,.9972962594,.9957241047,.9938316932,.9914957212,.9886847575
     3,.9853714996,.9815311496,.9771415146,.9721828747,.9666378516
     4,.9604912687,.9537300064,.9463428584,.9383203978,.9296548574
     5,.9203400255,.9103711570,.8997448998,.8884592329,.8765134145
     6,.8639079382,.8506444948,.8367259382,.8221562544,.8069035320
     7,.7910849338,.7745966692,.7574839664,.7397560444,.7214230854
     8,.7024962065,.6829874311,.6629096600,.6422766425,.6211029467
     9,.5994039302,.5771957101,.5544951326,.5313197436,.5076877575
     1,.4836180269,.4591300120,.4342437493,.4089798212,.3833593242
     2,.3574038378,.3311353933,.3045764416,.2777498220,.2506787303
     3,.2233866864,.1958975027,.1682352516,.1404242332,.11248894351
     4,.844540400E-1,.5634431304E-1,.2818464895E-1,.0000000000/
      DATA W64
     A/.5053609519E-4,.1807395645E-3,.3777466463E-3,.6326073194E-3
     B,.9383698485E-3,.1289524083E-2,.1681142865E-2,.2108815246E-2
     C,.2568764944E-2,.3057753410E-2,.3572892784E-2,.4111503979E-2
     D,.4671050372E-2,.5249123455E-2,.5843449876E-2,.6451900053E-2
     E,.7072489995E-2,.7703375233E-2,.8342838754E-2,.8989275784E-2
     F,.9641177730E-2,.1029711696E-1,.1095573339E-1,.1161572332E-1
     G,.1227583056E-1,.1293483966E-1,.1359157101E-1,.1424487737E-1
     H,.1489364166E-1,.1553677556E-1,.1617321873E-1,.1680193857E-1
     I,.1742193016E-1,.1803221639E-1,.1863184826E-1,.1921990512E-1
     J,.1979549505E-1,.2035775506E-1,.2090585145E-1,.2143898001E-1
     K,.2195636631E-1,.2245726583E-1,.2294096423E-1,.2340677750E-1
     L,.2385405211E-1,.2428215502E-1,.2469052474E-1,.2507856965E-1
     M,.2544557699E-1,.2579162698E-1,.2611567338E-1,.2641747340E-1
     N,.2669662293E-1,.2695274967E-1,.2718551323E-1,.2739460526E-1
     O,.2757974957E-1,.2774373218E-1,.2787725148E-1,.2798921826E-1
     P,.2807645579E-1,.2813884992E-1,.2817631903E-1,.2818881418E-1/
      DATA W32
     1/.3632214818E-3,.1265156556E-2,.2579049795E-2,.4217630442E-2
     2,.6115506822E-2,.8223007957E-2,.1049824691E-1,.1290380010E-1
     3,.1540675047E-1,.1797855157E-1,.2059423392E-1,.2323144664E-1
     4,.2586967933E-1,.2848975475E-1,.3107355111E-1,.3360387715E-1
     5,.3606443278E-1,.3843981025E-1,.4371551012E-1,.4287796003E-1
     6,.4491453165E-1,.4681355499E-1,.4856433041E-1,.5015713931E-1
     7,.5158325395E-1,.5283494679E-1,.5390549934E-1,.5478921053E-1
     8,.5548140543E-1,.5597843651E-1,.5627769983E-1,.5637762836E-1/
```

```
      XM=0.5*(X11+X22)
      XD=0.5*(X22-X11)
      SU11=0.0
      SU22=0.0
      K=1
      J=0
      DO 10 I=1,63
      DX=R64(I)*XD
      TEMP=FUN(XM-DX)+FUN(XM+DX)
      SU11=SU11+W64(I)*TEMP
      IF(K.GT.0) GO TO 10
      J=J+1
      SU22=SU22+W32(J)*TEMP
 10   K=-K
      TEMP=FUN(XM)
      SU11=SU11+W64(64)*TEMP
      SU22=SU22+W32(32)*TEMP
      AIG=XD*SU11
      DIG=XD*(SU11-SU22)
      RETURN
      END
C-----------------------------------------------------------------------
C     EXTERNAL FUNCTION IS GIVEN BELOW
C-----------------------------------------------------------------------
      FUNCTION FUNC(Z)
      COMMON RKA
      DATA PII/3.14159265358979323846264338327950288/
      RKA1=RKA*SIN(Z)
      R00=BESJP(RKA,0.0)
      R11=BESJP(RKA1,1.0)
      GM=R00*R11
      SU=0.0
      DO 773 KK=1,9,2
      BJ=FLOAT(KK)
      BJ1=FLOAT(KK+1)
      BJ2=FLOAT(KK-1)
      CK=BESJP(RKA,BJ)
      CK1=BESJP(RKA1,BJ1)
      CK2=BESJP(RKA1,BJ2)
      FST=CK*CK*((CK1-CK2)**2+COS(Z)*COS(Z)*(CK1+CK2)**2)**2/(BJ*BJ)
      SU=SU+FST
 773  CONTINUE
      FTA=GM*GM+2.0*SU/(PII*PII)
      FUNC=FTA*SIN(Z)
      RETURN
      END
      DOUBLE PRECISION FUNCTION BESJP(X,P)
C-----------------------------------------------------------------------
C     SUBROUTINE BESSEL(BESJP,X,P)
C-----------------------------------------------------------------------
C     COMPUTATION OF BESSEL FUNCTIONJ(X,J) OF THE ORDER OF P
C     LIMITATION X.GE.0.AND.P.GT.(-1)
C     RETERNS THE VALUE ZERO IF X.LT.0.OR.P.LT.(-1).OR.IF(X.EQ.0.
```

```
C      AND P.LT.0).OR.WHEN THE VALUE OF THE BESSEL FUNCTION WOULD CAUSE
C      AN UNDER FLOW.
C
       DOUBLE PRECISION A,A1 AK,AL,ALOGUF,BL,Y2,DABS,DCOS,DEXP,DLOG,
      +DSIN,DSQRT,EMPACH,FF,FI,P,PP,PN,QN,S,SIGN,U,UB,UU,U1,V,X,XB,
      +XX,Y,Y1,PI
       INTEGER I,K,L,NP,NU,NUB,NUM
C      THE CONSTANTS DEFINED IN THE FOLLOWING DATA STATEMENT ARE MACHINE
C      DEPENDENT
C      ALOGUF IS THE NATURAL LOGARITHM OF THE LAGEST MACHINE NUMBER.
C      EMPACH IS THE SMALLEST POSITIVE NUMBER SO THAT (1+EPMACH) > 1.
       DATA ALOGUF/1.70D+02/
       DATA EMPACH/1.0D-16/
       DATA PI/3.14159265358979323846264338327950288D+00/
       BESJP=0.0D+00
       IF(X.EQ.0.0D+00.AND.P.EQ.0.0D+00)BESJP=1.0D+00
       IF(X.LE.0.0D+00.OR.P.LE.(-1.0D+00))GO TO 110
       XB=(-6.0D-01)*(DLOG(EMPACH))
       IF(X.GE.XB.AND.P.LT.X)GO TO 60
       NP=X-P
       PP=NP
       IF(NP.GT.0)U=P+PP+1.0D+00
       IF(NP.LE.0)U=P
C      COMPUTATION OF THE LOGARITHM OF THE GAMMA FUNCTION
       UU=U
       AL=0.0D+00
       NUB=10
       IF(EMPACH.LT.1.0D-17)NUB=50
       UB=NUB
       IF(U.GE.UB)GO TO 20
       NU=U
       L=NUB-NU
       BL=L
       UU=U+BL
       S=1.0D+00
       DO 10 K=1,L
       AK=K
       S=S*(U+AK)
10     CONTINUE
       AL=DLOG(S)
20     A=2.5D-01*X*X/(U+1.0D+00)
       XX=1.0D+00/(UU+1.0D+00)**2
       F1=(((((XX/1.56D+02-6.91D+02/3.60360D+05)*XX+1.0D+00/1.188D+03)
      +*XX-1.0D+00/1.680D+03)*XX+1.0D+00/1.260D+03)*XX-1.0D+00/3.6D+02)
      +*XX+1.0D+00/1.2D+01)/(UU+1.0D+00)-AL
       FF=-F1-A+U*DLOG(5.0D-01*X)+UU*(1.0D+00-DLOG(UU+1.0D+00))+1.0D+00
      +-5.0D-01*DLOG(2.0D+00*PI*(UU+1.0D+00))
       IF(-FF.GT.(ALOGUF-1.0D+01))GO TO 110
       FF=DEXP(FF)
C      EVALUATION OF SERIES EXPANSION
       V=1.0D+00
       Y1=0.0D+00
       BESJP=1.0D+00
```

```
      S=U-A
      DO 30 I=2,200
      AI=I
      Y2=A*(Y1*(AI+AI-2.0D+00)-V*A)/(AI*(AI+U))
      BESJP=BESJP+Y2
      S=S+(U-A+AI)*Y2
      IF(X.LT.1.0D-01.AND.DABS(Y2).LT.(1.0D-02*EMPACH))GO TO 40
      IF((1.0D+01/EMPACH)*(U-A+AI)*(DABS(Y1)+DABS(Y2)).LT.DABS(S))GO TO
     +40
      V=Y1
      Y1=Y2
30    CONTINUE
40    BESJP=BESJP*FF
      IF(NP.LE.0)GO TO 110
C     START OF BACKWARD RECURSION(WHEN X.LT.XB.AND.P.LT.X)
      XX=2.0D+00/X
      V=S*XX*FF
      DO 50 K=1,NP
      AK=K
      Y=XX*(U-AK)*V-BESJP
      BESJP=V
      V=Y
50    CONTINUE
      BESJP=V
      GO TO 110
C     COMPUTATION WHEN X.GE.XB.AND.P.LT.X
60    NUM=1
      IF(P.GT.2.0D+00)NUM=2
      NP=P
      PP=NP
      UU=P-PP+1.0D+00
      IF(NUM.EQ.1)UU=P
      DO 90 K=1,NUM
      AK=K
      U=UU+1.0D+00-AK
C     HANKEL'S ASYMPTOTIC EXPANSION OF BESSEL FUNCTION
      V=1.0D+00
      U1=4.0D+00*U*U
      XX=8.0D+00*X
      PN=1.0D+00
      QN=0.0D+00
      SIGN=1.0D+00
      AI=-1.0D+00
      DO 70 I=1,100
      AI=AI+2.0D+00
      V=V*(U1-AK*AK)/(AI*XX)
      IF(DABS(V).LT.EMPACH)GO TO 80
      SIGN=-SIGN
70    CONTINUE
80    FI=X-(5.0D-01*U+2.5D-01)*PI
      Y1=DSQRT(2.0D+00/(PI*X))*(PN*X)*(PN*DCOS(FI)-QN*DSIN(FI))
      IF(NUM.EQ.1)Y2=Y1
90    CONTINUE
```

```
      BESJP=Y2
      IF(NUM.EQ.1)GO TO 110
C     START OF FORWARD RECURSION(WHEN X.GT.2.AND.P.LT.X)
      XX=2.0D+00/X
      DO 100 K=2,NP
      BESJP=XX*UU*Y2-Y1
      UU=UU+1.0D+00
      Y1=Y2
      Y2=BESJP
100   CONTINUE
110   RETURN
      END
```

DATA FOR RADIATED POWER, RADIATION RESISTANCE AND GAIN IN X,Y,Z-DIRECTION

L/LAM	RAD. POWER	RAD. RESIST.	GAIN-X	GAIN-Y	GAIN-Z
0.10	0.153481E-01	0.272643E-01	0.134439E+01	0.957359E+00	0.389950E+00
0.20	0.239833E+00	0.384690E+00	0.134292E+01	0.958398E+00	0.396292E+00
0.30	0.116728E+01	0.171647E+01	0.134019E+01	0.959960E+00	0.407070E+00
0.40	0.349154E+01	0.477407E+01	0.133578E+01	0.961798E+00	0.422613E+00
0.50	0.794233E+01	0.102341E+02	0.132910E+01	0.963553E+00	0.443401E+00
0.60	0.151073E+02	0.185812E+02	0.131940E+01	0.964758E+00	0.470094E+00
0.70	0.252770E+02	0.300448E+02	0.130576E+01	0.964828E+00	0.503572E+00
0.80	0.383431E+02	0.445786E+02	0.128717E+01	0.963071E+00	0.544984E+00
0.90	0.537669E+02	0.618747E+02	0.126246E+01	0.958680E+00	0.595833E+00
1.00	0.706217E+02	0.814018E+02	0.123046E+01	0.950744E+00	0.658077E+00
1.10	0.876961E+02	0.102456E+03	0.118997E+01	0.938263E+00	0.734304E+00
1.20	0.103641E+03	0.124219E+03	0.113989E+01	0.920149E+00	0.827947E+00
1.30	0.117132E+03	0.145814E+03	0.107934E+01	0.895248E+00	0.943627E+00
1.40	0.127025E+03	0.166357E+03	0.100776E+01	0.862329E+00	0.108765E+01
1.50	0.132495E+03	0.185008E+03	0.925133E+00	0.820067E+00	0.126871E+01
1.60	0.133129E+03	0.201031E+03	0.832296E+00	0.767005E+00	0.149889E+01
1.70	0.128990E+03	0.213866E+03	0.731456E+00	0.701500E+00	0.179496E+01
1.80	0.120627E+03	0.223251E+03	0.627149E+00	0.621721E+00	0.217989E+01
1.90	0.109044E+03	0.229407E+03	0.528041E+00	0.525872E+00	0.268349E+01
2.00	0.956157E+02	0.233365E+03	0.449926E+00	0.413037E+00	0.333947E+01
2.10	0.819609E+02	0.237532E+03	0.419888E+00	0.285633E+00	0.417047E+01
2.20	0.697749E+02	0.246726E+03	0.478068E+00	0.154642E+00	0.514574E+01
2.30	0.606324E+02	0.270241E+03	0.664751E+00	0.464503E-01	0.610299E+01
2.40	0.557884E+02	0.326285E+03	0.976191E+00	0.104012E-03	0.670508E+01
2.50	0.560018E+02	0.452646E+03	0.131857E+01	0.382300E-01	0.661859E+01
2.60	0.614154E+02	0.735977E+03	0.155597E+01	0.135401E+00	0.585579E+01
2.70	0.715181E+02	0.140790E+04	0.162526E+01	0.238859E+00	0.477070E+01
2.80	0.852058E+02	0.325637E+04	0.155523E+01	0.313155E+00	0.370688E+01
2.90	0.100937E+03	0.104061E+05	0.140287E+01	0.349905E+00	0.281843E+01
3.00	0.116964E+03	0.899832E+05	0.121163E+01	0.354251E+00	0.212301E+01
3.10	0.131600E+03	0.209361E+06	0.100611E+01	0.334025E+00	0.158702E+01
3.20	0.143476E+03	0.201295E+05	0.799106E+00	0.295940E+00	0.116991E+01
3.30	0.151735E+03	0.757145E+04	0.598221E+00	0.245310E+00	0.838712E+00
3.40	0.156135E+03	0.406160E+04	0.410374E+00	0.186902E+00	0.570779E+00
3.50	0.157034E+03	0.256292E+04	0.244446E+00	0.125974E+00	0.353333E+00
3.60	0.155269E+03	0.177709E+04	0.112468E+00	0.691385E-01	0.182567E+00
3.70	0.151959E+03	0.131530E+04	0.289785E-01	0.246423E-01	0.626608E-01

3.80	0.148265E+03	0.102593E+04	0.783034E-02	0.153628E-02	0.384218E-02
3.90	0.145170E+03	0.838521E+03	0.566042E-01	0.743578E-02	0.186643E-01
4.00	0.143311E+03	0.715771E+03	0.170870E+00	0.454844E-01	0.116873E+00
4.10	0.142889E+03	0.635760E+03	0.332199E+00	0.112243E+00	0.301133E+00
4.20	0.143679E+03	0.584487E+03	0.512309E+00	0.198171E+00	0.566420E+00
4.30	0.145114E+03	0.552454E+03	0.681250E+00	0.290571E+00	0.903591E+00
4.40	0.146426E+03	0.532966E+03	0.814763E+00	0.377114E+00	0.130476E+01
4.50	0.146805E+03	0.521247E+03	0.897601E+00	0.448082E+00	0.176745E+01
4.60	0.145551E+03	0.513939E+03	0.923135E+00	0.496927E+00	0.229650E+01
4.70	0.142191E+03	0.508813E+03	0.891403E+00	0.519762E+00	0.290398E+01
4.80	0.136550E+03	0.504596E+03	0.807440E+00	0.514623E+00	0.360820E+01
4.90	0.128769E+03	0.500903E+03	0.680785E+00	0.481023E+00	0.443171E+01
5.00	0.119287E+03	0.498280E+03	0.526357E+00	0.420047E+00	0.539745E+01
5.10	0.108792E+03	0.498392E+03	0.366553E+00	0.335155E+00	0.652026E+01
5.20	0.981429E+02	0.504483E+03	0.233789E+00	0.233789E+00	0.778953E+01
5.30	0.882900E+02	0.522285E+03	0.171151E+00	0.129573E+00	0.913913E+01
5.40	0.801794E+02	0.561787E+03	0.225684E+00	0.436198E-01	0.104098E+02
5.50	0.746573E+02	0.640824E+03	0.427432E+00	0.131005E-02	0.113367E+02
5.60	0.723755E+02	0.792810E+03	0.757590E+00	0.208640E-01	0.116239E+02
5.70	0.737064E+02	0.108501E+04	0.113462E+01	0.984754E-01	0.111158E+02
5.80	0.786808E+02	0.166748E+04	0.144965E+01	0.205969E+00	0.992649E+01
5.90	0.869620E+02	0.292849E+04	0.162731E+01	0.307501E+00	0.836851E+01
6.00	0.978644E+02	0.612787E+04	0.165263E+01	0.378449E+00	0.675858E+01
6.10	0.110424E+03	0.173337E+05	0.155302E+01	0.410624E+00	0.529453E+01
6.20	0.123514E+03	0.112818E+06	0.136908E+01	0.406942E+00	0.405208E+01
6.30	0.135994E+03	0.760546E+06	0.113771E+01	0.374859E+00	0.303292E+01
6.40	0.146859E+03	0.419987E+05	0.887536E+00	0.322583E+00	0.220841E+01
6.50	0.155374E+03	0.144273E+05	0.640427E+00	0.257813E+00	0.154455E+01
6.60	0.161161E+03	0.746857E+04	0.414306E+00	0.187757E+00	0.101325E+01
6.70	0.164215E+03	0.464095E+04	0.225382E+00	0.119575E+00	0.596367E+00
6.80	0.164867E+03	0.319834E+04	0.889851E-01	0.606863E-01	0.286308E+00
6.90	0.163679E+03	0.235989E+04	0.187009E-01	0.186456E-01	0.850368E-01
7.00	0.161309E+03	0.183178E+04	0.238238E-01	0.355158E-03	0.159849E-02
7.10	0.158369E+03	0.148170E+04	0.105833E+00	0.106657E-01	0.483346E-01
7.20	0.155314E+03	0.124184E+04	0.255442E+00	0.507929E-01	0.236435E+00
7.30	0.152357E+03	0.107373E+04	0.452132E+00	0.117307E+00	0.572329E+00
7.40	0.149466E+03	0.953733E+03	0.667203E+00	0.202369E+00	0.105671E+01
7.50	0.146392E+03	0.866369E+03	0.869388E+00	0.295250E+00	0.168686E+01
7.60	0.142760E+03	0.801068E+03	0.103074E+01	0.384468E+00	0.246147E+01
7.70	0.138162E+03	0.750444E+03	0.113059E+01	0.459624E+00	0.338579E+01
7.80	0.132273E+03	0.709366E+03	0.115696E+01	0.512415E+00	0.447570E+01
7.90	0.124929E+03	0.674434E+03	0.110629E+01	0.536861E+00	0.575973E+01
8.00	0.116186E+03	0.643712E+03	0.982795E+00	0.529120E+00	0.727824E+01

8.10	0.106341E+03	0.616610E+03	0.798969E+00	0.487451E+00	0.907837E+01
8.20	0.959090E+02	0.593975E+03	0.577768E+00	0.412763E+00	0.111999E+02
8.30	0.855792E+02	0.578383E+03	0.356855E+00	0.310272E+00	0.136430E+02
8.40	0.761446E+02	0.574806E+03	0.192602E+00	0.192438E+00	0.163073E+02
8.50	0.684186E+02	0.591926E+03	0.156975E+00	0.820457E-01	0.189054E+02
8.60	0.631475E+02	0.644696E+03	0.314273E+00	0.110328E-01	0.209120E+02
8.70	0.609258E+02	0.759557E+03	0.673020E+00	0.839343E-02	0.216905E+02
8.80	0.621220E+02	0.985737E+03	0.114779E+01	0.792413E-01	0.208631E+02
8.90	0.668241E+02	0.142215E+04	0.159117E+01	0.195728E+00	0.186297E+02
9.00	0.748126E+02	0.228992E+04	0.188262E+01	0.314847E+00	0.156371E+02
9.10	0.855661E+02	0.416386E+04	0.198205E+01	0.404064E+00	0.125481E+02
9.20	0.983065E+02	0.892577E+04	0.191386E+01	0.450654E+00	0.976690E+01
9.30	0.112077E+03	0.257955E+05	0.172700E+01	0.456217E+00	0.743897E+01
9.40	0.125851E+03	0.177296E+06	0.146906E+01	0.428609E+00	0.555898E+01
9.50	0.138646E+03	0.888876E+06	0.117788E+01	0.377008E+00	0.406280E+01
9.60	0.149644E+03	0.573070E+05	0.882107E+00	0.310056E+00	0.287736E+01
9.70	0.158272E+03	0.200624E+05	0.604102E+00	0.235601E+00	0.194103E+01
9.80	0.164256E+03	0.104641E+05	0.362626E+00	0.161011E+00	0.120951E+01
9.90	0.167617E+03	0.653451E+04	0.174261E+00	0.934939E-01	0.655976E+00
10.00	0.168623E+03	0.452191E+04	0.533632E-01	0.401423E-01	0.268979E+00

REFERENCES

[1] Hallen, E., "Theoretical investigations into transmitting and receiving qualities of antenna," Nova Acta Regiae. Soc. Sci. Upsaliensis, Vol. 4 pp. 1-44; 1938.

[2] Storer J.R., "Impedance of thin-wire loop antennas", Trans. Am. Inst. Elec. Engrs. Vol. 75, p. 606; 1956; also cruft Laboratory, Harvard University, Cambridge, Mass., Tech. Rept. No. 212; May 1955.

[3] Wu T. T., "Theory of thin circular Loop antenna," J. Math. Phys., Vol.3, pp. 1301-1304; November-December 1962.

[4] Kraichman M.B., "Impedance of a circular Loop in an infinite conducting medium," J. Research Natl. Bur. Standards, Vol. 66d, pp. 499-503; July-August 1962.

[5] Chen C. L and R. W. P. King," The small bare Loop antenna immersed in a dissipative medium," IEEE Trans. on Antennas and Propagation, Vol. AP-11, pp. 266-268; May 1963.

[6] King R. W. P., C. W. Harrison, Jr. and D. G. Tingley, "The Admittance of Bare circular Loop Antennas in a Dissipative Medium," IEEE Trans. on Antennas and Propagation, Vol. AP-12, pp. 434-438 July 1964.

[7] King R. W. P., C. W. Harrison, Jr., and D. G. Tingley, "The Current in Bare circular Loop Antennas in a Dissipative Medium," IEEE Trans. on Antennas and Propagation, Vol. AP-13, pp. 529-531, May 1965.

[8] Galejs J., "Admittance of Insulated Loop Antennas in a Dissipative Medium," IEEE Trans., on Antennas and Propagation, Vol. AP-13, pp. 229-235, March 1965.

[9] Whiteside H., and R. W. P. King., "The Loop Antenna as a Probe," IEEE Trans. on Antennas and Propagation, Vol. AP-11, pp. 291-297, May 1964.

[10] Richtscheid A., "Calculation of the Radiation Resistance of Loop Antennas with Sinusoidal Current Distribution," IEEE Trans. on Antennas and Propagation, Vol. AP-23, pp. 889-891, November 1976.

[11] Tsukiji T., and S. Tou., "On Polygonal Loop Antennas," IEEE Trans. on Antennas and Propagation, Vol. AP-28. No.4, pp. 571-575, July 1980.

[12] Michaski K. A., and L. W. Pearson, "Equivalent Circuit Synthesis for a Loop Antenna Based on the Singularity Expansion Method," IEEE Trans. on Antennas and Propagations Vol. AP-32, No.5, pp. 433-441, May 1984.

[13] Awadalla K.H., and A. A. Sharshar, "A Simple Method to Determine the Impedance of a Loop Antenna," IEEE Trans. on Antennas and Propagations, Vol. AP-32, No.11, pp.1248-1251, November 1984.

[14] Barrick D.E., "Miniloop Antenna Operation and Equivalent Circuit" IEEE Trans. Antennas and Propagation, Vol. AP-34 No.1, pp. 111-114, January 1986.

[15] Row R. V., "Insulated Loop Antenna in a conducting Spherical Shell," IEEE Trans. on Antennas and Propagation, Vol. AP-13, pp. 216-218, March 1965.

[16] Iizuka K., R. W. P. King, and C. W. Harrison, Jr., "Self-and Mutual Admittances of two Identical Circular Loop Antennas in a Conducting Medium and in Air," IEEE Trans. on Antennas and Propagation, Vol.AP-14, No.4, pp. 440-450, July 1966.

[17] Tsukiji T., "Analysis of Two Coupled Coplanar Loops," IEEE Trans. on Antennas and Propagation, Vol. AP-28, pp. 250-253, March 1975.

[18] Devore R., and P. Bohley, "The Electrically Small Magnetically Loaded Multiturn Loop Antenna," IEEE Trans on Antennas and Propagation, Vol. AP-25, No.4, pp. 496-505, July 1977.

[19] Pettengill, R. C., H. T. Garland, and J. D. Meindl, "Receiving Antenna Design for Miniature Receivers," IEEE Trans. on Antennas and Propagation, Vol. AP-25, pp. 528-530,July 1977.

[20] Abul-Kassem A. S., and D. C. Chang, "On Two Parallel Loop Antennas," IEEE Trans. on Antennas and Propagation, Vol. AP-28, No. 4, pp.491-496, July 1980.

[21] Shoamanesh A., and L. Shafai., "Characteristics of Yagi Arrays of Two Concentric Loops with Loaded Elements," IEEE Trans. on Antennas and Propagation, Vol. AP-28, No.6, pp. 871-874, November 1980.

[22] Burton R. W., R. W. P. King, and , T. T. Wu, "The Loop Antenna with a Cylindrical Core : Theory and Experiment," IEEE Trans. on Antennas and Propagation, Vol. AP-31, No. 2, pp. 225-231, March 1983.

[23] Ju X. D, D. M. Fu, and N. H. Mao, "VHF TV Full Channel Loaded Circular Loop Antenna," IEEE Trans. on Antennas and Propagation, Vol. AP-32, No. 4, pp. 425-428, April 1984.

[24] Metwally A. D., and S.F. Mahmoud, "Mutual Coupling between Loops on Layered Earth Using Images," IEEE Trans. on Antennas and Propagation, Vol. AP-32, No.6, pp. 574-579, 1984.

[25] Cheng D.K., "Analysis of Linear Systems," Addison Wesley Publishing Co. Inc. California, Ch. 5, 1972.

[26] Schelkunoff S. A., "A General Radiation Formula," Proc. IRE Vol. 27, pp. 660-666, October 1939.

[27] Abramowitz M. and I. A. Stegun, "Handbook of Mathematical Functions with Formulas Graphs and Mathematical Tables," Dover Publications Inc. New York, p. 360, 1972.

[28] Harrington R.F., "Field Computation by Moment Method," The Macmillan Company New York, 1968.

[29] Jasik H., "Antenna Engineering Handbook", McGraw-Hill Book Co., N.Y., Ch.1, 1961.

[30] Ramo S.,J. R. Whinnery, and T. V. Duzer, "Fields and Waves in Communication Electronics", John Wiley and Sons Inc., N.Y., Ch. 12, 1965.

[31] Collin R. E., and F. J. Zucker, "Antenna Theory Part-1", McGraw-Hill Book Co., N. Y., Ch. 2, 1969.

[32] Pipes L. A., and L. R. Harvill, "Applied Mathematics for Engineers and Physicists", McGraw-Hill Kogakusha, Ltd., 3rd Ed., p. 784, 1970.